



WORCESTER POLYTECHNIC INSTITUTE

MAJOR QUALIFYING PROJECT

Completed in partial fulfillment of the Bachelor of Science degree in Chemical  
Engineering at  
Worcester Polytechnic Institute

UNDERSTANDING THE PURPLE CLAY COMPOSTION AND  
ITS EFFECTS ON GREEN TEA

Sponsored by:

Yixing Liyong Pottery Co. Ltd, & Wuhan University of Technology (WUT)

Authors:

Xiaoqiu Hou

Saeed Alshahrani

Farraj Aldossary

Khalid Alsobhi

Advisor:

Jianyu Liang

## ABSTRACT

The project develops a scientific understanding of the chemical composition of purple clay and its interaction with green tea. The team utilized multiple characterization methods, including SEM, EDX, XRD, TGA, XRF, ICP-OES, and pH tests, and recommended future research directions based on analysis of the characterization results. The results suggest that purple clay is a safe material for tea environment and additional tests on different kinds of tea may help to fully understand health effects of tea.

## **ACKNOWLEDGEMENTS**

### **Yixing Liyong Pottery Co, Ltd:**

The team would like to thank our wonderful sponsors at Yixing Liyong Pottery Company, special thanks go to Ying Bin Shen, the Executive Director at the Liyong Pottery company, and Shuai Zheng, the Deputy Manager of Product R&D Department at the Liyong Pottery Company, for their great hospitality and for the valuable lectures and sources they have provided us.

### **Wuhan University of Technology (WUT):**

Also, we would like to thank the professors at Wuhan University of Technology: Xiang Xing, Fei Chen, Yuanlu Xiong, and Xianfeng Chen, for providing access to their labs in order for our experiments to be conducted and assisting us with understanding the results provided from the experiments. Specific thanks to our WUT student partners Wenying Wei, Xiaofeng Gao, Jinwei Lin, and Yujie Shen, for their enormous support in helping us running tests, collecting data, and analyzing the results.

### **Professors Jianyu Liang:**

Finally, we would like to thank our advisor, Professor Jianyu Liang for preparing us for this project, and assisting with the completion of our goal. She was instrumental in guiding us in every step of our project.

## **AUTHORSHIP**

Understanding the Purple Clay Compositions and Effects on Green Tea major qualifying project and paper was equally divided amongst the four project team members: Xiaoqiu Hou, Saeed Alshahrani, Farraj Aldossary and Khalid Alsobhi. The project paper went through many stages of writing, editing, and formatting. Each of the project team members contributed to the final completion of the project and paper equally based on his or her set of skills.

# TABLE OF CONTENTS

ABSTRACT .....	i
ACKNOWLEDGEMENTS .....	ii
AUTHORSHIP.....	iii
TABLE OF FIGURES .....	vi
TABLE OF TABLES .....	vii
EXECUTIVE SUMMARY .....	viii
CHAPTER ONE: INTRODUCTION.....	1
CHAPTER TWO: BACKGROUND .....	3
2.1 The origin of the purple clay .....	3
2.2 The history of the usage of purple clay teapot .....	5
2.2.1 The initial period: Song dynasty .....	6
2.2.2 The canonical period: Ming dynasty .....	6
2.2.3 The transformation period: Qing dynasty .....	6
2.2.4 The reviving period: The republic of China .....	7
2.3 History of the sponsor .....	7
2.4 The cultural tradition of purple clay art.....	8
2.4.1 The birth of purple sand.....	8
2.4.2 The complexity and uniqueness of the purple clay technique .....	9
2.4.3 The development of the purple clay technology .....	9
2.4.4 Technological and spiritual inheritance of purple clay art .....	10
2.5 The process of creating the purple clay .....	11
2.5.1 Mining the purple clay.....	11
2.5.2 Preparation of purple clay ware .....	12
2.5.3 Preparation of purple clay theory .....	14
2.6 Property of the purple clay.....	14
2.6.1 The characteristics .....	14
2.6.2 Distribution.....	16
2.6.3 The chemical composition .....	17
2.6.4 Classification of purple clay .....	17
CHAPTER THREE: METHODOLOGY .....	19
3.1 Scanning Electron Microscope (SEM).....	22
3.2 Energy Dispersive X-ray spectroscopy (EDX) .....	26
3.3 X-ray Diffraction (XRD) .....	27
3.4 Thermogravimetric Analyzer (TGA).....	29
3.5 X-Ray Fluorescence spectroscopy (XRF).....	31
3.6 Inductively Coupled Plasma Optical Emission Spectrometer (ICP-OES).....	33
3.7 pH test.....	35
CHAPTER FOUR: RESULTS AND DISCUSSION.....	37
4.1 Scanning Electron Microscope (SEM).....	37
4.2 Energy Dispersive X-ray spectroscopy (EDX) .....	39

4.3 Thermogravimetric Analyzer (TGA).....	46
4.4 X-ray Diffraction (XRD) .....	50
4.5 X-Ray Fluorescence spectroscopy (XRF).....	54
4.6 Inductively Coupled Plasma Optical Emission Spectrometer (ICP-OES).....	57
4.7 pH value measurement .....	63
<b>CHAPTER FIVE: CONCLUSION AND RECOMMENDATIONS .....</b>	<b>65</b>
<b>WORKS CITED.....</b>	<b>67</b>
<b>APPENDIXES.....</b>	<b>71</b>
<b>A. EDX Pure Powder Sample Report .....</b>	<b>71</b>
<b>B. EDX non-sintered Sample report.....</b>	<b>80</b>
<b>C. EDX Sintered Sample report .....</b>	<b>89</b>

## TABLE OF FIGURES

Figure 1: Location of Yixing within China map (Sucaidao, 2018) .....	4
Figure 2: Timeline of the development of purple clay teapot through China history.....	5
Figure 3: Gong Chun learning teapot art, (Tao Lu, 2018) .....	9
Figure 4: Different layers of rocks in terms of depth (Chao Wang, 2018).....	12
Figure 5: Flowchart process of making the Yixing clay teapots. ....	13
Figure 6: Different sintering temperature of purple clay (Chao Wang, 2018). ....	16
Figure 7: Timeline of the MQP Schedule .....	19
Figure 8: Summarize of experiments applied and the information provided from each experiment machine. ....	20
Figure 9: Chinese Lipton green tea (M, 2018).....	21
Figure 10: Teapots provided from the sponsor “Yixing Liyong Pottery Co”. (A) plastic teapot, (B) glass teapot, (C) porcelain teapot, (D) purple clay teapot, and (E) stainless steel teapot. ....	21
Figure 11: Purple clay samples used in the experiments: (A) pure purple clay powder, (B) purple clay non-sintered, (C) purple clay sintered. ....	22
Figure 12: Scanning Electron Microscope and Energy Dispersive X ray spectroscopy machine (R, 2016). ....	23
Figure 13: Picture of abrasive papers (M, 2018). ....	24
Figure 14: Q150R ES, a machine coats samples with electrons (QT, 2018).....	25
Figure 15: X-ray diffraction machine (T, 2017). ....	28
Figure 16: Thermogravimetric analyzer (U, 2012).....	30
Figure 17: X-ray fluorescence spectroscopy (F, 2018).....	32
Figure 18: laboratory grinder (T, 2009).....	33
Figure 19: Inductively Coupled Plasma Optical Emission Spectrometer (ICP-OES) (S, 2015)..	34
Figure 20: Corresponding morphology pictures of the SEM test. ....	38
Figure 21: The powder EDX and elements peaks in different spots .....	41
Figure 22: The non-sintered EDX and elements peaks in different spots .....	43
Figure 23: The sintered EDX and elements peaks in different spots.....	46
Figure 24: The total results of the Sintered, non-sintered, pure purple clay powder for the TGA test.....	47
Figure 25: TGA graph of powder sample .....	48
Figure 26: TGA graph of Unsintered Sample.....	48
Figure 27: TGA graph of Sintered Purple Clay Sample .....	49
Figure 28: XRD graph of powder sample.....	50
Figure 29: XRD graph of non-sintered sample.....	51
Figure 30: XRD graph of sintered sample .....	52
Figure 31: Element concentration distribution within the powder purple clay, non-sintered and sintered samples. ....	56
Figure 32: Barium chart for the ICP-OES. ....	59
Figure 33: Barium chart for the ICP-OES. ....	60
Figure 34: Strontium chart for the ICP-OES. ....	60
Figure 35: Chlorine chart for the ICP-OES. ....	61
Figure 36: Barium chart for the ICP-OES test 2. ....	62
Figure 37: Aluminum chart for the ICP-OES test 2. ....	62
Figure 38: Strontium chart for the ICP-OES test 2.....	63
Figure 39: Chlorine chart for the ICP-OES test 2.....	63

## TABLE OF TABLES

Table 1: The chemical composition of the clay (Chao Wang, 2018). .....	17
Table 2: Concentration of non-oxide elements .....	55
Table 3: Corresponding shortcut name for testing sample .....	57
Table 4:: pH experiment results of testing sample listed in ICP-OES experiment.....	64

## EXECUTIVE SUMMARY

Yixing, China is a city with a long and complex history and is known as the capital of China's pottery. Yixing is also considered to be the origin of the purple clay, where the Yixing Liyong Pottery Company was founded. The Liyong Pottery Co is a leading company in making the purple clay teapots (Also known as Zisha ware). These teapots are very famous due to the complexity and time consumption of creating such wares, as well as the cultural importance of them since the tea traditions are essential in the Chinese culture.

To comprehend the chemical compositions of the purple clay, a team of chemical engineering students from Worcester Polytechnic Institute (WPI) cooperated with another team of material science students from Wuhan University of Technology (WUT) to run five sets of experiments on purple clay samples, which were collected in different stages of creating the teapots (pure powder, non-sintered, and sintered). Also, the group conducted another two sets of experiments for understanding the leaching elements from different kind of teapots and one kind of green tea. These samples were provided from the project's sponsors "Yixing Liyong Pottery Co".

The goal of the project is to develop a scientific understanding of the chemical compositions of the purple clay interacting with green tea. In order to achieve this goal, the team have set three objectives to be completed. The first objective was to study the structure and phase of purple clay material, including the pure powder purple clay, the non-sintered and the sintered clay. The second objective was to understand the chemical elements in the purple clay material. Finally, the third objective was to identify potential harmful elements and study their effects on green tea. The project was limited in seven weeks' period of time; thus, the team have narrowed

the samples of the experiments to one type of the Zisha ware which is the purple clay ware, and one product of pure green tea which is the Lipton Chinese green tea.

As for the results, SEM and EDX tests revealed the morphology and composition difference in three samples from different stages of tea pot manufacturing process. The TGA test clearly showed the loss of free and structural water in the material at temperatures in pure powder and non-sintered samples, but not in sintered sample. The XRD provided phase information that agrees with the TGA and SEM results. XRF identified the detailed chemical elements within the samples. Four elements that may be of health concern have been identified by the team and ICP tests were conducted to gather the concentration of these four elements in tea solutions made in tea pots of different materials. The results suggest that the purple clay teapots are safe for tea and may better preserve the original taste of the tea solution. Most of the extracted elements may be from the green tea itself. Therefore, the project team recommended that testing various tea to develop a better understanding of health effects by tea as a future direction.

## CHAPTER ONE: INTRODUCTION

Zisha ware (purple clay) teapots are one of the most expensive and luxurious kits in Chinese culture and traditions that are used in ceremonies as well as in daily life. The importance of the purple clay teapots comes from the significance of the tea in the Chinese culture, the scarcity of the purple clay minerals, which only exist in Yixing, China, the linkage of associating purple clay teapots to the emperors and noble families back in history, the artist who crafted that piece of art, as well as most of the nationwide, believe that drinking tea in purple clay teapots are healthier and beneficial to human bodies compared to other teapots made of different materials. (Tao Lu, 2018)

The distinctive features of the purple clay vitalize itself with fame and majesty throughout the Chinese history. Serving as one of the characteristics of purple clay, the strong plasticity enables the purple clay to turn into pottery without additional raw materials. The superior air permeability, exceptional stability, and unique kiln color also help the purple clay to stand out from other luxurious potteries in the world. The process of making pottery out of purple clay is been kept and preserved for more than 1000 years. It is being transferred from a generation to another from 960 until now (Chao Wang, 2018).

Though there are numerous companies that specialized in making and producing potteries from purple clay, Yixing Liyong Pottery Co., Ltd is the leading company and the biggest company in this industry. Despite the fact that the company sales and production are booming, they are seeking to use the modern technologies and research capabilities to enhance their product quality and look forward to the future (Liyong Pottery Co, 2018). Therefore, Yixing Liyong Potter Co cooperated with Worcester Polytechnic Institute (WPI) in order to conduct an extensive research on the characteristic of powder, non-sintered and sintered purple clay. The

objective of this research is to analyze the material in depth and find out what kind of elements are leaching out from purple clay teapots when using hot water and green tea.

In this project, a team of Worcester Polytechnic Institute (WPI) and Wuhan University of Technology (WUT) students worked together in order to design a methodology of conducting this research, executing the experiments, and finally, analyzing and finalizing the results founded from the experiments.

In this report, the engineering team discussed in detail the research and testing the project team conducted in order to provide Yixing Liyon Potter Co with efficient data and information about the microstructure of purple clay as well as identifying which elements are leaching out from the purple clay teapots when water or green tea were used. The report consists of the following chapters: introduction, which is this chapter, background, methodology, results and discussions and conclusion. The background consists of the history of purple clay and pottery in Chinese history, the characteristics and chemical compositions of purple clay and the process of mining and making the purple clay teapots. The different experiments that were conducted to better understand what purple clay contains and what kind of elements are leaching out when using water or green tea and their results were discussed in the methodology and results and discussion chapters, respectively. The end of the report includes a conclusion that wrap up the findings from the results and recommendations for further researches in the future.

## CHAPTER TWO: BACKGROUND

In this chapter, we explain the origin of the purple clay and the history of using the purple clay teapots, along with the cultural tradition of purple clay art, and the process of creating the teapots as well as its properties. In section 1, we discussed the geological origin location of purple clay which is Yixing, known as the capital of China's pottery and the importance of the city throughout the Chinese history. In section 2, we demonstrated the usage of purple teapots throughout the history, which could be divided by six essential periods. Starting with the initial period that came from the Song dynasty to early Ming dynasty, and ends up to the Republic of China's period. Lastly, we introduced our sponsors "Yixing Liyong Pottery Co" and illustrated its originality, history, and its role in the pottery industry. In section 3, we looked at the birth of purple sand that extracted from the general pottery with its complexity and uniqueness. As well as the development of the purple clay art that took over five hundred years of evolution. In section 4, we explained the process of creating the purple clay, beginning with mining mineral materials which are divided to the open depth and the tunnel mining, to end up in creating the needed design of teapots. In section 5, we elucidated the property of the purple clay and its characteristics. Also, we discussed the distribution that take place in the hilly area of Huanglongshan. Finally, we illustrated the chemical composition of purple clay and its classifications.

### 2.1 The origin of the purple clay

Previously called 'Yang Xian', Yixing, along with its century history and cultural background, is known as the capital of China's pottery. Located in the south of Jiangsu province in China, Yixing has taken advantage of the delta area near the Yangtze River to help itself become one of the rapidly developing cities in modern China (Santangelo, P, 1992) (Figure 1).



Figure 1: Location of Yixing within China map (Sucaidao, 2018).

The importance of Yixing can be traced by to the ancient China history. From Wen Zhengming "The tale of Xianju in the jade pond", "The map of the wonderland of Taoyuan" and "The map of the jade cave", Yixing's natural beauty has been shown to the public. In the scenes of four seasons, such as the spring and stream, the waterfalls, the mountain path and the luxuriant woods, the shape of the spiritual source and the spiritual home are drawn. This is the charm of "Yixing", and the integration of landscape and human environment is a glimpse of the power of integrating art and the beauty of nature (Santangelo, P, 1992).

Yixing's superior geographical location has provided the city not only the scenic landscape but also the origin of the purple clay. As one of the biggest discoveries in Chinese archaeology, the Neolithic culture in the Taihu river basin is the cultural type of camel pier, with the pottery flat bottom kettle as its main feature. It is a unique and self-contained cultural type in

the West Bank of Taihu, which is parallel to Hemudu Site culture and majibang culture. Since the Neolithic age, the kiln has been firing, and the famous "Yixing kiln" system has been formed (Santangelo, P, 1992).

## 2.2 The history of the usage of purple clay teapot

There is a total of six important periods in the history of purple clay ware. The initial period which is from Song dynasty to early Ming dynasty, the canonical period which is from middle Ming dynasty to late Ming dynasty, the flourishing period which is during the Kangxi, Yongzheng and Qianlong period n Qing dynasty, the transformation period which is from Jiaqing and Daoguang in Qing dynasty to the end of the Qing dynasty, the reviving period which is during the establishment of the Republic of China and the innovation period which starts from 50 years ago (Wu, 2010).

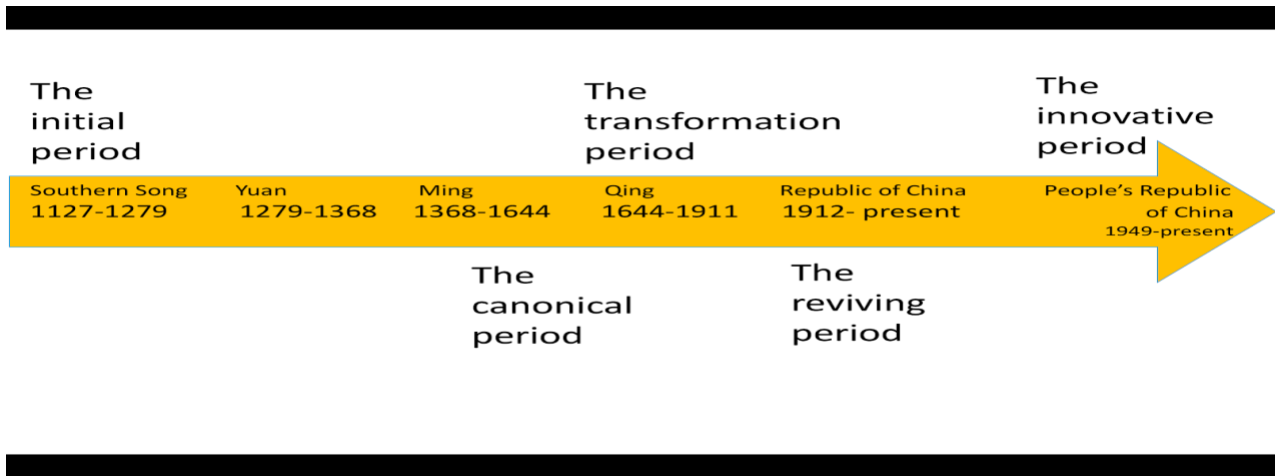


Figure 2: Timeline of the development of purple clay teapot through China history.

### **2.2.1 The initial period: Song dynasty**

When it comes to the Song dynasty, marvelous architectures, profound cultural heritage were the first things that come to mind. The effortless shape, immaculate shading, and coating of the wares of the Song Dynasty marked a unique point in Chinese decorative art. Besides the purple clay wares, Song is also known for the production of Jingdezhen whiteware, Jizhou wares, and Celadons. Before the establishment of the Southern Song dynasty, the former Northern Song Dynasty has already started its literature and art renewal. It is a major breakthrough during the ancient Chinese history that poets and painter were allowed to attend court along with imperial families and generals (Wu, 2010).

### **2.2.2 The canonical period: Ming dynasty**

According to historical records, the real purple teapot was actually founded during the Zhengde period of the Ming Dynasty. The Jinsha Temple and the Gongchun can be regarded as the pioneers of the professionalization and artistic in the field of purple clay teapot. From Jiajing to Wanli, purple clay gradually formed its own technological system from the daily use of ceramics. During this period, Dabin was a landmark figure in the history of purple clay. He helped to establish the standard for the basic technology of purple sand molding and cultivated a large number of talents. The innovation of the sand adjustment, color matching, and different styles was also brought by Dabin. Moreover, he connected the art of teapot making to the literati which adjusted the size of the teapot and eventually formed the style of pottery in Park Athens.

### **2.2.3 The transformation period: Qing dynasty**

During the Jiaqing period of the Qing Dynasty, Chen Mansheng, one of the 'Xi'an Eight', designed a new style of the teapot along with his fellows during his tenure as the Shuyang

County magistrate. He then handed the teapot to a famous artist called Yang Pengnian to engrave it. The piece was then named as the Mansheng pot regarding its simple and elegant style.

Later, in the late Qing Dynasty, the Zhejiang calligrapher Mei Ting Ding created the Yucheng Kiln. The famous craftsmen Wang Dongshi and He Xinzhou made the pots, and they had the praise of words by pots and pots with words. The pot art style of this period is a wash-up of the literati, which can be called the conversion period of purple sand (Wu, 2010).

#### **2.2.4 The reviving period: The republic of China**

The purple clay industry during the Republic of China experienced a dramatic rise to decline. From the beginning of the Republic of China to the year of 1937, under the influence of the industrial revolution, the purple clay industry developed vigorously and showed a scene of prosperity. At that time, almost everyone from Lushan, Chuanxiong, Qian Luo and the surrounding countryside devoted themselves to making the homemade muddy and household-made billets. The dragon kiln did not stop day and night. The production and sales of the products were booming and exported to the countries of Toyo and Nanyang.

In terms of talent cultivation, besides family biography and teacher management, the purple clay company also established a pottery workshop and later the Jiangsu Provincial Yixing Primary Ceramics Vocational School. Ren Qiting, Gu Jingzhou, and other famous artists also learned their talents during the Republic of China. From the outbreak of the War of Resistance Against Japanese in the year of 1937, the Dingyu kiln was bombed by the Japanese. A year later, the Japanese colonized the area which put the whole industry in danger (Bossler. B, 2002).

### **2.3 History of the sponsor**

At the beginning of the Republic of China, a number of purple sand enterprises and pottery shops have sprung up, such as Liyong, Yufeng, Fukang, Wu Desheng, Tiehuaxuan, and

even a short-lived state-owned Jiangsu Yixing pottery. Industry factory. Yixing Liyong Pottery Co., Ltd. is one of the earliest companies with the best performance and the longest operation time. Liyong pottery company was incorporated in Shanghai in the second year of the Republic of China of 1913. The company reached its peak in the 1930s. After the founding of New China, the government supported the development of purple sand production (Liyong Pottery Co, 2018).

During the year of 1951, the “Yixing Zisha Production and Marketing Joint Marketing Office” was established to organize production and sales. Thirty-seven Zisha artists then established Zisha Workshop (under the Tangdu Ceramics Production Cooperative) in the year of 1954. Two years later, Yixing County Shushan Ceramics Production Cooperative Zisha Workshop was established. In 1958, “Yixing Zisha Craft Factory” was established. Since then, the factory has become the only professional factory in Yixing Zisha production for nearly 30 years (Liyong Pottery Co, 2018).

## **2.4 The cultural tradition of purple clay art**

### **2.4.1 The birth of purple sand**

From the middle of the Northern Song Dynasty, the craft of making the purple clay ware was extracted from the general pottery, and the soil was refined, the processing was meticulous, the plain billet was fired, and the mud plate was formed. In Ming Dynasty, Gong Chun, a student of the scholar Wu Shi, learned the method of pottery from a monk, and opened the door of teapot art. In the last years of Ming Dynasty, Zhou Gaoqi introduced the process of purple clay teapot technique growing from the beginning to the maturity, in the book “Yang Xian Teapot”. It can be seen that in the middle and late Ming Dynasty, the purple clay ware was not only a general appliance for living and drinking tea but also a device for playing among the Zen masters, literati and scholars (Tao Lu, 2018).



*Figure 3: Gong Chun learning teapot art (Tao Lu, 2018).*

#### **2.4.2 The complexity and uniqueness of the purple clay technique**

The Yixing purple clay pottery technique entered the first batch of national intangible cultural heritage list in 2006. Purple clay technique is not only a production technology, but it also includes a series of techniques such as the preparation of the clay, the art design, the kiln firing the final product, so the whole process is accomplished by individuals. As a kind of artistic creation material, purple clay has its uniqueness and its own special characteristics. Its plasticity is strong, its color is steady and rich, and it does not glaze as well as it can become pottery independently (Tao Lu, 2018).

#### **2.4.3 The development of the purple clay technology**

In the five hundred years of the development of purple clay art, each period's works have distinct features of that time, reflecting the different cultural background, the aesthetic trend of thought, and the characteristics of the craft. And since the founding of the purple clay art, the author has signed the teapot, which continues to modern days. Shi Dabin, Chen Mingyuan, Shao

Daheng and Gu Jingzhou are also conscious of the inheritance and innovation of the purple clay technique, leaving one by one wonderful pieces of work (Tao Lu, 2018).

There are two ways for the royal court purple clay wares in Ming and Qing Dynasties. The first is for local officials, and the second one is created for the Emperor that he is using by himself. The palace office draw sketches and even made wood model, delivered to the officials in Yixing to customize. Therefore, all the purple clay sent to the palace must be selected high quality clay and made by the best craftsmen. The style of court purple clay teapot is dignified and embodies the classical artistic style. The main achievement is in the decoration, the creation of a variety of new techniques, presenting a magnificent, elegant and noble, showing the imperial style of emperor (Tao Lu, 2018).

#### **2.4.4 Technological and spiritual inheritance of purple clay art**

The technology of purple clay is a highly inheriting technology category. In the past five hundred years, the core technology has been well preserved and developed very well. In the pluralistic era of information, it is not enough to simply inherit and talk about tradition only. The artistic creation of purple clay is complex and difficult. It needs not only the perfect traditional technology, and the understanding of the literary feelings of purple clay but also invested with tea culture, and more importantly, the thinking and practice of contemporary aesthetics. To find the balance between the traditional technology and the aesthetic of the times, it can be seen that the graduates of many art colleges and universities have become the new "craftsmen" of purple clay and apply their study into the art of purple clay to deduce modern design ideas. From technological inheritance to design innovation to the evolution of artistic creation that became essentially related to the spiritual life of the Chinese culture (Tao Lu, 2018).

Purple clay is the spiritual support and life culture carrier and embodiment of ancient literati. Therefore, the inheritance is not only the imitation of the form and the craft but also the cultural spiritual connotation and the spiritual demand and lifestyle of the times.

## **2.5 The process of creating the purple clay**

### **2.5.1 Mining the purple clay**

There are two ways of mining mineral materials. One is the open depth, also known as the bright depth, which is suitable for mineral materials close to the surface of the stratum. Most of this method is to collect tender mud, generally, only one or two meters of waste soil needs to be bound to collect it. The second one is tunnel mining, also called dark excavation, which mainly mines armor clay and purple clay minerals. Due to the deep burial of purple clay minerals and the multi-star slope shape of ore bodies, inclined shafts are generally used for mining. First paste into a mine, and then through the Huangshi rock for mining, or directly in the lower part of the Huangshi rock tooth crossing tunnel to the mud layer for mining (Liyong Pottery Co, 2018).

Mining of mineral materials is divided into two stages. The first stage is prior to July 1955, and it belonged to individual manual mining. The tools and mining techniques were very primitive and belonged to the early stage of mining. The distribution of early mining sites is relatively extensive, and the seams are different. Although the amount of purple clay minerals mined is limited, the types are quite diverse. Purple clay is also called "rich soil" because of its low content in mineral seams and its "golden value" for a long time. Yixing Guokuang company was set up in July 1955 to receive all the individual mines and pits mined by local clay. The state and local governments are in charge of mining and have entered the stage of modern mining. With the intervention of modern technology, the mining conditions have been continuously improved, and the efficiency has also been greatly enhanced (Chao Wang, 2018).



*Figure 4: Different layers of rocks in terms of depth (Chao Wang, 2018).*

### **2.5.2 Preparation of purple clay ware**

Purple clay shale is formed in the interlayer of a mud seam. It is mostly mined from the depth of underground mines as deep as hundreds of meters or even kilometers, and the texture of deep ore bodies is excellent. However, the newly mined purple clay ore body (often called raw materials) is as good as stone and needs a series of processing treatments before it can be made into clay (clinker) for production. The technological process is as follows: mining ore bodies; selecting ore materials (raw materials); stacking them in the open air (wind, rain, sun and night exposure for months or even years); naturally weathering (ore bodies become loose and small particles); removing impurities; crushing ore materials (grinding with a stone mill or a rotary rolling machine), sieving ore materials (screening with screens of different specifications according to the mesh number required by the mud department, mixing ingredients (pure crude ore mud does not have this procedure), mixing with water (in a large cylinder).

One practice mud (manual mud uses artificial wooden pestle to practice foot treading or uses rolling stones to protect it from rotting. Machine-made mud is used by machine and

equipment for vacuum lifting) one shot into wet test blocks (manual mud slicing into blocks and machine-made mud extruding and cutting into strips). stale nurse (put more wet places and overstocks and the longer the stale time, the better). One clinker (it is necessary to train the pug once more before use in order to achieve ideal plasticity and uniformity). Finally, creating the needed form (only manually by a special artist) (Liyong Pottery Co, 2018).

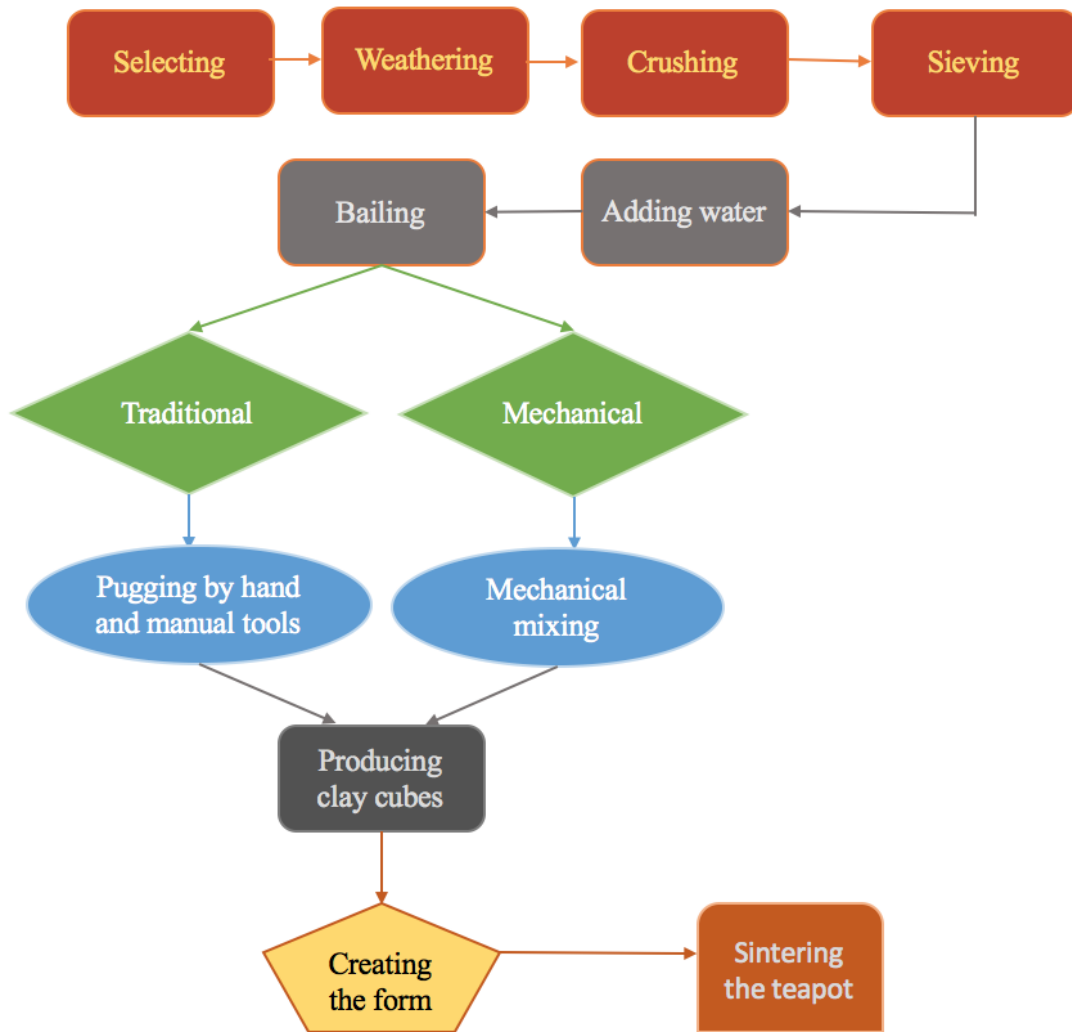


Figure 5: Process flowchart of making the Yixing clay teapots.

### **2.5.3 Preparation of purple clay theory**

Basically, divided into manual and mechanical processing. The manual method of grinding mud powder with stone mill continued until 1957. In 1958, the processing of purple clay was realized by mechanization. Rolling and crushing with a stone wheel and controlling the processing composition to be around the 6th sieve. In 1959, a Mongolia-saving crusher was started to be used. The rigidity was above 100 mesh sieves. After warm water was carried out by a vacuum mill, it became cooked mud for billet making.

From raw materials to match each other, there are primary color mud and match each other. However, no matter how the raw materials are processed, the finished product is called cooked mud, which can be formed after being aged. There are many good sandstones in the history. Different periods and different historical years have different representative sandstones. This provides collectors and connoisseurs with the connotation of historical works appreciation (Liyong Pottery Co, 2018).

## **2.6 Property of the purple clay**

In this section, the team major source was our sponsor's sources. One research has been found that is only discussing how the infusion of the tea in the Yixing clay pots are different in terms of taste. The company sources were the lectures that have been represented during our visit to the manufactory, which were mostly explaining the history and the cultural tradition of the purple clay with not significant background of the property and chemical composition of the teapots. Therefore, we faced some lack of information on this regard.

### **2.6.1 The characteristics**

Purple clay is a kind of clay with excellent quality. Its excellent performance and characteristics are as follows:

**1. Strong plasticity:** Purple clay can be made into pottery by itself without adding other raw materials along with the whole process of making it.

**2. Good air permeability:** The finished ceramic has a double pore structure: one is closed pore, which is the pore inside the agglomerate; the other is open pore, which is the pore group surrounding the agglomerate. This makes purple clay pottery have good air permeability. High pore density has a strong adsorption force, while glazed ceramic teapot lacks this function. At the same time, the teapot itself is a precise and reasonable shape. The lid of the teapot is closely matched, thus reducing the channel through which the air with *Aspergillus flavus* and *Shaw* in the mud flows into the egg. Therefore, the color and fragrance of the tea can be maintained for a long time, and the time for deterioration and spoilage of the tea can be relatively delayed.

**3. Good physical stability:** Purple clay pots do not crack when heated by heat and shrunk by cold even if they are poured alternately with cold and hot water. Where the shrinkage rate of drying is 3-5%, shrinkage rate of sintering is 6-8%, and a total shrinkage rate: about 10%.

**4. Kiln color:** Purple clay does not need to be glazed after being burnt. it is colored by its own primitive clay after being kiln-changed, and the kettle surface is bright and smooth. Manipulation of firing temperatures, as well as regulating the kiln atmosphere can create different colors for the purple clay (Chao Wang, 2018). (See figure 6)



*Figure 6: Different sintering temperature of purple clay (Chao Wang, 2018).*

## **2.6.2 Distribution**

The Ding Shu Town of Yixing City belongs to the lake basin along the edge of the continent. The heavy particles sunk underground, and the light particles are floating above forming two sedimentary clay. The light quality of silicon and aluminum forms the clay layer of the Yellowstone. The large proportion of quartz and iron are in the lower part of the clay layer, and the loose two clays is covered for a long time. The quartz sand is distributed in cemented clay, forming hard and semi-hard clay silt. Only produced in the hilly area of Huanglongshan area, it covers an area of about 2.5 km<sup>2</sup>, and Huanglong Mountain raw ore is about 100 meters high. After mining, it has gradually formed a pool of about 35m. The samples of other clays they can get: Green, yellow, and brown clays (Liyong Pottery Co, 2018).

### 2.6.3 The chemical composition

Most of the chemical and mineral composition of the purple clay are from silicon dioxide with more than 60% of the whole material, comes after it is the aluminum oxide with a 21%. You can see in the figure (Figure 13) the other chemical composition of the clay (Chao Wang, 2018).

SiO <sub>2</sub>	Al <sub>2</sub> O <sub>3</sub>	Fe <sub>2</sub> O <sub>3</sub>	CaO	MgO	I.L.
63.40	21.06	6.34	1.000	0.23	7.52

*Table 1: The chemical composition of the clay (Chao Wang, 2018).*

### 2.6.4 Classification of purple clay

Yixing's clay has a wide variety and is widely distributed in the hilly and mountainous areas in the south of Yixing. The raw materials used in purple clay pottery including purple clay, green clay and red clay, collectively referred to as the purple mud.

Purple mud is an interlayer of a mud seam. The ore body is thin and lenticular. The thickness of the seam is usually about tens of centimeters to one meter. The stability is poor, and the color of the raw materials are uniformed purple and purple with light green spots. After burning, the color of the raw materials is purple, purple brown and purple black. Purple mud is mainly composed of hydromica and contains different amounts of kaolin, Shi Ying, mica dust and iron. Based on the comprehensive analysis, purple clay belongs to the granular soil - Shi Ying mica system, which is quite characteristic of porcelain raw materials. Therefore, a single raw material is ideal (Liyong Pottery Co, 2018).

In the next chapter, the team discussed the different methods for analyzing the purple clay in terms of scientific experiments. Also, we examined the green tea along with its substantial minerals when the tea gets heated in the teapot.

## CHAPTER THREE: METHODOLOGY

The team members developed a clear plan for the research duration that illustrates the experiments applied, the project paper writing, the results analyzed, and performing the final presentation during the project of the MQP which consumed seven weeks (Figure 7). The goal of our project is to develop a scientific understanding of the chemical composition especially metals of the purple clay and its interaction with green tea.

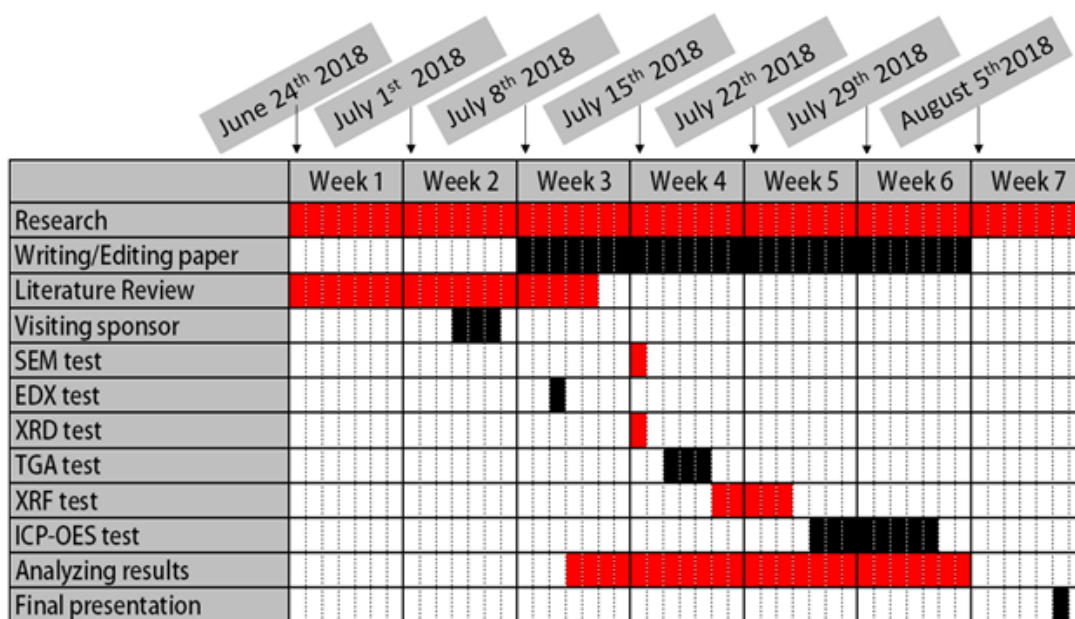


*Figure 7: Timeline of the MQP Schedule.*

The team setup clear objectives and guideline for testing and analyzing the chemical composition of the Purple Clay and its interaction with the green tea. In order to achieve the project goal, three objectives were established:

1. Study the structure and phase of purple clay material, including the pure purple clay powder, the non-sintered and sintered clay.
2. Understand the chemical elements in the purple clay material.
3. Identify potential harmful elements and study their effects on green tea.

In order to be able to achieve these objectives, several machines were used in conducting the experiments, such as SEM, EDX, XRD, TGA, XRF, ICP-OES and pH. All these instruments will be explained later in this chapter in advance, in how they are helpful to us and what kind of results each machine provided. (Figure 8).

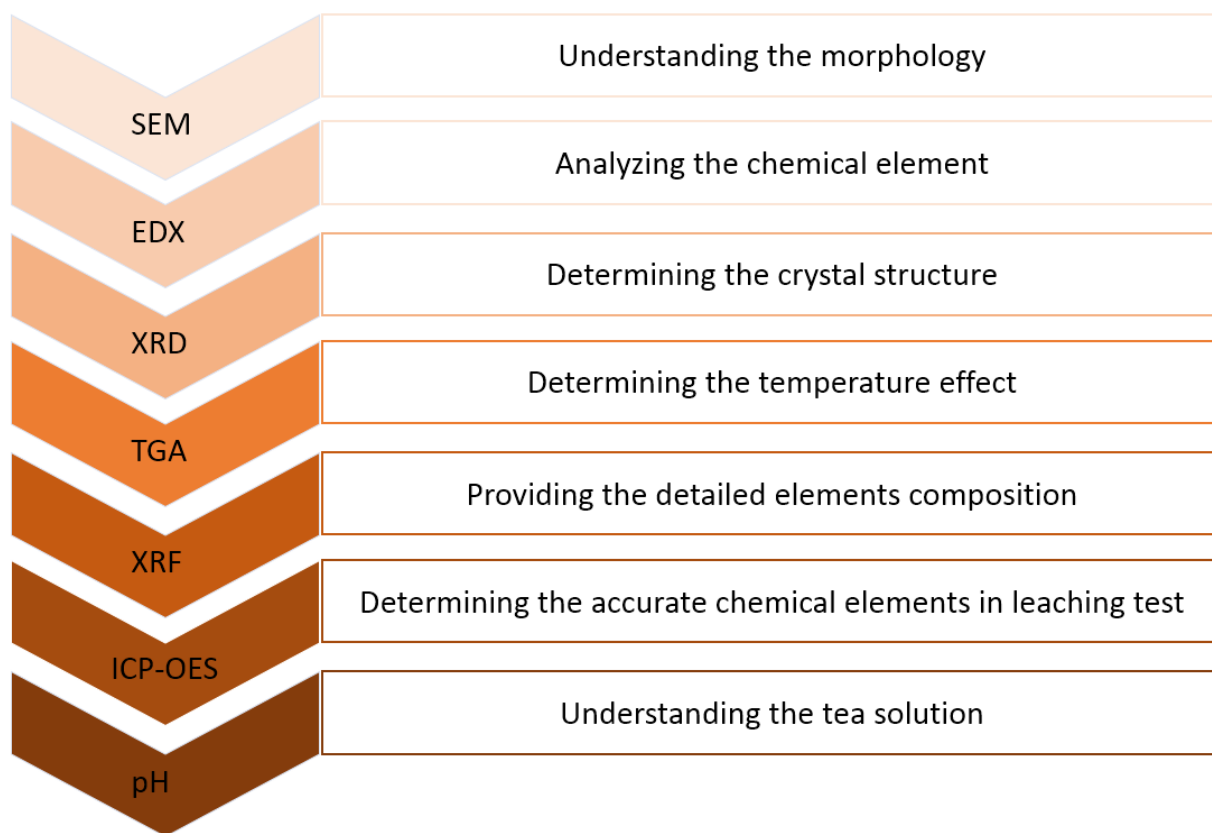


*Figure 8: Summarize of experiments applied and the information provided from each experiment machine.*

The green tea used in all experiments in this project is the Lipton pure Chinese Green Tea (Figure 9). The water used to make the green tea is the demineralization water (DI water).



Figure 9: Chinese Lipton green tea (M, 2018).

All the teapot containers were provided from our sponsor the “Yixing Liyong Pottery Co”. The teapots used in the experiments are (A) Plastic teapot, (B) glass teapot, (C) porcelain teapot, (D) purple clay teapot, and (E) stainless steel teapot.

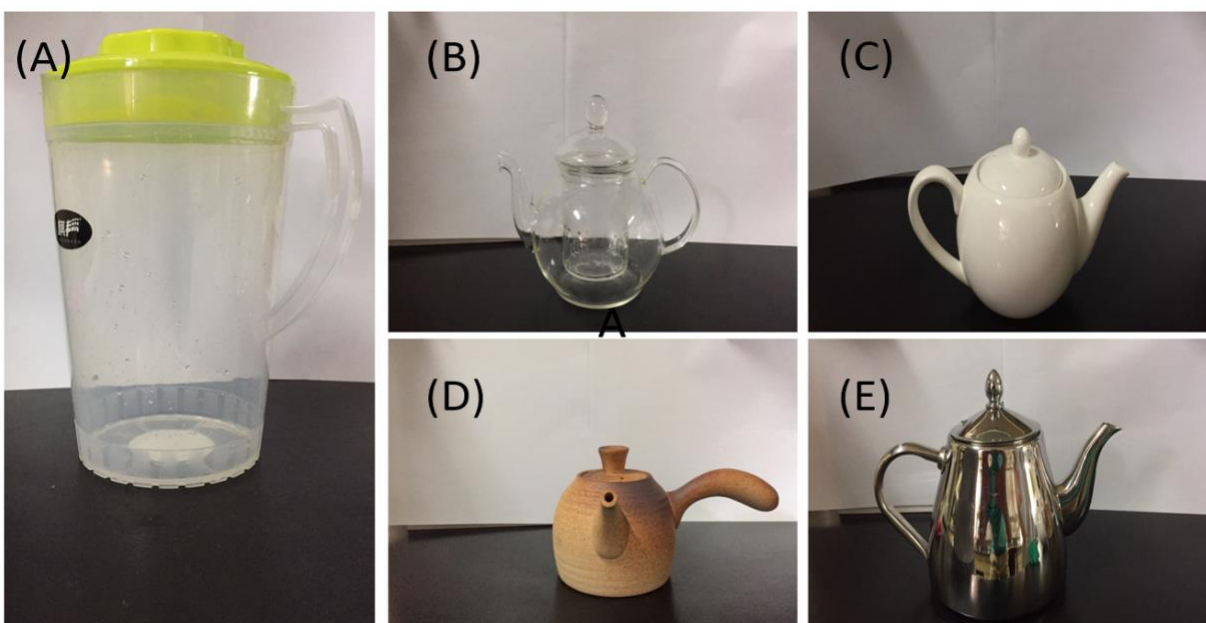


Figure 10: Teapots provided from the sponsor “Yixing Liyong Pottery Co”. (A) plastic teapot, (B) glass teapot, (C) porcelain teapot, (D) purple clay teapot, and (E) stainless steel teapot.

The purple clay samples tested in the project experiments are pure purple clay powder (Figure 11A), non-sintered purple clay (Figure 11B), and the sintered purple clay (Figure 11C).

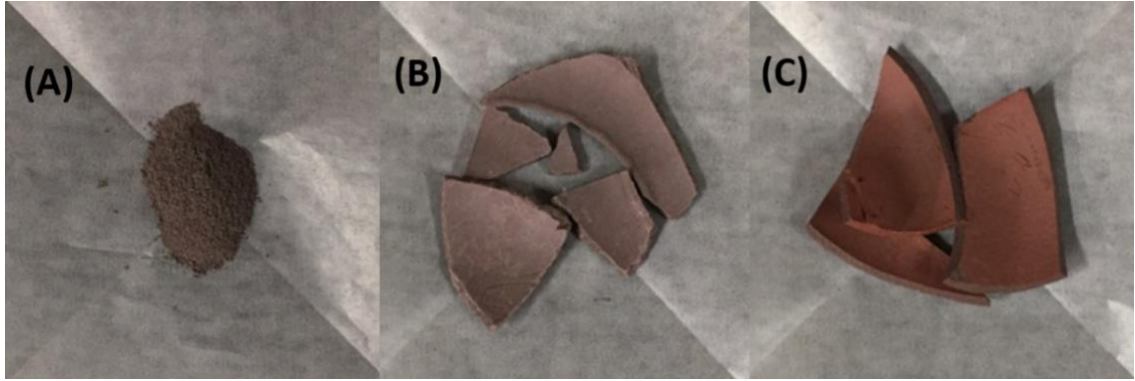


Figure 11: Purple clay samples used in the experiments: (A) pure purple clay powder, (B) purple clay non-sintered, (C) purple clay sintered.

### 3.1 Scanning Electron Microscope (SEM)

SEM is a chemical machine used in laboratories to scan the surface of tested samples in order to provide the chemical composition (D. Stokes, 2008). The tested samples must be charged by electrons to interact with the sample atoms in order to finally provide the compositions. Then, using the SEM machine to have a clear vision of the tested sample surface. SEM can test its samples in high or low vacuum and that could change the clearance of the scanning vision. (D. Stokes). The Scanning Electron Microscope shows the molecules of thin specimens, Energy-Dispersive X-Ray Spectroscopy detector, and pictures of the morphology (Figure 12).



*Figure 12: Scanning Electron Microscope and Energy Dispersive X ray spectroscopy machine (R, 2016).*

The tested samples which were the pure purple clay powder (Figure 11A), non-sintered purple clay broken parts (Figure 11B), and sintered purple clay broken parts (Figure 11C) were prepared (Figure 11). The samples were clean and dry before testing. The pure purple clay powder sample was cleaned using ethanol ( $C_2H_6O$ ) then it let to be dry overnight. After making sure that the sample was cleaned and totally dried, it was saved in a small clean plastic bag. For the second and third samples, which were the non-sintered and the sintered purple clay broken parts, a very small parts were taken and scrubbed using abrasive papers to adjust the surface of the samples (Figure 13).



*Figure 13: Picture of abrasive papers (M, 2018).*

Then, the second and third samples were cleaned using ethanol ( $C_2H_6O$ ) and let to be dried overnight. After making sure that the samples were completely dried, they were placed in clean separated bags. On the following day, a platinum tab was placed on the top of the aluminum stub then the samples were loaded in the aluminum stub using a sticky platinum tab. Then, the aluminum stub was placed in a machine called Q150R ES, which is “a compact rotary pumped coating system suitable for SEM sputtering with non-oxidizing (noble) materials” (QT, 2018). (Figure 14).

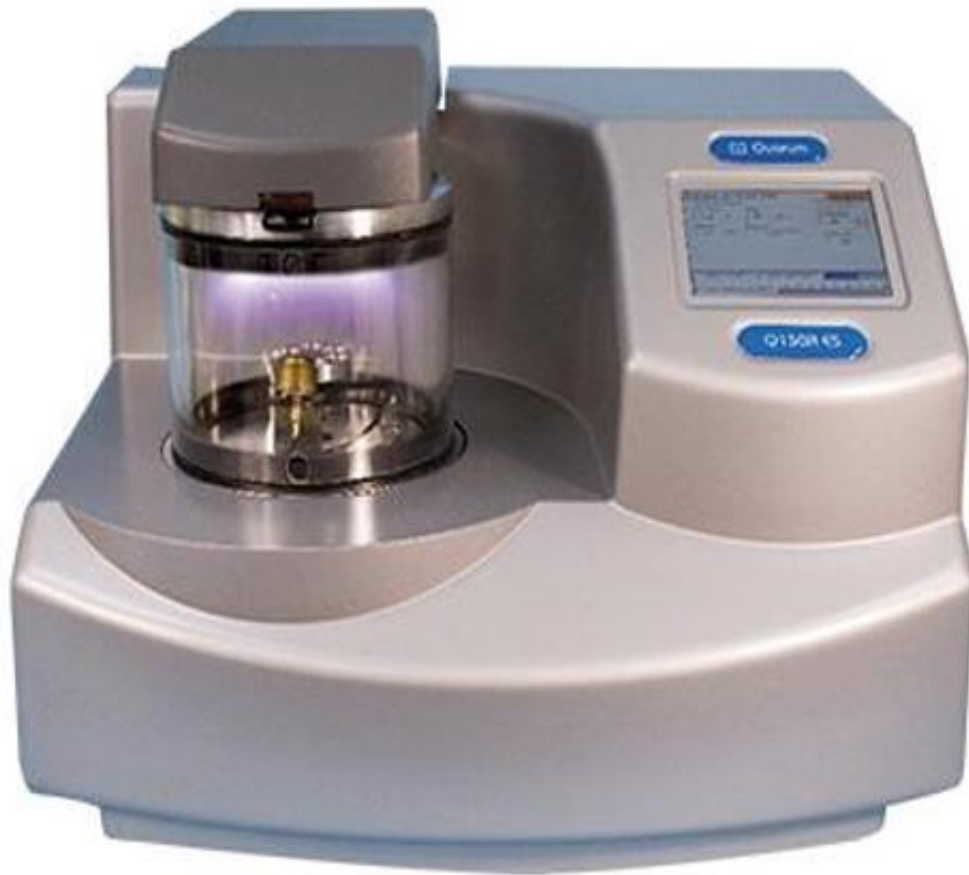


*Figure 14: Q150R ES, a machine coats samples with electrons (QT,2018).*

Placing the aluminum stub in the Q150R ES was to charge the tested materials to make them conductive in order to have a better vision of the samples. The aluminum stub was placed for around 6 minutes, until it was completed coating 20 nm layer of electrical platinum coating, 54 mA of current and  $1 \times 10^{-3}$  mBar of vacuum were applied. Then the aluminum stub was placed in the Quanta FEG 450 machine, which tests the SEM and the EDX later on. Then, the Quanta FEG 450 machine for testing the SEM started venting. After venting, the chamber door of the machine was opened, and samples were placed in the sample holder carefully and the height of the specimen was adjusted to be 10 mm. Then, in the computer screen, the HiVac mode was selected then Pump button was clicked. After that the machine started vacuuming for a while until it showed a VacOK on the screen, which means that it finished vacuuming. After vacuuming

Detectors and SE bottoms were selected then the beam was chosen to be 10,000 kV and the spot size, brightness, and contrast were adjusted until a clear vision of the samples appeared. Pictures were improved and taken at a magnification of 10000, 5000, 2000, 1000, and 500. The previous steps worked well with the pure powder purple clay sample, though neither the non-sintered nor the sintered purple clay samples were conductive. Therefore, the electrical platinum coating amount was increased to improve the vision of the non-sintered and sintered purple clay samples. Therefore, the electrical platinum coating was increased to be a total of 30 nm in both samples. The non-sintered purple clay sample was conductive, but the sintered purple clay sample was not conductive. Therefore the electrical platinum coating was increased to be a total of 40 nm in the Sintered purple clay sample, then it was finally conductive.

### **3.2 Energy Dispersive X-ray spectroscopy (EDX)**

EDX is a chemical machine used to analyze elements and chemical characteristics of typically thin film samples by applying the X-ray radiations to identify the atomic structure of each element and detect them on the spectrum peak (*J. Goldstein 2018*). The Energy Dispersive X-ray spectroscopy identifies the elements and quantitative compositional but not very accurately (*S. n.d.*) (Figure 12).

EDX test is an extension process of the SEM test. EDX identifies the sample elements, provides the amounts of each atoms, and maps the distribution of the atoms in the tested samples. (*Litzinger, R*) The chamber door of the Quanta FEG 450 machine was opened and the aluminum stub was gotten out to sputter some platinum in top of the samples in order to ensure the film is very conductive. Then, the samples were loaded again in the sample holder inside the Quanta FEG 450 machine. Then pump click was pressed to evacuate the chamber. After that the electron beam was turned on to generate the image on the monitor. Then the vision for the images was

adjusted in order to take great pictures of the morphology. After that a high voltage amount was applied to excite the samples in order to have clear peak results. Then the process time and the range of the energy of the beam were selected, and the start button was clicked. Then, eight spots were pointed in the picture in different places to measure the composition of these selected points, and then peaks appeared.

### **3.3 X-ray Diffraction (XRD)**

XRD is a chemistry lab machine used to measure the crystal structure of a thin film material of tested samples by producing incident X-ray to different directions (ISU). X-ray diffraction provides the crystal structure, quantitative analysis of phase composition, electron density, crystallite size, micro strain, residual strain in the macro stain, detect defects, characterize polymorphs, texture orientation, unit cell lattice parameters and the lattice symmetry. (ISU) (J. Fink, 2013) (Luuk J.P, 2011). (Figure 15). The X-ray diffraction identifies the phase of a crystalline material. It provides information about the dimensions of a single cell and determines the molecular and atomic structure of a crystal, (L. n.d.).



*Figure 15: X-ray diffraction machine (T, 2017).*

Starting with the sample preparation, it is important to have a well-defined polycrystalline material and the individual particle size should be below 45 microns. The loading sample holders must be filled that when the beam hits at a particular angle, it represents all the planes of the peak. The first sample, which was the pure purple clay powder, was not completely powder. Therefore, the mill was cleaned by ethanol then the pure purple clay powder was grinded. After that the pure purple clay powder sample was loaded in the sample holder and pressed gently using a glass cell with estimating the amount of the sample needed to fill the sample holder hole and adjusting the service of the sample holder. Then the sample holder was loaded in the XRD machine, and chamber door was closed. After that, the values of the volts and the current were inputted in the computer screen. The process started with a very low values of voltage and

current then increased the values to the amount needed. Thirty minutes was the waiting time to let the machine soak at the giving power conditions for each increase step. Then the values needed were selected in order to start applying the experiment. Then around 5 minutes was the waiting time to let the machine match the giving voltage and current values, after that the Start button was clicked to start running the experiment then finally the XRD results were saved.

*(TUT,2018) (UW)*

### **3.4 Thermogravimetric Analyzer (TGA)**

TGA is a chemical test instrument uses to analysis the characterize materials tested mass sample over the time with changing the temperature (Coats, 1963). The internal calibration weights and parallel guided balances guarantee unsurpassed accuracy. The multi star TGA sensors has six different thermocouples amplifies the measurement signals and thereby increases the sensitivity. The TGA works of modular concept, which is different sensor and gas box options easily changeable depending on the tested materials. TGA provides chemisorption, thermal decomposition, phase transitions and many other information about the tested samples *(C&R, 1963)* (Figure 16). The Thermogravimetric analyzer evaluates the material mass change over a given temperature range of heating. Analyses polymers and ceramics tested *(Luuk J.P, 2011) (S. n.d.) (J. Fink)*.



*Figure 16: Thermogravimetric analyzer (U, 2012).*

To set up the TGA instrument, first the air was turned on the maximum flow since the teapots will be surrounded by air not nitrogen. Then, the “Pyris Manager” was selected from the computer screen. After that the TGA instrument was turned on and the “Pyris Manager” was clicked on the top of the computer screen. Then the sample information was filled, which are the sample ID, Operator ID, Comment, File Name, Directory. Then the Program tab was clicked and the Initial Temperature, Final Temperature, Rate of the temperature increases, and Seconds between points, for testing the experiment were entered. Then the temperature on the right edge was set at 3-4 degrees below your initial temperature enter to be 37<sup>0</sup>C. Then, the small testing container was placed on the testing plate. Then, on the computer screen, Module Control Window was clicked, and then the experiment file was right clicked then the Auto option and

Pan were choosing, then OK was clicked. After that the sample DSC, TG, P1, P2, PG have appeared on the screen of the computer which represents the weight and some other important information of the tested sample. Then the tested Pure Purple Clay Powder was loaded into the sample crucible. Then, the experiment was started by clicking on the Start button. The results of the experiment were collected and saved on the computer desktop. These steps were applied on the other two samples which are the Non-Sintered Purple Clay, and Sintered Purple Clay (A.n,d).

### **3.5 X-Ray Fluorescence spectroscopy (XRF)**

XRF is a chemical instrument that measures the elemental composition of a tested sample (Stanford, 2015). X-ray fluorescence spectroscopy works on measuring the elemental composition and getting helpful information about the tested sample by measuring the energy and the intensity of its characters of the x-ray radiation that comes out of the tested material during the relaxations process (Viguerie, 2009) X-ray fluorescence spectroscopy emits sufficient x-ray radiation to the tested sample, so that the tested sample will interact with the atoms inner shell electrons causing some kicked out atoms, almost immediately a relaxation process takes a place where one of the outer shell electrons falls into the inner shell, as a result a specific amount of energy is released. The energy of the emitted X-ray depends on the energy difference between the higher and lower states and therefore the radiation also carries information about the atom (Stanford, 2015) (Viguerie, 2009) (Figure 17). The X-ray fluorescence spectroscopy determines the materials composition of the tested sample element as well as the chemistry of the tested sample, measures the sample fluorescent, and provide the elements of the tested sample quantities. (X, n.d).



*Figure 17: X-ray fluorescence spectroscopy (F, 2018).*

The tested samples which were pure purple clay powder, non-sintered purple clay, sintered purple clay were grinded by a lab grinder to be powder in order to easily test them (Figure 18). Five mg of each of the tested samples were grinded and placed in three different containers. Then the pure purple clay powder was the first sample to test. Therefore, the XRF top cover was opened, and the first sample was placed carefully on a special holder then the top cover was closed to start the experiment. After that the experiment started running. The X-ray fluorescence spectroscopy started emitting x-ray radiation to the sample atoms to excite them. Then the results chart is partially appearing, after waiting until the experiment finished the results spectrum is eventually obtained and appeared. (O, 2009).



*Figure 18: laboratory grinder (T, 2009).*

### **3.6 Inductively Coupled Plasma Optical Emission Spectrometer (ICP-OES)**

ICP-OES is divided into two parts, the first part is the Inductively Coupled Plasma and the second part is the Optical Emission Spectrometer (*DMW, 2002*). The tested sample introduced with peristaltic pump into a nebulizer then to a torch, so the nebulizer turns the tested samples into tiny droplets then the sample goes into an argon plasma which is extremely hot and get emitted by the coil to produce plasma which atomizes and excites the tested sample molecules to a higher state to emit light which gives special information about each metal (*DMW, 2002*). Then the light goes to the second part which is the Optical Emission Spectrometer. The light gets separated by prisms and grating so the detector measures the intensity of the light. The intensity of the light shows how much of each metal is in there, and the identity of the metal can be shown from the wavelength (*R, G,H, &B, 1982*). The Inductively coupled Plasma Optical Emission Spectrometer detects the chemical elements, metals, and several non-metals at concentrations as low as one part in  $10^{15}$  on non-interfered low-background

isotopes. It works by measuring the wavelengths and the lights of the emitted x-ray (DMW, 2002).



*Figure 19: Inductively Coupled Plasma Optical Emission Spectrometer (ICP-OES) (S, 2015).*

The testing containers which are plastic teapot (Figure 10A), glass teapot (Figure 10B), porcelain teapot (Figure 10C) purple clay teapot (Figure 10D), and stainless-steel teapot (Figure 10E) were cleaned by DI water and then placed in an oven under 60<sup>0</sup>C for around 15 minutes to be will dried. Then the boiler pot was cleaned using DI water. After that 2 liters of DI water were poured in the boiler pot and the water started heating. The containers were gotten out dry, clean, and ready to use. 100 ml of boiling DI water was poured in each container. After waiting 5-minute, 20 ml of each container was poured in different testing tube as ready samples. Then after waiting for 24 hours, 20 ml of each container was poured in different testing tubes as ready samples. Then the containers were cleaned by DI water and dried in oven under 81<sup>0</sup>C and placed for around 20 minutes. The containers were well cleaned, dry, and ready to be used. Around 2

Liters of DI water was poured in the boiler pot and start boiling. Then 2g of green tea was placed in each container. After that 100 ml of boiling DI water was poured in each container. After waiting for 5 minutes, 20 ml of each container was poured in different testing. Then after waiting for 24 hours, another 20 ml of each container was poured in different testing tubes and saved for the ICP-OES tests. Finally, the prepared samples for testing are water purple clay 5 minutes, water purple clay 24 hours, green tea purple clay 5 minutes, green tea purple clay 24 hours, green tea plastic 24 hours, green tea stainless steel 24 hours, green tea glass 24 hours, green tea porcelain 24 hours.

A diluent of nitric acid and an internal standard were prepared. The internal standard was added to the blank standard. On the screen of the computer the location of the 8 samples stock standards was listed. Then the experiment was started. After that the results appeared on the screen (Elmer, P. 1998).

As a part of the ICP-OES experiment a pure DI water and a pure green tea were tested in order to know the chemical elements that contained in both samples. 500 ml of pure DI water was boiled using a water boiler. Two clean flasks were prepared by placing 2 mg of green tea in one of them and the second one was empty. Then 100 ml of boiling DI water was poured in both flasks. Both flasks were closed up and stored for 24 hours. After 24 hours, 20 ml of each samples were taken for ICP-OES testing as pure DI water, and pure green tea.

### **3.7 pH test**

In addition to the ICP-OES experiment, many pH tastings of the green tea were applied in order to compare the different pH results of different green tea containers. The pH test was applied in total of 10 samples. Two samples of each container were taken in different times, the

first sample was taken after 5 minutes, and the second sample was taken after 24 hours. All samples were placed in different tubes and names of each sample was labeled on them.

After ensuring the temperature of each sample to be below 25 degrees Celsius, the protective cap that is attach to the electrode of the pH meter was removed. Then the electrode was washed using a DI water then dried using a clean tissue and filtration papers. After that the Cal button on the meter was pressed. Then the pH/mV button was pressed to appear the pH results on the screen of the meter when testing. Then the pH electrode was dipped in the first sample tube and the result appears on the screen of the pH meter. Then the electrode was cleaned and washed using DI water. And the steps were repeated for the rest of the samples.

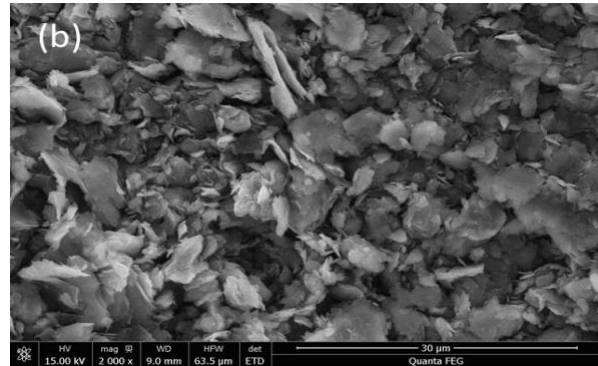
# CHAPTER FOUR: RESULTS AND DISCUSSION

## 4.1 Scanning Electron Microscope (SEM)

In order to get further information on the surface structures of the powder, non-sintered and sintered phase respectively, SEM experiments have been conducted. Both the tested sample and the corresponding experimental results are listed below.



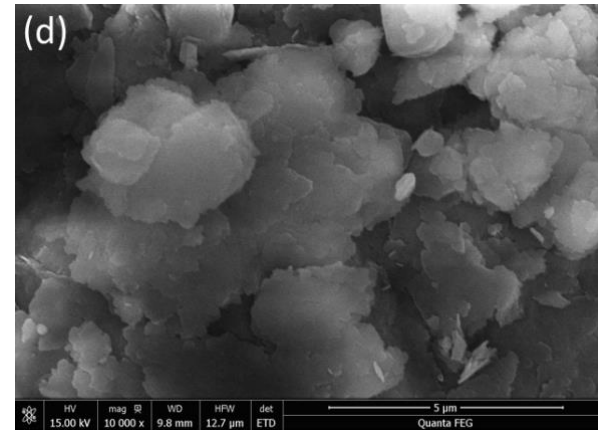
20(a): Powder phase of test sample.



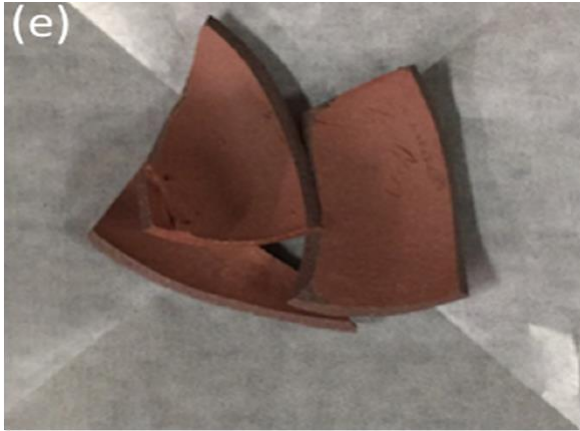
20(b): Morphology of powder phase.



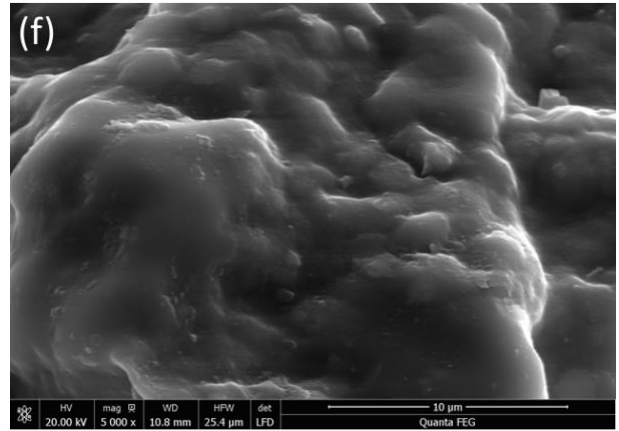
20(c): Non-sintered phase of test sample.



20(d): Morphology of non-sintered phase.



20(e): Sintered phase of test sample.



20(f): Morphology of sintered phase.

Figure 20: Corresponding morphology pictures of the SEM test.

As the pictures show in figure (20b), the morphology of the powder phase presented a relatively irregular form. The lamellar surface of the powder sample existed in the form of rolled sheets and distributed in an unpredictable pattern (Brindley, G). Spongy mica was detected in figure (20b) which probably results in the soil environment. Also, the relatively hot and humid weather might also become one of the factors of the characteristic of the powder clay sample. The patch formation of the impurities was also detected. Further experiments need to be conducted to analyze the composition of the impurities.

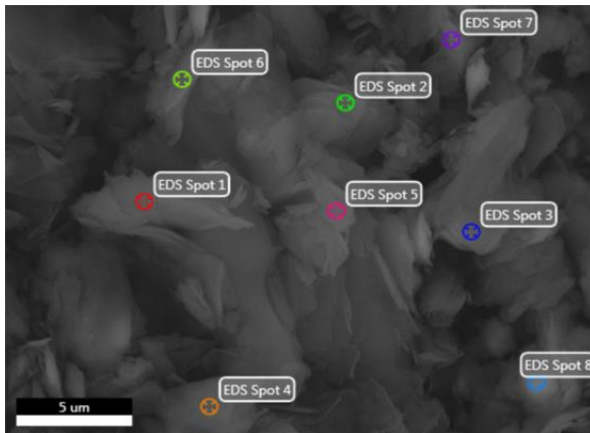
In the case of the figure (20d), the non-sintered phase has presented an amorphous structure. The powder particles are not of a uniform size, and they seem to exhibit a sheet-like structure. After sintering which is shown in the figure (20f), the densification is basically completely realized, and substantially no pores are formed.

In the phase of pre-sintering, the pattern is in the configuration of a sheet. There are single pieces and laminations. Although the surface structure still shows the pattern of flakes after firing, the flaky particles are connected together. Both the number of single pieces and the gap between the particles are significantly reduced after the firing. During the process of

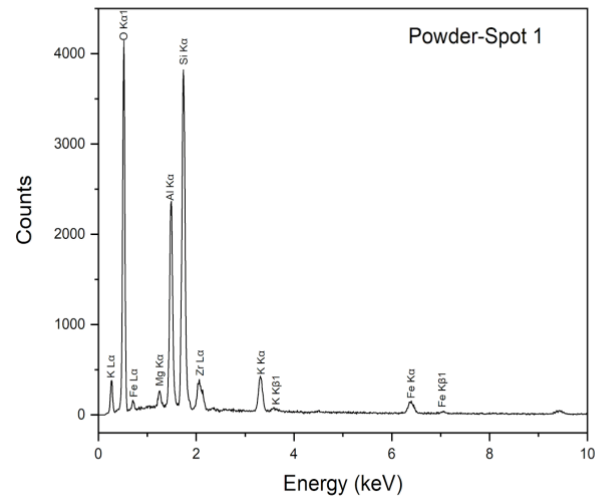
sintering, the hydroxyl group is removed from the sample which results in the distortion of the crystal lattice and the expansion of the agglomeration.

## 4.2 Energy Dispersive X-ray spectroscopy (EDX)

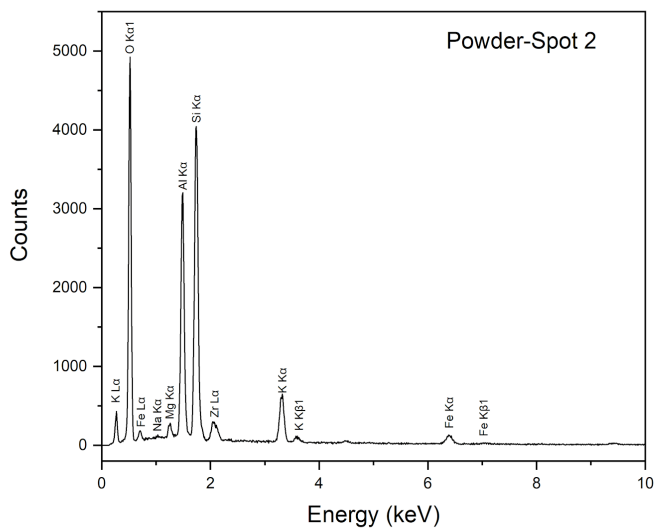
The SEM results have provided a fundamental understanding of the surface structure of each sample. In order for a semi-quantitative element results, energy-dispersive x-ray spectroscopy (EDX or EDS) was conducted at the location of interest. The X-ray radiations were practiced on the powder, non-sintered, and sintered sample respectively to detect the chemical elements that emitted. Each sample has multiple spots where they differ in terms of elements peaks due to the different emission of the elements that came out from the sample from each spot. The spectrum peaks and EDX results were presented in figure (21,22,23). Further information can be found in the **Appendix A, B and C**.



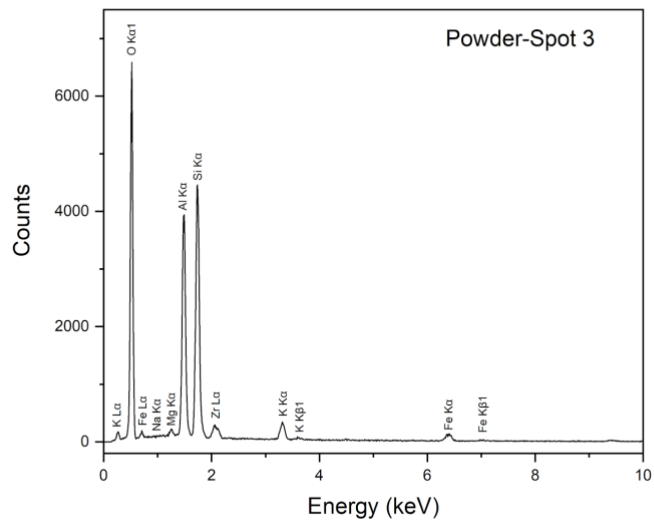
21(a): Selected EDX test location of powder phase.



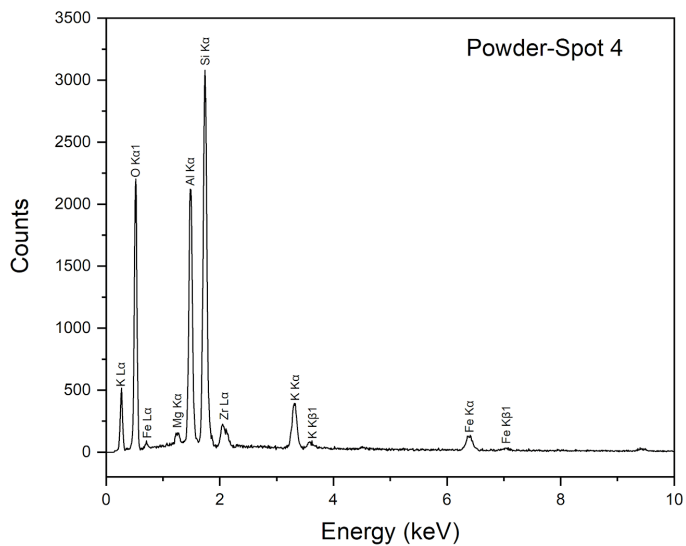
21(b): EDX spectrum at spot 1.



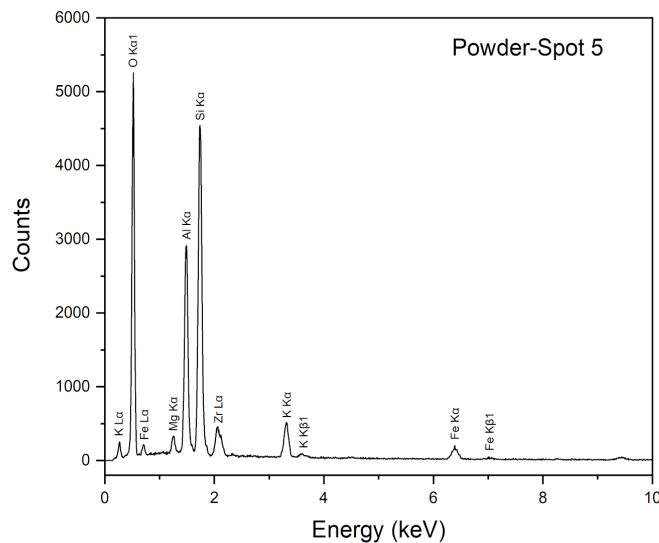
21(c): EDX spectrum at spot 2.



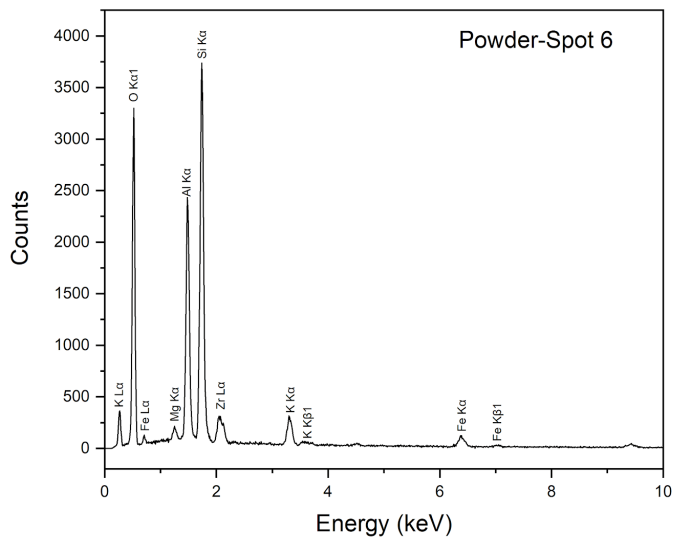
21(d): EDX spectrum at spot 3.



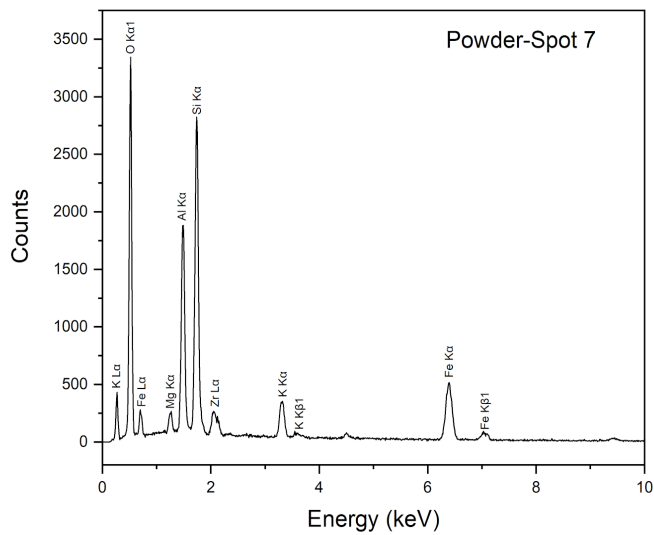
21(e): EDX spectrum at spot 4.



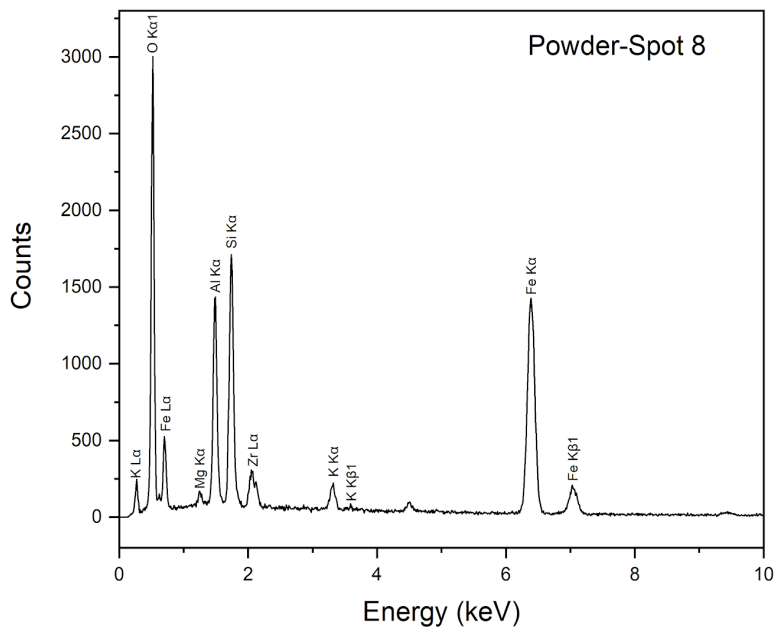
21(f): EDX spectrum at spot 5.



21(g): EDX spectrum at spot 6.



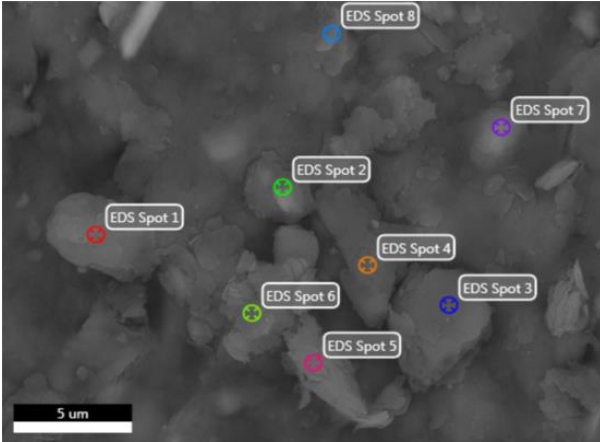
21(h): EDX spectrum at spot 7.



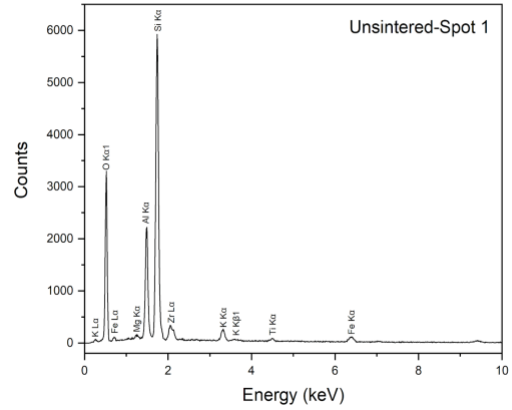
21(i): EDX spectrum at spot 8.

Figure 21: The powder EDX and elements peaks in different spots.

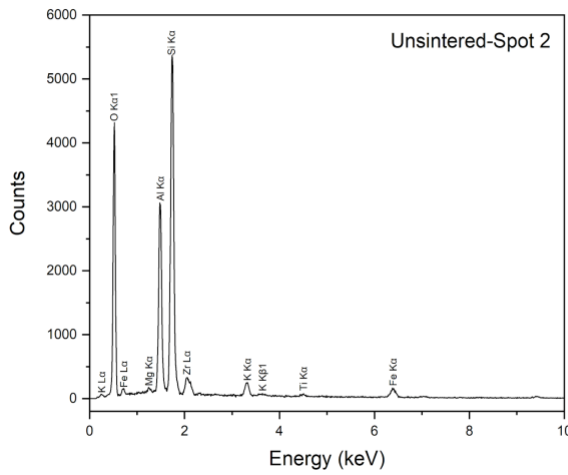
EDX spectrum of the powder phase in figure 21 shows a great amount of (SI)Silicon and (Al) Aluminum and a minor amount of Manganese, potassium, and iron in the selected 5 $\mu$ m spot.



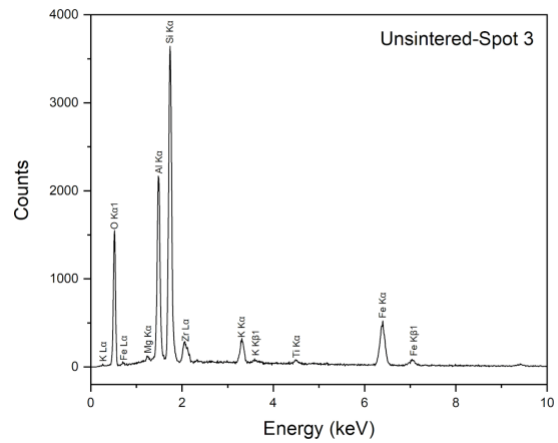
22(a): Selected EDX test location of non-sintered phase.



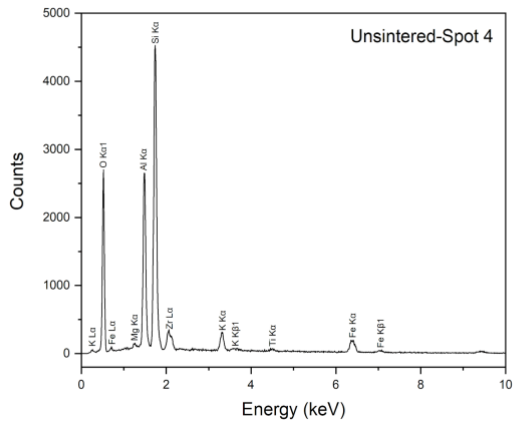
22(b): EDX spectrum at spot 1.



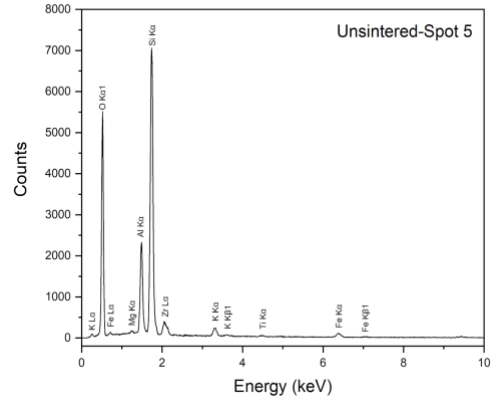
22(c): EDX spectrum at spot 2.



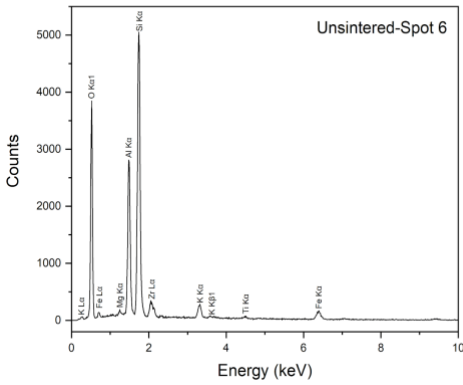
22(d): EDX spectrum at spot 3.



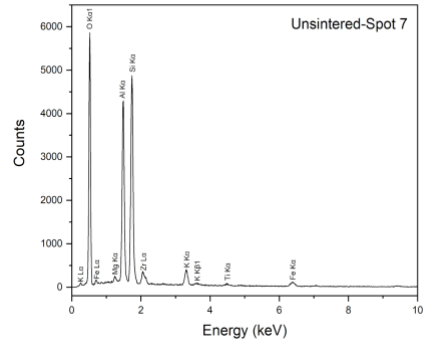
22(e): EDX spectrum at spot 4.



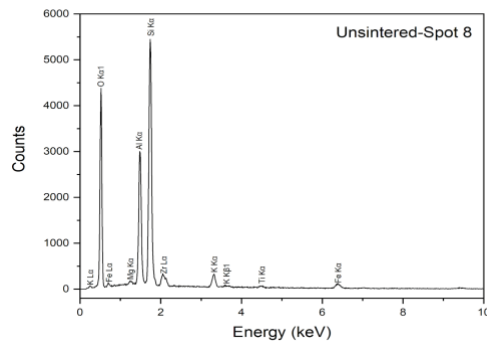
22(f): EDX spectrum at spot .5



22(g): EDX spectrum at spot 6.



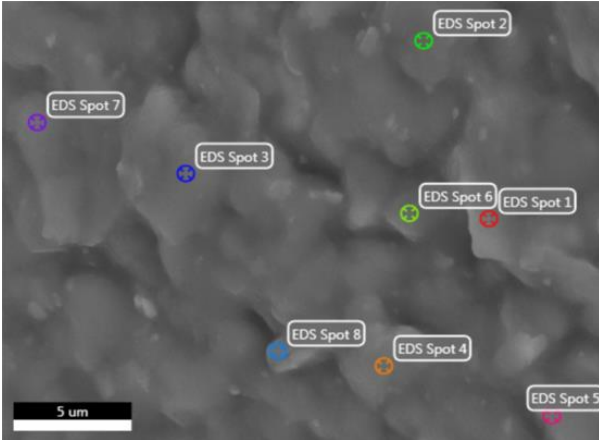
22(h): EDX spectrum at spot 7.



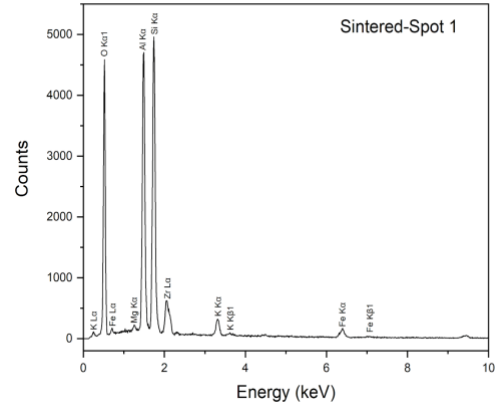
22(i): EDX spectrum at spot 8

Figure 22: The non-sintered EDX and elements peaks in different spots.

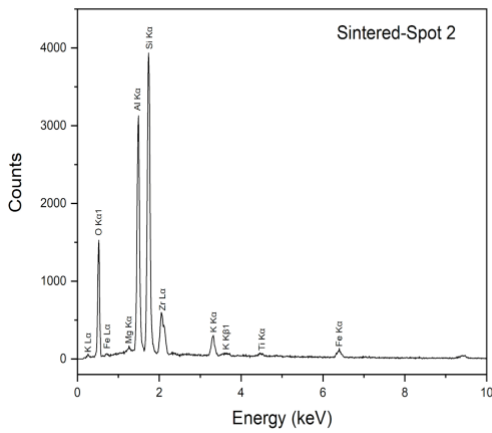
EDX spectrum of the powder phase in figure 22 shows a great amount of Si and Al and a minor amount of Mn, K, and iron in the selected 5 $\mu\text{m}$  EDX spot. The oxygen's peak ratio of the first spot is much smaller than the peak in the second spot.



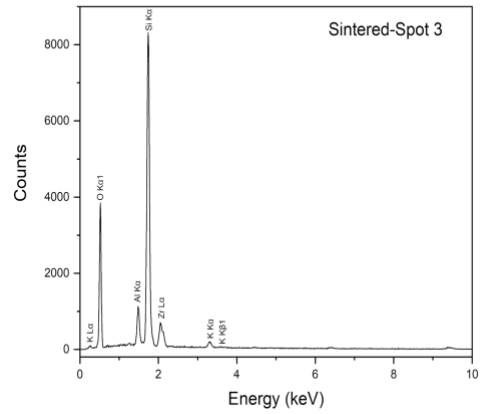
23(a): Selected EDX test location of sintered phase



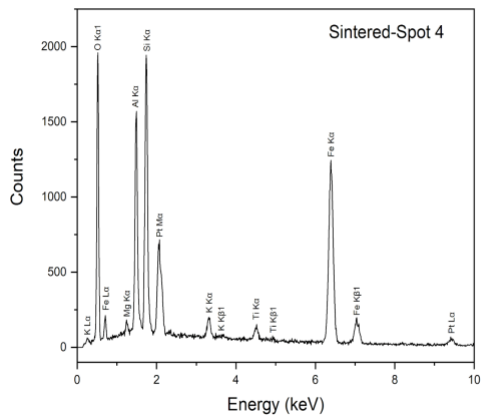
23(b): EDX spectrum at spot 1.



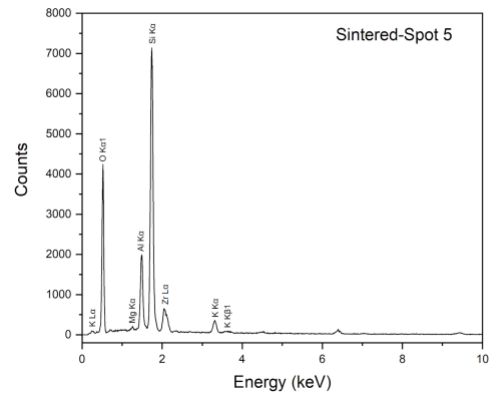
23(b): EDX spectrum at spot 2



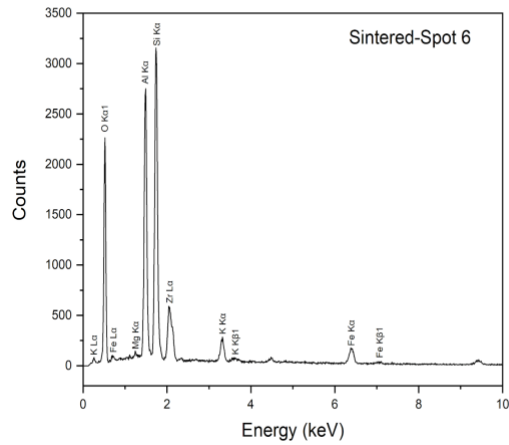
23(c): EDX spectrum at spot 3.



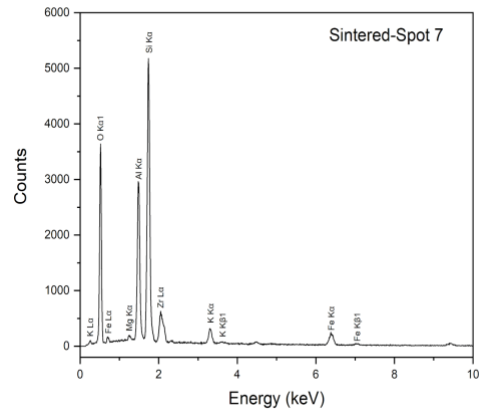
23(d): EDX spectrum at spot 4



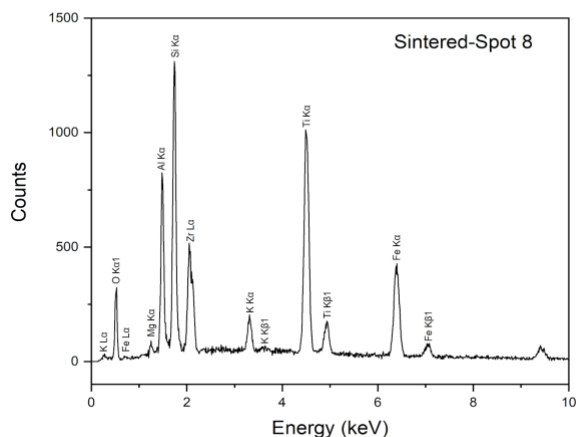
23(e): EDX spectrum at spot 5



23(f): EDX spectrum at spot 6



23(g): EDX spectrum at spot 7



23(i): EDX spectrum at spot 8

Figure 23: The sintered EDX and elements peaks in different spots.

EDX spectrum of the powder phase in figure 23 shows a great amount of Si, Al, and Fe. A minor amount of Mn, K, (Ti) titanium, and (Pt) platinum was also observed in the selected 5 $\mu$ m EDX spot.

From all three EDX graphs, oxygen has taken a great portion which was due to the early stages of creating teapots. The amount of oxygen tends to decrease from the powder form to the non-sintered form which results in the time-costed method of bailing. The oxygen gets recovered after the sintering procedure. Silicon also takes a large percentage among all the three samples. The amount of silicon dramatically increases from powder phase to non-sintered phase. Other coated elements including Fe, Ti, Mn, and Pt were the potential coating composition. The presence of Zr samples may result from the existence of Pt since the similarity between those two elements.

### 4.3 Thermogravimetric Analyzer (TGA)

The results of the EDX test didn't provide enough information about the detailed composition of the purple clay teapot. In order to get a full picture of the stability and oxidative

capability of the composition property, the thermal gravimetric analysis was conducted which generally measures the rate of mass change over variable temperature.

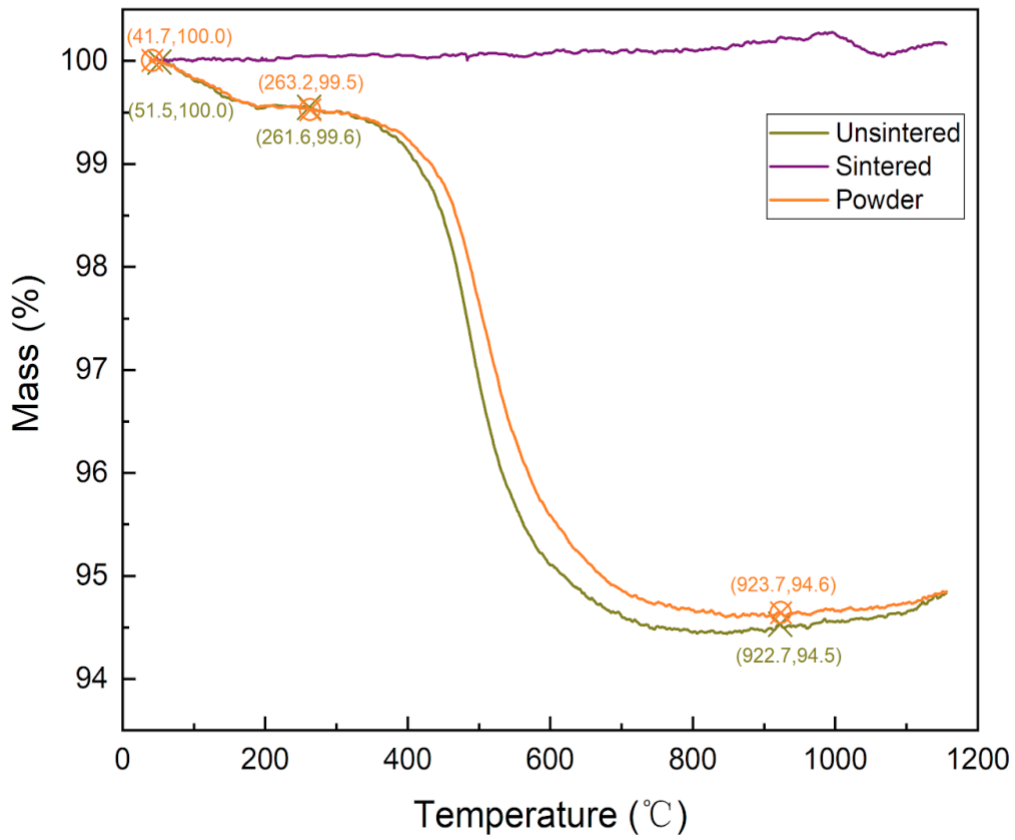


Figure 24: The total results of the Sintered, non-sintered, pure purple clay powder for the TGA test.

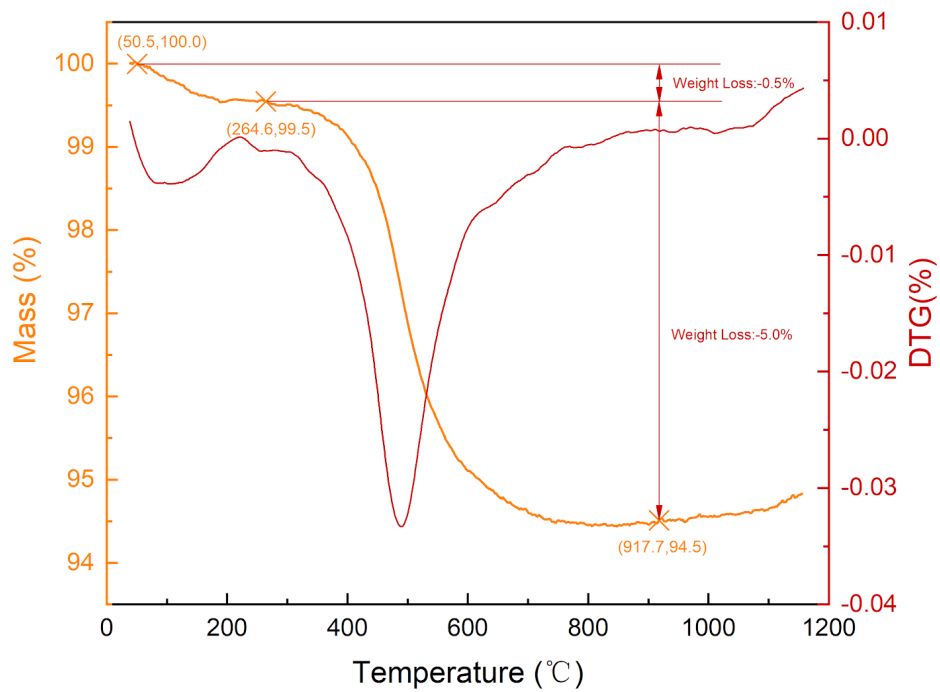


Figure 25: TGA graph of powder sample.

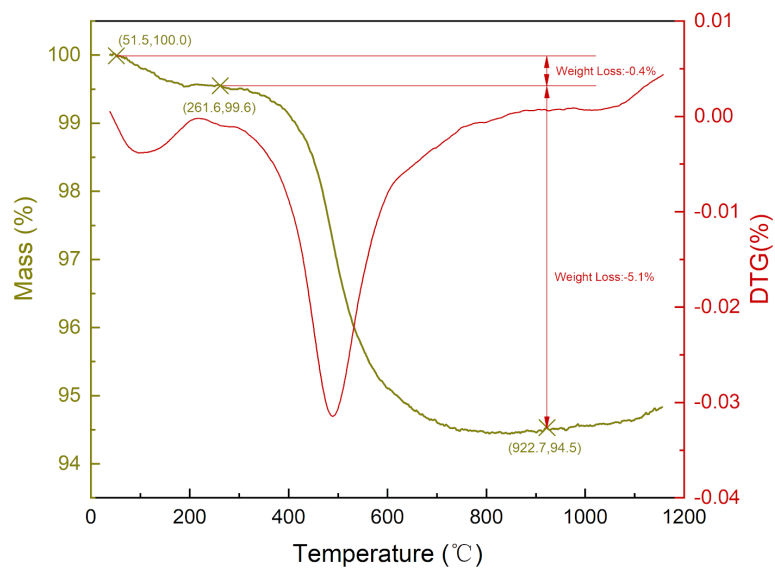
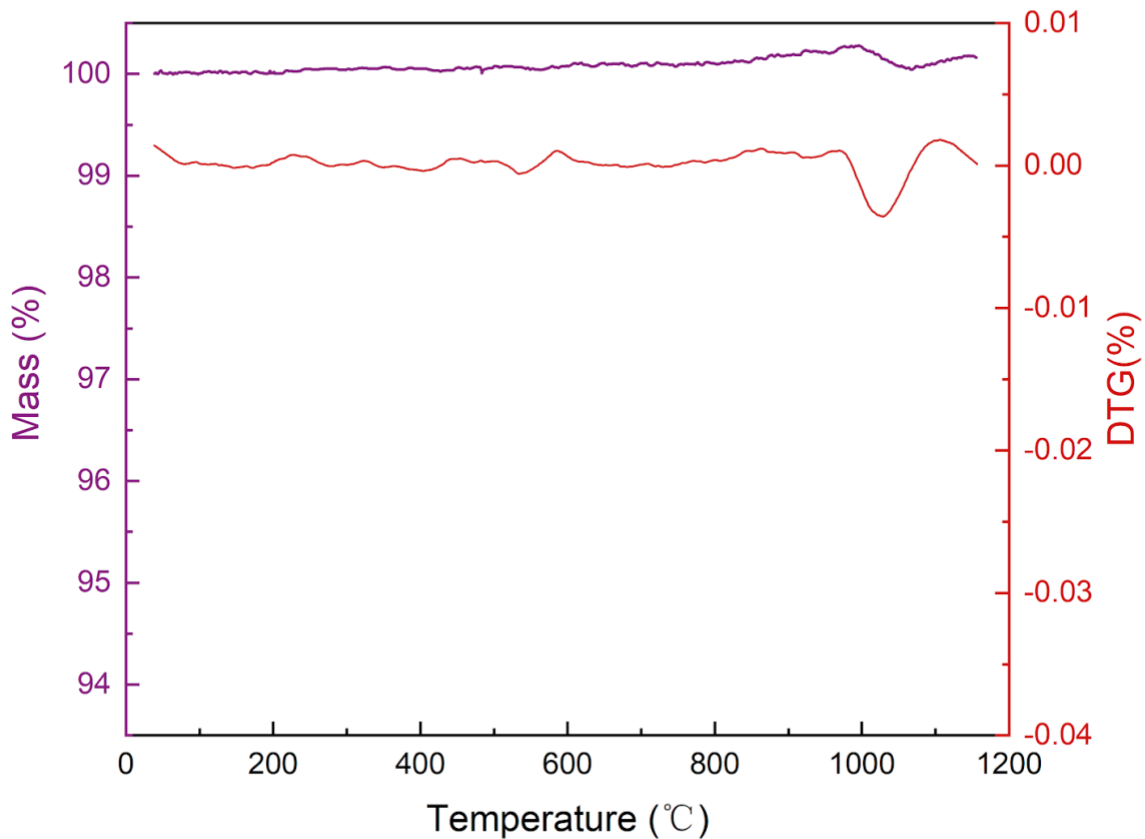


Figure 26: TGA graph of non-sintered sample.



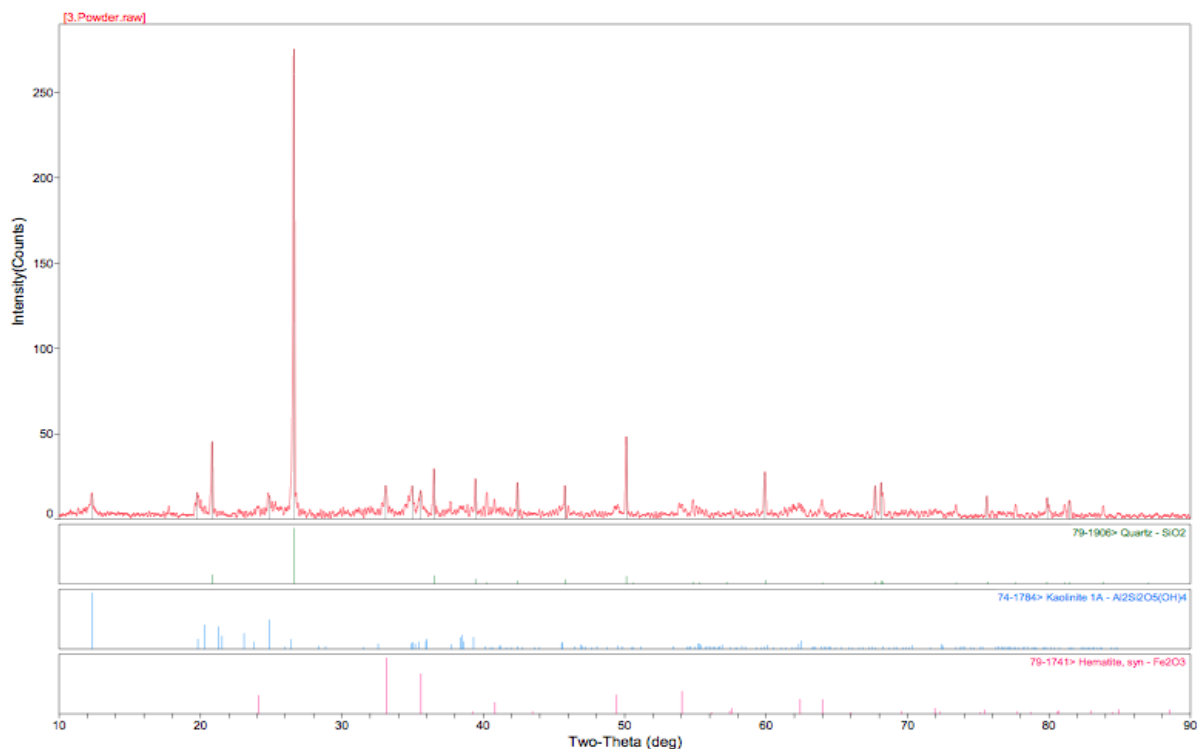
*Figure 27: TGA graph of sintered purple clay sample.*

From the diagram there's generally weight loss due to increase in temperature, but there are two major drops on weight for the non-sintered and powder samples. The weight loss is at two different temperature: the first one is at 100<sup>0</sup>C which is related to free water loss (Free water evaporation) which can be attributed to water present in the structural channels. The second one is at 500<sup>0</sup>C and it is due to structural water loss which means both samples have humidity in their structures. Therefore, the total loss of the free water was about 0.5% in both samples. However, the structural water loss reached about 5.5% of the total mass. On the other hand, the sintered sample did not show any major loss in weight. The reason behind that is the sintered sample has

been heated during the scintillation process of making the teapot, which means mostly all the water molecules have been evaporated during the scintillation process indicating the absence of humidity in its structure.

#### 4.4 X-ray Diffraction (XRD)

After obtaining the TGA results which provide a general picture of the thermal activity of the chemical property within the purple clay sample, the x-ray powder diffraction test was conducted to classify the crystal phase of the sample.



Materials Data, Inc.

[VIVIAN-LAB\Myron]\C:\Users\Myron\Desktop\WPI 2018\XRD> Wednesday, Jul 18, 2018 10:11p (MDI\JADE6)

Figure 28: XRD graph of pure purple clay powder sample.

The X-ray diffraction (XRD) patterns of samples were obtained on an RU-200B/D/MAX-RB X-ray diffractometer with Cu K $\alpha$  radiation ( $\lambda=1.5406 \text{ \AA}$ ) generated at 40 kV and 40 mA from 10°C to 90°C at a scanning speed of 4°/min<sup>-1</sup>.

Figure (28) is depicted the XRD spectra of the pure purple clay powder. It can be found that the values of significant peaks match well with the peaks of quartz (Silicon dioxide) (JCPDS Card No.79-1906), kaolinite 1A (JCPDS Card No.74-1784) and hematite (JCPDS Card No.79-1741). The sharp and intense peaks located at  $2\theta=20.8^\circ$ ,  $26.6^\circ$ ,  $36.5^\circ$  and  $50.1^\circ$  are assigned to quartz, which corresponds to the crystal face of (100), (011), (110) and (112) respectively. The peaks at  $12.3^\circ$ ,  $19.7^\circ$  and  $24.8^\circ$  result from kaolinite 1A, corresponding to (001), (020) and (002) crystal face. The detection of the peaks at  $33.1^\circ$  and  $35.6^\circ$  indicate the presence of hematite and correspond respectively to its crystal face of (104) and (110).

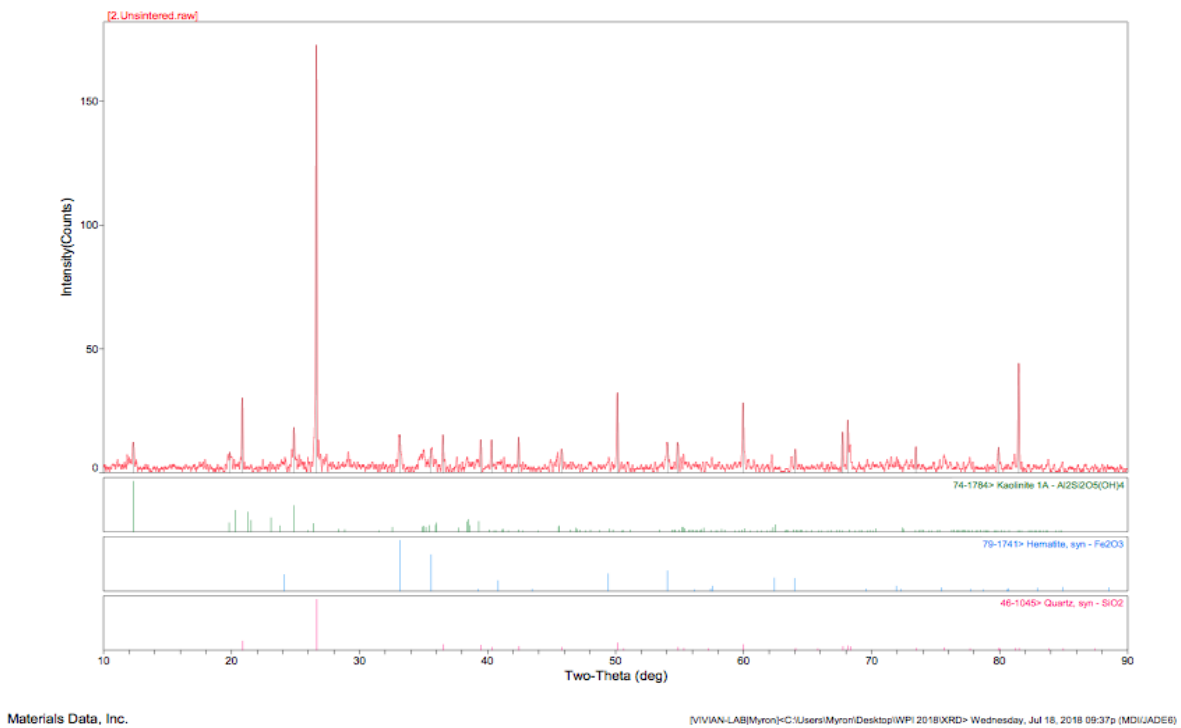
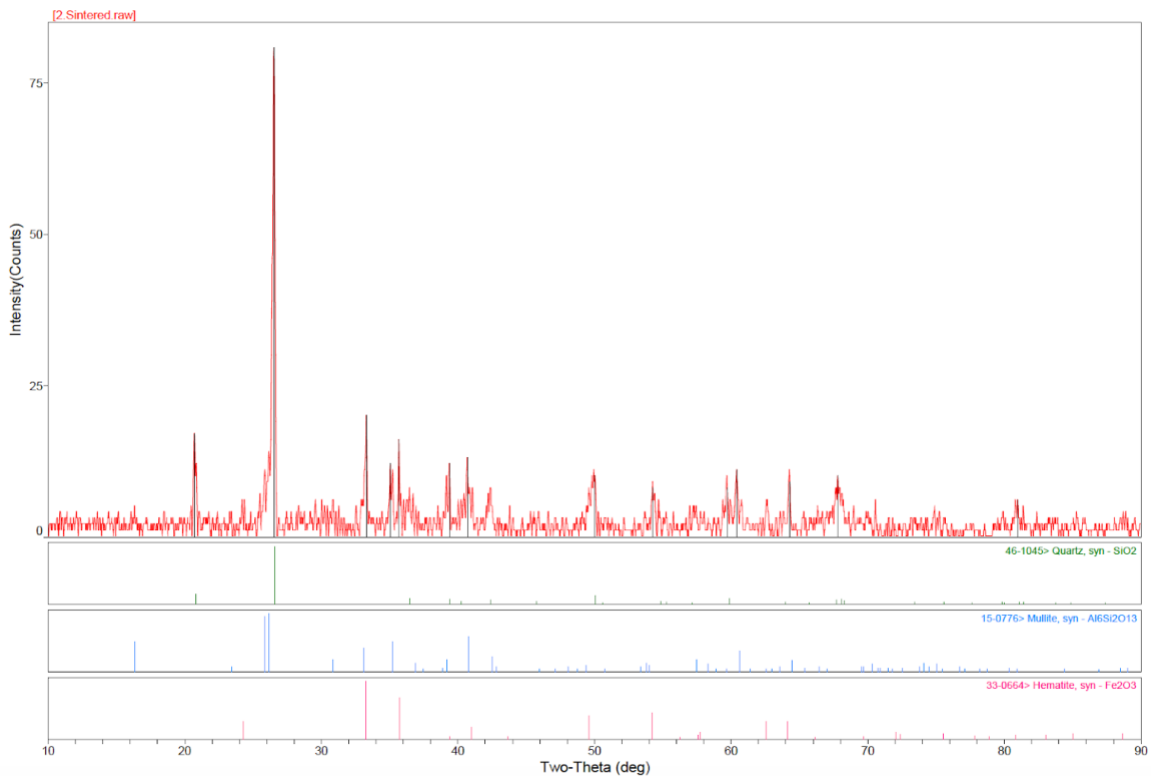


Figure 29: XRD graph of non-sintered sample.

The result of X-ray Diffraction pattern in Figure 29 showed that the main phase composition of the non-sintered purple clay includes quartz (JCPDS Card No.46-1054), kaolinite 1A (JCPDS Card No.74-1784) and hematite (JCPDS Card No.79-1741). The sharp diffraction

peaks at  $2\theta=20.9^\circ$ ,  $26.6^\circ$ ,  $36.5^\circ$  and  $50.1^\circ$  correspond to the (100), (011), (110) and (112) crystal face of quartz respectively. The observed peaks at  $12.3^\circ$ ,  $19.8^\circ$  and  $24.9^\circ$  result from kaolinite 1A, correspond respectively to its crystal face of (001), (020) and (002). The detection of the peaks at  $33.1^\circ$ ,  $35.6^\circ$  and  $54.0^\circ$  indicate the presence of hematite, resulting from the crystal face of (104), (110) and (116) respectively.



*Figure 30: XRD graph of sintered sample.*

The result of X-ray Diffraction pattern in Figure 30 showed that the main phase composition of the sintered purple clay includes quartz (JCPDS Card No.46-1054), mullite (JCPDS Card No.15-0776) and hematite (JCPDS Card No.33-0664). The sharp diffraction peaks at  $2\theta=20.6^\circ$ ,  $26.5^\circ$ ,  $50.0^\circ$  and  $67.8^\circ$  correspond to the (100), (101), (112) and (212) crystal face of quartz respectively. The observed peaks at  $25.9^\circ$ ,  $26.2^\circ$ ,  $35.1^\circ$  and  $40.7^\circ$  result from mullite, correspond respectively to its crystal face of (120), (210), (111) and (121). The detection of the

peaks at  $33.3^\circ$ ,  $35.7^\circ$  and  $54.3^\circ$  indicate the presence of hematite, resulting from the crystal face of (104), (110) and (116) respectively.

Silicon dioxide has a generally chemical equation of  $\text{SiO}_2$  and is often found within quartz and other living bodies. Often appears as transparent solid, Silicon dioxide has a melting point at  $1713^\circ\text{C}$  and boiling point at  $2950^\circ\text{C}$ . Serving as major composition of sand, other silicon dioxide related materials play important roles in the field of manufacturing or food industry. Although studies have shown that orally injection of Silicon dioxide is nontoxic and can effectively decrease the chance of dementia, breathing in finely isolated crystalline silica is lethal and can prompt serious irritation of the lung tissue, silicosis, bronchitis, lung malignancy, and foundational immune system infections, such as lupus and rheumatoid joint pain.

Wildly known as a dirt mineral, Kaolinite, with a chemical formula of  $\text{Al}_2\text{Si}_2\text{O}_5(\text{OH})_4$ , is related to the family of constructional mineral. It is a layered silicate mineral, with one tetrahedral sheet of silica ( $\text{SiO}_4$ ) connected through oxygen molecules to one octahedral sheet of alumina ( $\text{AlO}_6$ ) octahedra. Rocks that are wealthy in kaolinite are known as kaolin or china clay. With a relatively low shrink-well limit and cation exchange limit, kaolinite is a delicate, natural, generally white, mineral (decahedral phyllosilicate mud), created by the synthetic weathering of aluminum silicate minerals like feldspar. Besides China, Kaolinite also shows the color of pink-orange-red under the effect of iron oxide. Other unique colors also include white, yellow or light orange depends on the concentration.

Serving as the mineral form of iron oxide, hematite is one of the most common iron minerals which exists mainly in rocks and soils. Having a similar crystal structure as ilmenite and corundum, Hematite crystallizes in the rhombohedral lattice system. Moreover, Hematite can also form a complete solid solution at temperatures above  $950^\circ\text{C}$  along with ilmenite.

Large portions of hematite are often detected in banded iron. The variety of hematite also leads to a different characteristic. For instance, the present of gray hematite can be easily traced with still water or mineral hot springs. Since the mineral can be found as the sediment at the bottom of the water, it is relatively easy to collect. Other cases such as the volcanic activity can also induce the presence of hematite. Often appears as the secondary mineral product via weathering processes in soil, clay-sized hematite can form reddish colored soils which mostly occurred in tropical or ancient areas with the help of other iron oxides and oxyhydroxides.

#### **4.5 X-Ray Fluorescence spectroscopy (XRF)**

Due to the lack of information derived from the previous EDX test, X-ray fluorescence test was operated for the determination of the composition property in elemental phase.

<b>Elements</b>	<b>Pure Purple Clay Powder concentration %</b>	<b>Purple Clay Non-Sintered concentration %</b>	<b>Purple Clay Sintered concentration %</b>
<b>O</b>	<b>52.373</b>	<b>45.362</b>	<b>50.697</b>
<b>Si</b>	<b>21.062</b>	<b>24.293</b>	<b>22.149</b>
<b>Al</b>	<b>17.095</b>	<b>19.095</b>	<b>16.312</b>
<b>Fe</b>	<b>3.529</b>	<b>4.361</b>	<b>4.161</b>
<b>K</b>	<b>2.583</b>	<b>2.854</b>	<b>2.603</b>
<b>Mg</b>	<b>2.201</b>	<b>1.583</b>	<b>1.434</b>
<b>Ti</b>	<b>0.730</b>	<b>0.957</b>	<b>1.014</b>

<b>Na</b>	<b>0.186</b>	<b>0.241</b>	<b>0.440</b>
<b>Ca</b>	<b>0.150</b>	<b>0.220</b>	<b>0.221</b>
<b>P</b>	<b>0.053</b>	<b>0.061</b>	<b>0.116</b>
<b>Zr</b>	<b>0.020</b>	<b>0.025</b>	<b>0.011</b>
<b>S</b>	<b>0.014</b>	<b>0.042</b>	<b>0.057</b>
<b>Sr</b>	<b>0.004</b>	<b>0.006</b>	<b>0.006</b>
<b>Ba</b>	<b>-----</b>	<b>0.892</b>	<b>0.778</b>

*Table 2: Concentration of non-oxide elements.*

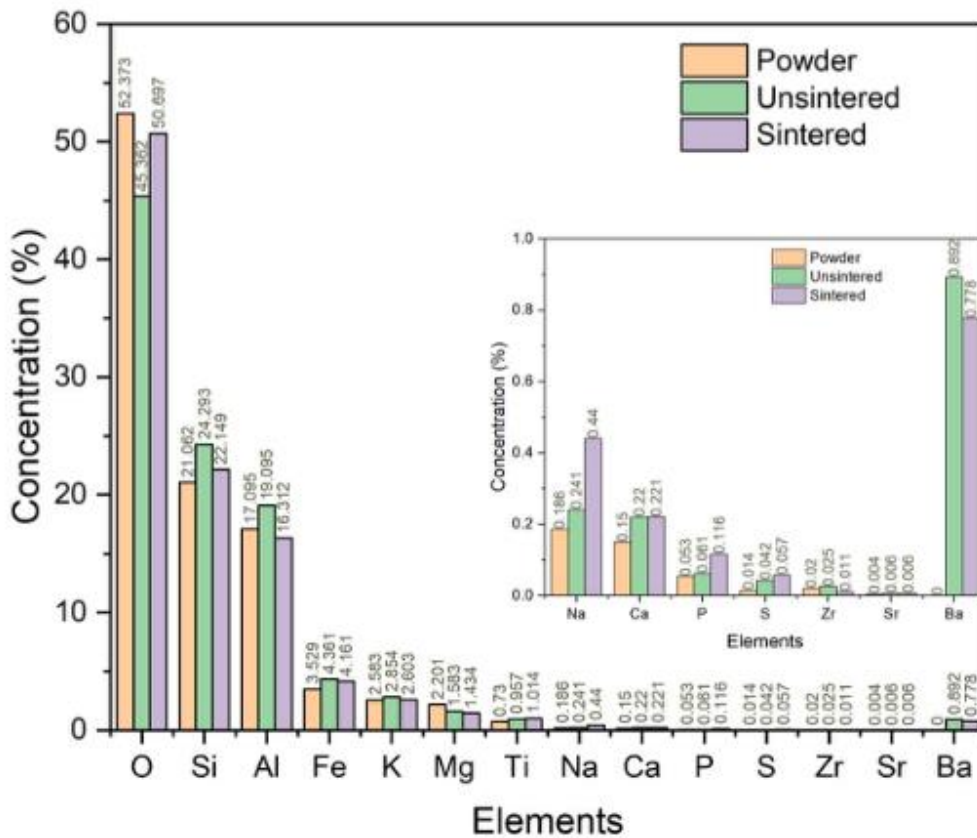


Figure 31: Element concentration distribution within the pure powder purple clay, non-sintered and sintered samples.

It is shown by the non-oxide element (Table 2) and distribution graph (Figure 31) that Oxygen got reduced by 7% after it transformed from a pure powder phase to non-sintered phase. During the process of the conversion, which in this case is the process called bailing, manual mud uses the artificial wooden pestle to practice foot treading or uses rolling stones to protect it from rotting. The sample experienced intensive pressing which ultimately leads to the decreasing of the oxygen. And the concentration of oxygen went back to 50% after the sample was sintered. The heating and the scintillating process helps the sample to get back its oxygen concentration. Al got slightly increased by 2% from the pure powder sample compared to the non-sintered sample which is due to the substance that was added during the process. Same reason in the case

of Si which is increased by 2.2% after bailing; however, both of the elements got reduced during the heating process. It was believed that the lost elements were oxidized.

The element Ba did not experience any concentration change since it was introduced to the process later on. Its concentration only shows in the non-sintered and sintered phase. The remaining elements including Sr, Zr, Fe, Ti, Ca, K, S, P, Mg, and Na did not experience dramatically concentration change.

#### 4.6 Inductively Coupled Plasma Optical Emission Spectrometer (ICP-OES)

Sample Numbers	Sample Shortcut Name
Purple clay, water, 5-min	PC-W5
Purple clay, water, 24-h	PC-W24
Purple clay, green tea, 5-min	PC-G5
Purple clay, green tea, 24-h	PC-G24
Plastic, green tea, 24-h	PL-G24
Iron, green tea, 24-h	I-G24
Glass, green tea, 24-h	G-G24
Porcelain, green tea, 24-h	PO-G24

*Table 3: Corresponding shortcut name for testing sample.*

After reviewing the XRF results to find the harmful elements for the human being, Barium (Ba), Chlorine (Cl), Strontium (Sr), and Aluminum (Al) (M.n.d.) were selected for further testing. The selection criteria were explained as followed:

Though no existing studies show the toxicity of the barium element in the metal form, barium related compound can be harmful. Studies have shown that low measurements of Ba can induce muscle stimulant and higher measurements can even induce dysfunctional nerve system.

Since the presence of Ba was added through the bailing process, there's no guarantee that after the bailing procedure the teapot wasn't contaminated.

The classification of Al is in the non-carcinogen catalog due to the current experimental results of having barely any toxic effect on human health. But considering the high portion of Al metal, it is necessary to conduct the ICP-OES test on Al as well.

In the case of Sr, although its high reactivity and the hazardous effect of its isotope can post a huge problem, the majority of Sr is pretty stable. Possessing a similar structure of Calcium makes Sr tend to cause mineral bone growth problems. Thus, it's still necessary to conduct the ICP-OES test on Sr.

As one of the most recognized elements in the halogen group, Cl was known for its high reactivity and bleaching capability. The history of using chlorine as chemical weapons during the first World War has already demonstrated the toxicity of high concentration of Chlorine. Although it was believed that most of the chlorine was brought by the tea-leaf itself, further experiments such as the ICP-OES need to be conducted.

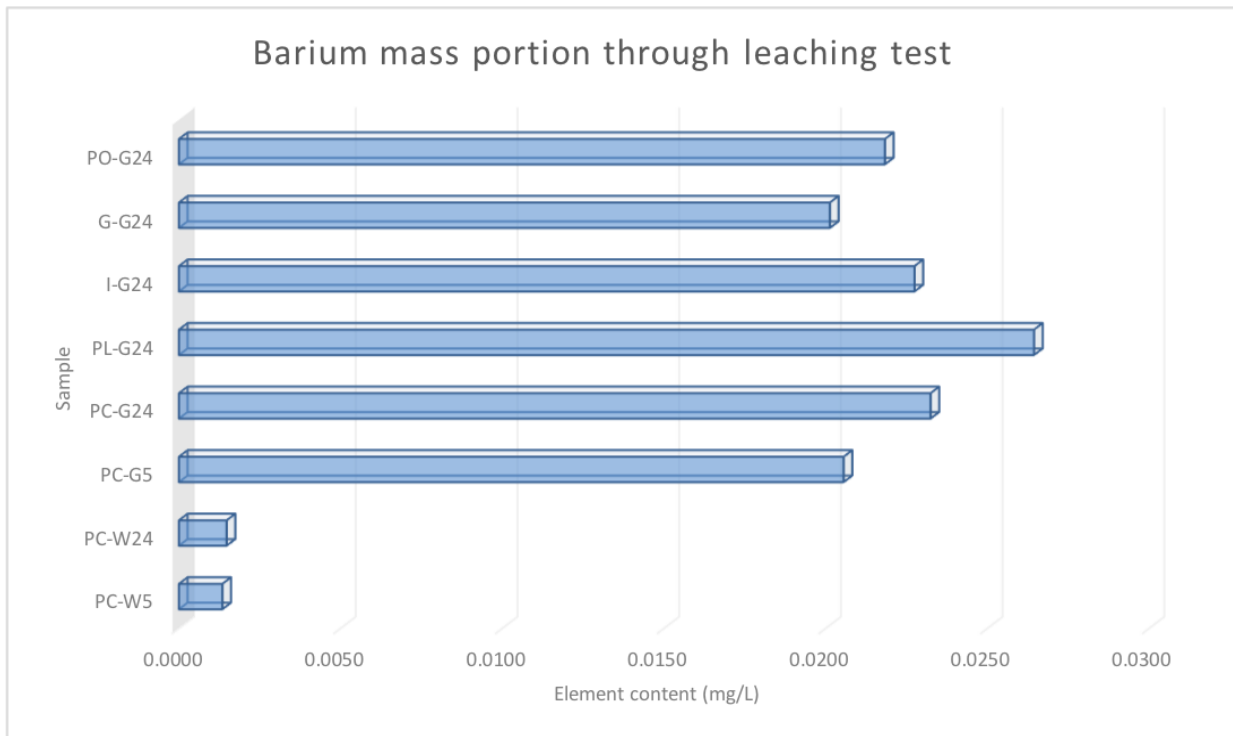


*Figure 32: Barium chart for the ICP-OES.*

As what is shown here in the Barium chart (Figure 32), that the highest amount of the harmful element Barium (Ba) for the green tea is stored at the Plastic container after 24 hours, while the lowest amount of the harmful element Barium for the green tea is in the glass after 24 hours and after that the Purple Clay after 5 minutes.

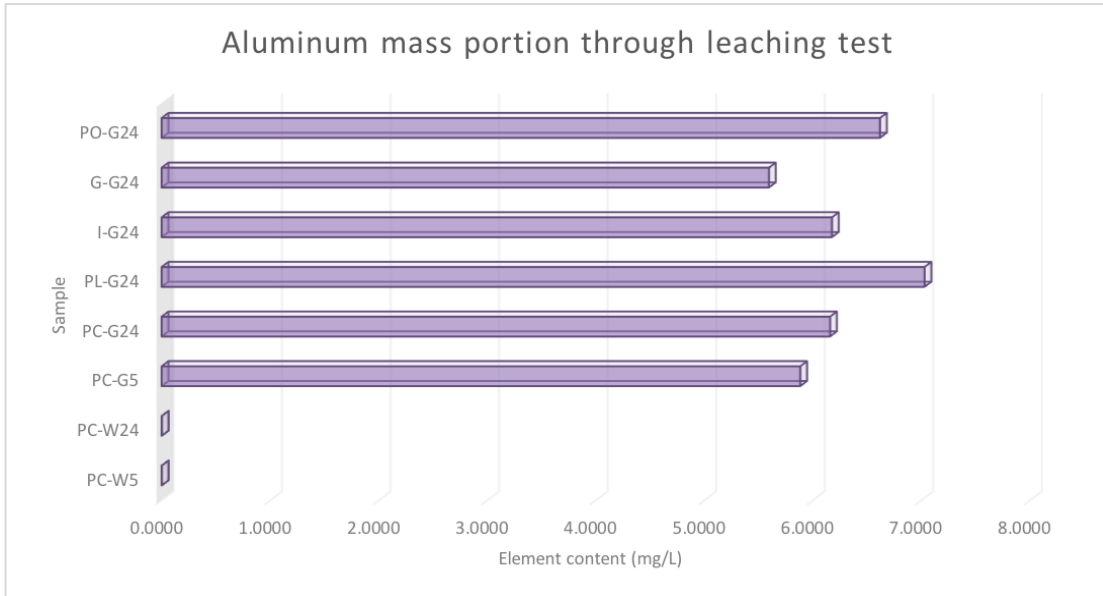


Figure 33: Barium chart for the ICP-OES.

As what it appears in the aluminum chart (Figure 33), that the lowest amount of the harmful element Aluminum (Al) for the green tea is stored in the glass container after 24 hours then the Purple Clay container comes to be the second least harmful to the green tea and 5 minutes, while the highest amount of the harmful element Aluminum Al for the green tea is in the plastic container after 24 hours and after that the porcelain container after 24 hours.

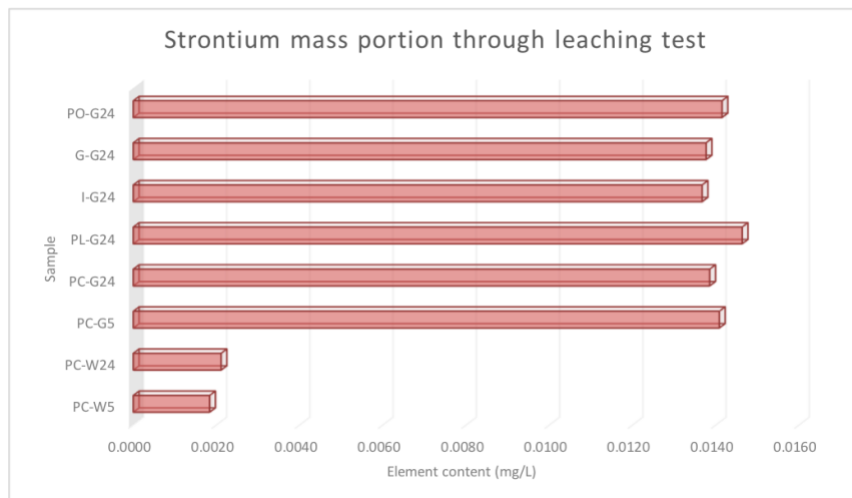


Figure 34: Strontium chart for the ICP-OES.

As what is provided here in the Strontium Sr chart (Figure 34), that the lowest amount of the harmful element Strontium (Sr) for the green tea is at the iron container after 24 hours then the second container is the Purple Clay which contains the least harmful Strontium (Sr) for the green tea and 24 hours, while the highest amount of the harmful element Strontium (Sr) for the green tea is stored in the plastic container after 24 hours then comes after that the porcelain container for the green tea after 24 hours.

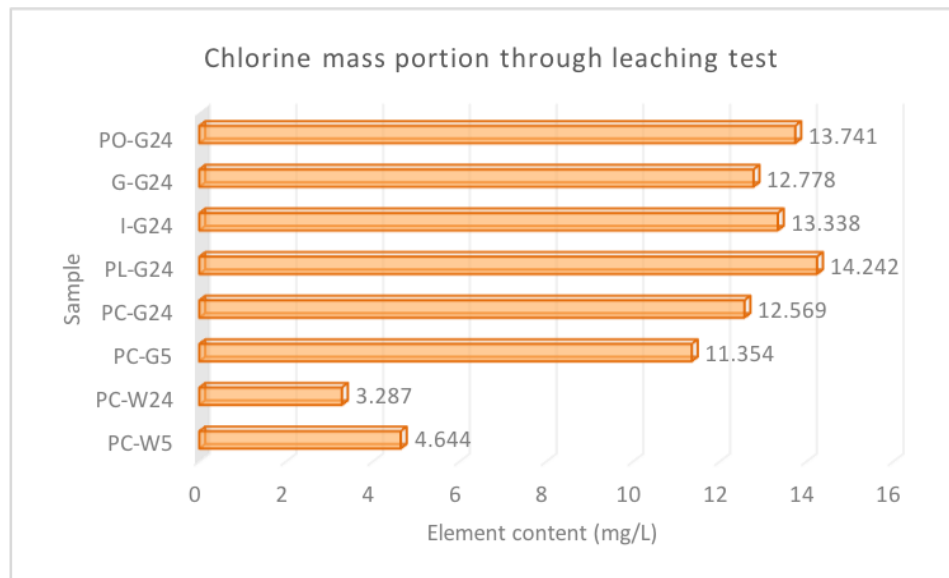


Figure 35: Chlorine chart for the ICP-OES.

As what is provided here in the Chlorine Cl chart (Figure 35), that the lowest amount of the harmful element Chlorine(Cl) for the green tea is at the purple clay container after 24 hours while the highest amount of the harmful element Chlorine (Cl) for the green tea is stored in the plastic container after 24 hours then comes after that the porcelain container for the green tea after 24 hours.

After comparing all those four selected elements experience data, it can be seen that among all the cases, purple clay container with water is the least toxic case. And the plastic container was the most hazardous. Thus, further ICP-OES test including the comparison of water and green tea needs to be conducted in order for reaching the final conclusion.

After reviewing the results from the first ICP-OES test, the green tea in all containers tends to contain a relatively large portion of Al, Sr, Ba, and Cl elements than the one with the water especially the glass pot. The material or the manufacturing process of the container were unknown at this moment since they were all sent by the sponsor. In order to eliminate the potential contamination to the final results. Lab glassware were used to conduct the second experiment. The green tea and the DI water were placed in the lab container for 24 hours. The final ICP-OES test results were listed below.

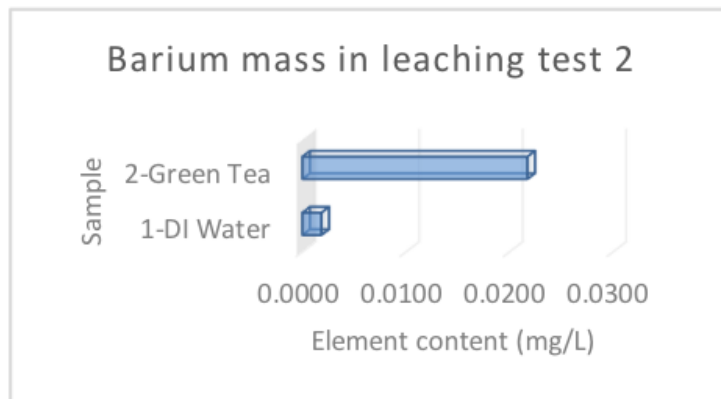


Figure 36: Barium chart for the ICP-OES test 2.

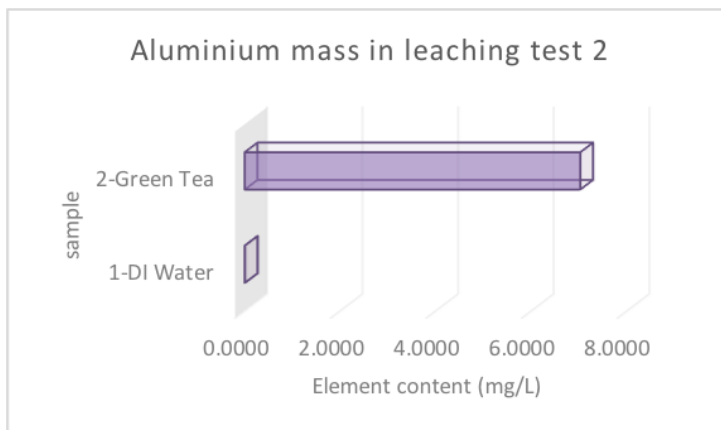


Figure 37: Aluminum chart for the ICP-OES test 2.

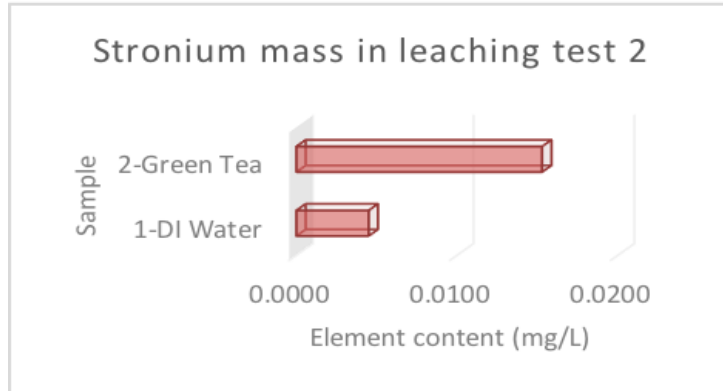


Figure 38: Strontium chart for the ICP-OES test 2.

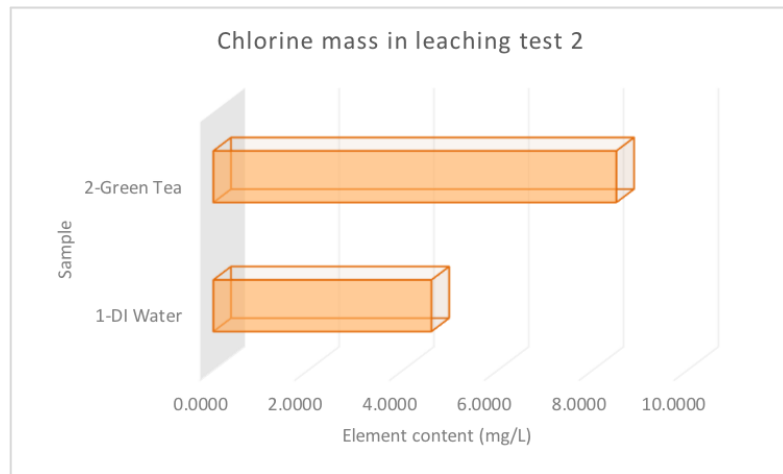


Figure 39: Chlorine chart for the ICP-OES test 2.

In order to testify the presence of harmful elements after leaching test, ICP-OES experiment two was conducted. As what is presented here in the Barium chart (Figure 36), Aluminum chart (Figure 37), Strontium chart (Figure 38), and Chlorine chart (Figure 39), green tea tends to separate out more elements than the DI water under the same circumstance within 24 hours. With the existing test results, the possibility of the side effect of purple clay container can be eliminated.

#### 4.7 pH value measurement

The original intention of the pH test is to evaluate the acidity of the green tea solution. All the groups show the value of sub-acidity. Although it has long believed that the use of green

tea had certain health treatment effect, recent studies have reported certain harmful effects of concentrated GTE consumption on the liver (Graham,1992). Studies also show that the internal use of green tea can cause potential GI toxicity, hepatobiliary toxicity. (Hu, 2018) As we conducted in the last experiment, Aluminum took a large portion in the composition of tea solution as well as the teapot itself. From previous studies conducted by Fernandez-Calvino in 2008, green tea accounted for 25% of the Al solubility which ranked the third along with other types of teas. The characteristic that Metals tend to dissolve more in the acid environment can even increase the Al contained in the tea solution. The pH test was then operated on the testing samples of the ICP-OES experiment to get the acidity value.

<b>Containers</b>	<b>pH of 5 minutes</b>	<b>pH of 24 hours</b>
<b>Iron</b>	5.21	5.68
<b>Glass</b>	5.27	5.72
<b>Porcelain</b>	5.25	5.68
<b>Plastic</b>	5.22	5.74
<b>Purple clay</b>	5.79	5.75

*Table 4: pH experiment results of testing sample listed in ICP-OES experiment.*

From table 4, all of the testing samples showed a pH value of around 5 which indicates that after conducting the leaching test of both 5 mins and 24 hours, the solution appears to be acidic. The solution sample within the Iron, Glass, Porcelain and plastic container shows a level of increase after 24 hours. In contrast, the sample within the purple clay container displays a slight decrease in the pH value.

## CHAPTER FIVE: CONCLUSION AND RECOMMENDATIONS

This study focused on the specific characteristic of the purple clay teapot samples in pure powder, non-sintered, and sintered phases. Our literature study revealed that most of the existing studies on purple clay material were outdated. We hope to generate a more thorough database for further reference for following studies. A total of 7 sets of experiments were conducted. The SEM and EDX tests showed that the pure purple clay powder has a relatively irregular form compared to both non-sintered and sintered sample. The existence of metal elements including Fe, Ti, Mn, and Pt was observed along with the coating composition. Both the non-sintered and sintered sample displays layers over layers, the sintered sample tends to have built connections over each piece. Oxygen and silicon also took a large portion in the composition in all the three phases. TGA test has shown that besides the sintered sample, both the pure powder purple clay and non-sintered purple clay have experienced the loss of free water and structural water during heating. The sintered sample was heated during manufacturing process and does not contain water in its structure anymore. The XRD test displayed the crystal phase of the samples which indicates the existence of silicon dioxide, kaolinite, and hematite and a phase change in sintered sample that agreed with the SEM and TGA results. XRF test provided the detailed information on specific elements contained within the sample. From this list, four elements were identified as with potential detrimental health concerns. The leaching test, ICP-OES helped to testify the amount of elements extractions in tea in teapots of different materials. Without further information of the constitution of the given containers, we cannot jump into the conclusion after the first ICP test. The second ICP test demonstrated that the green tea itself may be the main sources of the larger amount of Barium, Aluminum, and Strontium than DI water. The pH test also showed that purple clay wares have a better capability of maintaining the pH value of the

solution. The use of purple clay teapot may better reserve the original taste of the tea solution. From previous studies, purple clay contained less amount of potentially harmful compound including caffeine or minerals (Liao, Z, 2018).

This study helps to demonstrate the benefit of using the purple clay wares. Though through the leaching test, ICP-OES, the extraction from the green tea solution contained in the purple clay wares showed a high concentration of metal and mineral elements, further studies help to justify that most of the extraction was brought by the green tea itself. In this case, the concentration extraction was largely dependent on the tea itself not the property of the containers. Testing various tea may help develop a better understanding of health effects by tea could be a future research topic.

## WORKS CITED

“中国地图矢量图。”卡通喜庆元宵佳节海报背景设计素材\_素材岛, 2018, [www.sucaidao.com/view-1-77612.html](http://www.sucaidao.com/view-1-77612.html).

5-37. doi:10.2307/4126583

79-86. doi:10.1007/s12665-009-0321-0

Accessed July 22th, 2018 <https://terebess.hu/english/yixing2.html>

Basics. Retrieved July 15, 2018, from

Bossler, B. (2002). *Shifting identities: Courtesans and literati in song china*. Harvard

Brindley, G. (1955). *The Structure and Morphology of a Kaolin Clay from Les Eyzies (France)*. *Clays and Clay Minerals*, 4(1), 61–66. doi:10.1346/CCMN.1955.0040109

*Bruker D8 Discover with I $\mu$ S 2-D XRD System*. Retrieved July 15, 2018, from <https://www.moles.washington.edu/maf/research-tools/d8-xrd-2/> (UW) U. (n.d.).

C. (n.d.). *Diffraction Chao Wang*. (2018, July 4). *Materials of Yixing Zisha Stoneware*. Lecture presented in China, Yixing.

*Chemical Technology of Thermogravimetric analyzer*. Retrieved July 24, 2018, from [http://www.nait.ca/program\\_home\\_76429.htm\(n.d.\)](http://www.nait.ca/program_home_76429.htm(n.d.)). chemistry. *PrevMed* 21:334–350 (1992)

Coat A E, and Redfern J P. *Thermogravimetric Analysis. A Review*. 1963, [adsabs.harvard.edu/abs/1963Ana....88..906C](https://adsabs.harvard.edu/abs/1963Ana....88..906C). (C&R, 1963).

Coats, B., & Donleavy, J. (n.d.). Retrieved August 5, 2018, from <http://pubs.rsc.org/en/Content/ArticleLanding/1963/AN/an9638800906#!divAbstract>

*Crystallography*. Retrieved July 15, 2018, from <http://www.utoledo.edu/nsm/ic/instruments/xray.html> and C. (2018, May 25). *Center for Materials and Sensor Characterization*. Retrieved July 15, 2018, from <http://www.utoledo.edu/engineering/cmsc/> (TUT, 2018) U. (2018, January 11).

De, L. O., Das, S., Da, E. S., Gao, P., Gress, J., & Liu, Y., et al. (2018). Metal concentrations in traditional and herbal teas and their potential risks to human health. *The science of the Total Environment*, 633, 649-657.

Determination of metals in wine with atomic spectroscopy (flame-AAS, GF-AAS and ICP-AES); a review. (n.d.). Retrieved July 23, 2018, from <https://doi.org/10.1080/02652030110071336> (DMW, 2002)

Dorland, L. M., Ms. (n.d.). Ms Lin Marvin-Dorland. Retrieved July 06, 2018, from <https://www2.le.ac.uk/departments/geology/analytical/semnew2> University Of Leicester (Dorland, L)

Dutrow, B. L. (n.d.). X-ray Powder Diffraction (XRD). Retrieved July 23, 2018, from [https://serc.carleton.edu/research\\_education/geochemsheets/techniques/XRD.html](https://serc.carleton.edu/research_education/geochemsheets/techniques/XRD.html) (D, BL)

elementary excitations. *Rev. Mod. Phys.* 83, 705 (2011) (Luuk J.P, 2011)

Elmer, P. (1998). Simplify Your ICP-OES Sample Preparation. Retrieved July 23, 2018, from [http://info.perkinelmer.com/4-16-AvioPrep3-NA-LP?utm\\_source=YouTube-PerkinEmer&utm\\_medium=social&utm\\_content=EH-PROMO-Q4-16-AvioPrep3-NA-2016Q4&utm\\_campaign=EH-PROMO-Q4-16-AvioPrep3-NA&utm\\_keyword=824](http://info.perkinelmer.com/4-16-AvioPrep3-NA-LP?utm_source=YouTube-PerkinEmer&utm_medium=social&utm_content=EH-PROMO-Q4-16-AvioPrep3-NA-2016Q4&utm_campaign=EH-PROMO-Q4-16-AvioPrep3-NA&utm_keyword=824)

*Environmental Earth Sciences*, 61(1),

F. (2018). Retrieved from [http://www.futurelabs.co.in/?page\\_id=28](http://www.futurelabs.co.in/?page_id=28)

Goldstein, J., Newbury, D. E., Michael, J. R., Ritchie, N. W., Scott, J. H., & Joy, D. C. (2018). *Scanning electron microscopy and x-ray microanalysis*. New York, NY: Springer. (J.Goldstein 2018).

Graham HN, *Green tea composition, consumption, and polyphenol*

Haswell, S.J., 1991. *Atomic Absorption Spectrometry; Theory, Design and Applications*. Elsevier, Amsterdam. (Haswell, S.J., 1991)<https://www.cif.iastate.edu/acide/xrd-tutorial/xrd> IOWA STATE UNIVERSITY (ISU)

Hu, J., Webster, D., Cao, J., & Shao, A. (2018). The safety of green tea and green tea extracts consumption in adults - results of a systematic review. *Regulatory Toxicology & Pharmacology Rtp*, 95. J. Fink et al. *Journal of Asiatic Studies*, 62(1),

L. (n.d.). *Scanning Electron Microscopy (SEM) with Energy Dispersive X-Ray Analysis (EDX)*. Retrieved July 23, 2018, from <https://www.lucideon.com/testing-characterization/techniques/sem-edx> (L. n.d.).

Litzinger, R. (n.d.). *Energy Dispersive X-ray Spectroscopy*. Retrieved July 15, 2018, from [www.cei.washington.edu/education/science-of-solar/energy-dispersive-x-ray-spectroscopy/](http://www.cei.washington.edu/education/science-of-solar/energy-dispersive-x-ray-spectroscopy/) CLEAN ENERGY INSTITUTE (Litzinger, R)

Liyong Pottery Co, L. (2018, June 28). *Basic knowledge of purple clay*. Reading presented in China, Yixing.

Luuk J.P. Ament et al. *Resonant inelastic x-ray scattering studies of*

M. (2018). *Lipton Green Tea*. Retrieved from [https://item.m.jd.com/product/859381.html?utm\\_source=iosapp&utm\\_medium=appshare&utm\\_campaign=t\\_335139774&utm\\_term=Wxfriends&ad\\_od=share&ShareTm=dlBZJyV9cuentq3o6T4QbYqF5G GHeZVx9iJEjvx kvw6gFaRAAtLzsDoEf7UNStJ3kUll PVxzm9Hsfhc98S5D9VYNDY4rGFniKeMyUZFLQJIXH K56dJ0Vx4QpOaGTXcLiRQezFI6mQfaoTQRufkIsCf6CS96Sm5jwSts1M=&from=singlemessage&isappinstalled=0](https://item.m.jd.com/product/859381.html?utm_source=iosapp&utm_medium=appshare&utm_campaign=t_335139774&utm_term=Wxfriends&ad_od=share&ShareTm=dlBZJyV9cuentq3o6T4QbYqF5G GHeZVx9iJEjvx kvw6gFaRAAtLzsDoEf7UNStJ3kUll PVxzm9Hsfhc98S5D9VYNDY4rGFniKeMyUZFLQJIXH K56dJ0Vx4QpOaGTXcLiRQezFI6mQfaoTQRufkIsCf6CS96Sm5jwSts1M=&from=singlemessage&isappinstalled=0)

M. (2018). Retrieved from [https://www.mt.com/es/es/home/products/Laboratory\\_Analytics\\_Browse/TA\\_Family\\_Browse/DSC.html](https://www.mt.com/es/es/home/products/Laboratory_Analytics_Browse/TA_Family_Browse/DSC.html)

M. (n.d.). *SAFETY DATA SHEET*. Retrieved July 27, 2018, from <https://www.sigmaaldrich.com/MSDS/MSDS/DisplayMSDSPage.do?country=US&language=en&productNumber=441899&brand=ALDRICH&PageToGoToURL=https://www.sigmaaldrich.com/catalog/search?term=Strontium&interface=Product Name&N=0 &mode=mode matchpartialmax&lang=en@ion=US&focus=productN=0 220003048 219853286 219853269>

M. (n.d.). *SAFETY DATA SHEET*. Retrieved July 27, 2018, from <https://www.sigmaaldrich.com/MSDS/MSDS/DisplayMSDSPage.do?country=US&language=en&productNumber=11009&brand=ALDRICH&PageToGoToURL=https://www.sigmaaldrich.com/catalog/search?term=aluminum&interface=All&N=0&mode=match partialmax&lang=en@ion=US&focus=product>

M. (n.d.). *SAFETY DATA SHEET*. Retrieved July 27, 2018, from <https://www.sigmaaldrich.com/MSDS/MSDS/DisplayMSDSPage.do?country=US&language=en&productNumber=474711&brand=ALDRICH&PageToGoToURL=https://www.sigmaaldrich.com/catalog/search?term=Barium&interface=All&N=0&mode=match partialmax&lang=en@ion=US&focus=product>

M. (n.d.). *SAFETY DATA SHEET*. Retrieved July 27, 2018, from <https://www.sigmaaldrich.com/MSDS/MSDS/DisplayMSDSPage.do?country=US&language=en&productNumber=295132&brand=ALDRICH&PageToGoToURL=https://www.sigmaaldrich.com/catalog/search?term=Chlorine&interface=All&N=0&mode=match partialmax&lang=en@ion=US&focus=product>

O. (2009). *Qualitative X-ray fluorescence analysis of powder samples*. Retrieved July 23, 2018, from <https://www.phywe.com/en/qualitative-x-ray-fluorescence-analysis-of-powder-samples.html>

*pressure/environmental scanning electron microscopy (VP-ESEM)*. Chichester, U.K.: Wiley. (D. Stokes, 2008)

Quorum Technologies. (2018). Retrieved July 15, 2018, from <https://www.quorumtech.com/quorum-product/q150r-rotary-pumped-sputter-coatercarbon-coater> (QT,2018)

R. (2016). Retrieved from <http://www.rocklandcountybusiness.com/business-products/x-ray-spectrometer.jsp>

*Resonant elastic soft x-ray scattering*. *Rep. Prog. Phys.* 76, 056502 (2013) (J. Fink, 2013)

Reynolds, R.J. et al.,1970. *Atomic Absorption Spectroscopy*. Barnes & Noble Inc., New York.(Reynolds, R.J. et al.,1970)

Rezaaiyaan, R., Hieftje, G. M., Anderson, H., & Meddlings, B. (1982). *Design and Construction of a Low-Flow, Low-Power Torch for Inductively Coupled Plasma Spectrometry*. Retrieved July 23, 2018, from <https://www.osapublishing.org/as/abstract.cfm?uri=as-36-6-627>

S. (2015). Retrieved August 8, 2018, from <https://ardec.ca/en/p/505/siatur-siasoft-abrasive-paper>

S. (n.d.). *Resonant X-ray Scattering*. Retrieved July 23, 2018, from <https://arpes.stanford.edu/research/tool-development/resonant-x-ray-scattering> (S. n.d.).

Santangelo, P. (1992). *Ming qing shidai yincha shenghuo 明清時代飲茶生活 / the world of tea during ming and qing dynasties* ÉDITIONS DE L'ÉCOLE DES HAUTES ÉTUDES EN SCIENCES

Schrenk, W.G., 1975. *Analytical Atomic Spectroscopy*. Plenum Press, New York. (Schrenk, W.G., 1975) SOCIALES.

Stokes, D. (2008). *Principles and practice of variable*

Swapp, S. (n.d.). *Geochemical Instrumentation and Analysis*. Retrieved July 23, 2018, from [https://serc.carleton.edu/research\\_education/geochemsheets/techniques/SEM.html](https://serc.carleton.edu/research_education/geochemsheets/techniques/SEM.html) , (S. n.d.).

T. (2009). Retrieved August 8, 2018, from <https://www.tokopedia.com/terasmedis/lumpang-alu-mortar-stamper-diameter-16-cm-porselen>

T. (2017). Retrieved from <http://cste.sut.ac.th/2014/?p=1920&lang=en> Tao Lu. (2018, July 5). *The History and Culture of Purple Clay Art*. Lecture presented in China, Yixing.

U. (2012). Retrieved August 8, 2018, from <https://www.selectscience.net/products/optima-8x00-icp-oes-spectrometers/?prodID=113734>

U. (2012). Retrieved August 8, 2018, from [https://www.utwente.nl/en/mechlab/thermal\\_characterization/Thermo-gravimetric analyser.whlink/](https://www.utwente.nl/en/mechlab/thermal_characterization/Thermo-gravimetric_analyser.whlink/)

Varma, A., 1985. *Handbook of Atomic Absorption Analysis. Vol. I.* CRC Press, Boca Raton. (Varma, A., 1985)

Viguerie, D. L., VA, S., & F, W. (2009, December). *Multilayers quantitative X-ray fluorescence analysis applied to easel paintings.* Retrieved July 23, 2018, from <https://www.ncbi.nlm.nih.gov/pubmed/19688344>

Wu, S., Zhou, S., Li, X., Johnson, W. C., Zhang, H., & Shi, J. (2010). *Heavy-metal accumulation trends in yixing, china: An area of rapid economic development.*

*X-Ray Fluorescence.* Retrieved July 23, 2018, from <https://colourlex.com/project/x-ray-fluorescence/> S. (2015, November).

*XRF Technology.* (n.d.). Retrieved from <https://www.thermofisher.com/us/en/home/industrial/spectroscopy-elemental-isotope-analysis/spectroscopy-elemental-isotope-analysis-learning-center/elemental-analysis-information/xrf-technology.html> (X, n.d)

# APPENDIXES

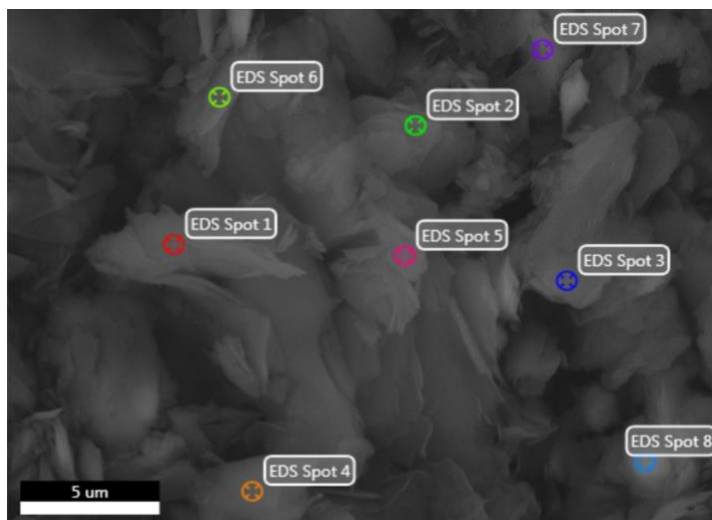
## A. EDX Pure Powder Sample Report EDAX TEAM

Page1

xiangxing

Author: edax  
Creation: 7/13/2018  
Sample Name: New Sample

### Area 1

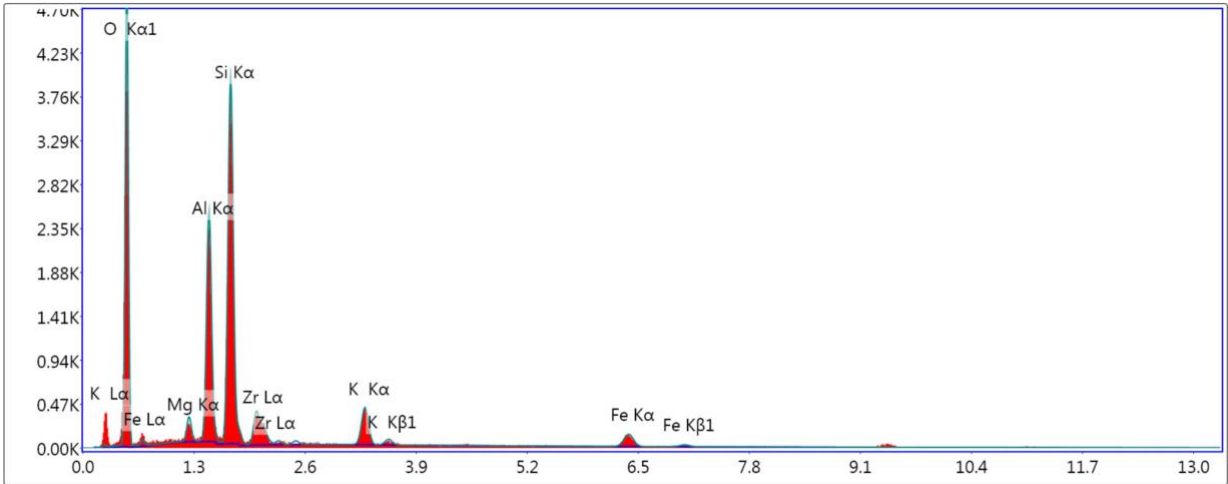


Notes:

EDS Spot 1

kV: 20      Mag: 5008      Takeoff: 6.2      Live Time(s): 30      Amp Time(μs): 3.84      Resolution:(eV)124

EDS Spot 1



Lsec: 30.0 0 Cnts 0.000 keV Det: Apollo X-SDD Det

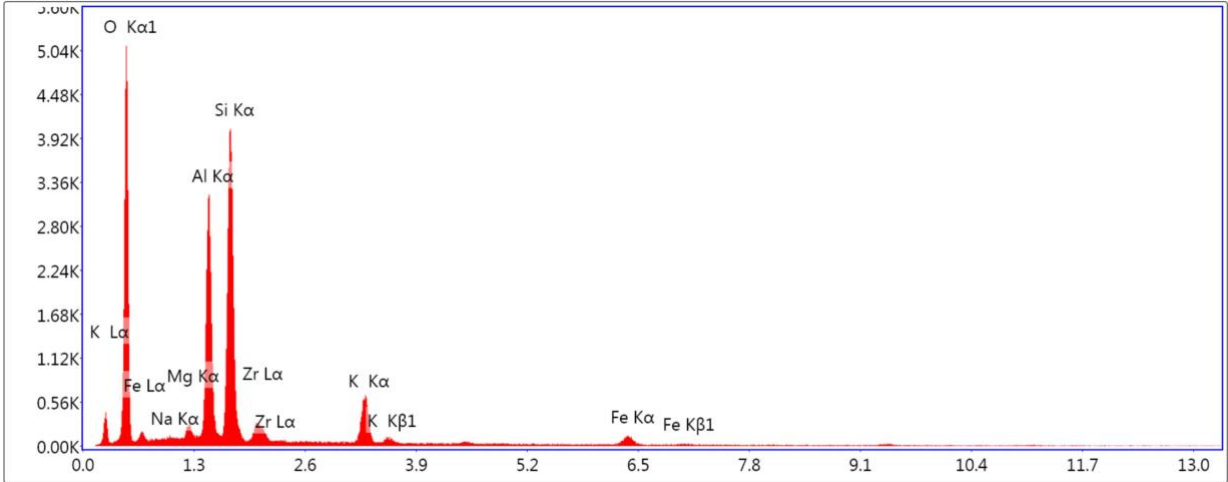
**eZAF Smart Quant Results**

Element	Weight %	Atomic %	Net Int.	Error %	Kratio	Z	R	A	F
O K	52.76	68.86	754.54	8.25	0.19	1.06	0.97	0.34	1
MgK	1.67	1.43	62.60	9.34	0.01	0.98	1	0.51	1.01
AlK	12.47	9.65	573.21	5.38	0.08	0.95	1.01	0.65	1.01
SiK	20.99	15.61	962.68	5.03	0.13	0.97	1.01	0.66	1
ZrL	4.58	1.05	86.15	9.02	0.03	0.75	1.2	0.79	1.01
K K	3.65	1.95	130.76	4.94	0.03	0.9	1.04	0.89	1
FeK	3.89	1.45	59.90	7.46	0.03	0.82	1.07	1	1

EDS Spot 2

kV: 20      Mag: 5008      Takeoff: 6.2      Live Time(s): 30      Amp Time(μs): 3.84      Resolution:(eV)124

EDS Spot 2



Lsec: 30.0 0 Cnts 0.000 keV Det: Apollo X-SDD Det

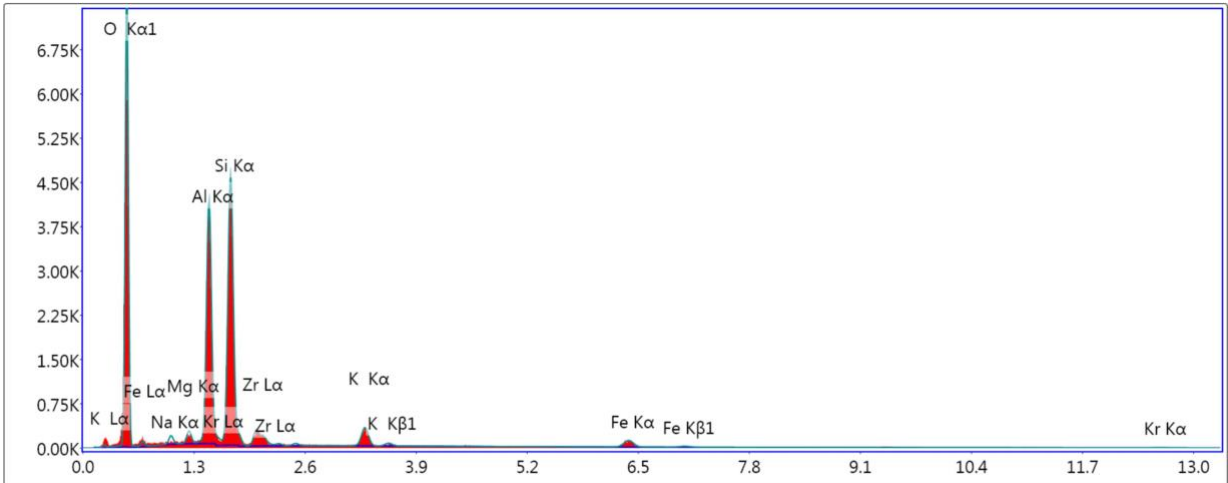
**eZAF Smart Quant Results**

Element	Weight %	Atomic %	Net Int.	Error %	Kratio	Z	R	A	F
O K	52.75	68.01	900.07	8.18	0.19	1.06	0.97	0.34	1
NaK	1.50	1.34	36.37	12.66	0.01	0.96	1	0.36	1.01
MgK	1.58	1.34	70.35	9.26	0.01	0.98	1	0.51	1.01
AlK	13.95	10.67	762.42	5.28	0.09	0.94	1.01	0.65	1.01
SiK	19.66	14.44	1,052.78	5.13	0.12	0.96	1.02	0.64	1
ZrL	3.09	0.70	69.38	9.58	0.02	0.74	1.21	0.79	1.01
K K	4.68	2.47	200.82	4.10	0.04	0.89	1.05	0.9	1
FeK	2.79	1.03	51.15	8.92	0.02	0.81	1.07	1	1

EDS Spot 3

kV: 20      Mag: 5008      Takeoff: 6.2      Live Time(s): 30      Amp Time(μs): 3.84      Resolution:(eV)124

EDS Spot 3



Lsec: 30.0 0 Cnts 0.000 keV Det: Apollo X-SDD Det

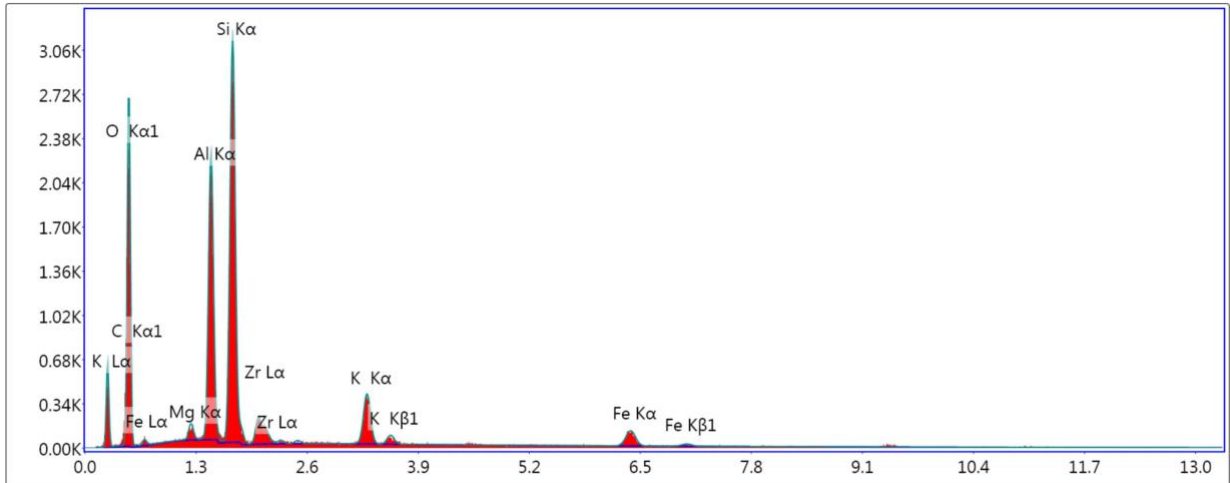
**eZAF Smart Quant Results**

Element	Weight %	Atomic %	Net Int.	Error %	Kratio	Z	R	A	F
O K	55.21	69.87	1,168.91	7.72	0.22	1.05	0.97	0.37	1
NaK	1.28	1.13	34.67	12.78	0.00	0.96	1	0.36	1.01
MgK	1.06	0.88	52.88	10.20	0.01	0.98	1.01	0.51	1.01
AlK	15.42	11.57	951.47	5.06	0.10	0.94	1.01	0.66	1.01
KrL	0.68	0.16	18.91	13.45	0.00	0.73	1.19	0.78	1.03
SiK	19.17	13.82	1,120.70	5.23	0.12	0.96	1.02	0.63	1
ZrL	2.61	0.58	64.27	10.46	0.02	0.74	1.21	0.78	1
K K	2.11	1.09	100.60	5.74	0.02	0.89	1.05	0.9	1
FeK	2.47	0.90	50.58	8.99	0.02	0.81	1.07	1	1

EDS Spot 4

kV: 20      Mag: 5008      Takeoff: 6.2      Live Time(s): 30      Amp Time(μs): 3.84      Resolution:(eV)124

EDS Spot 4



Lsec: 30.0 0 Cnts 0.000 keV Det: Apollo X-SDD Det

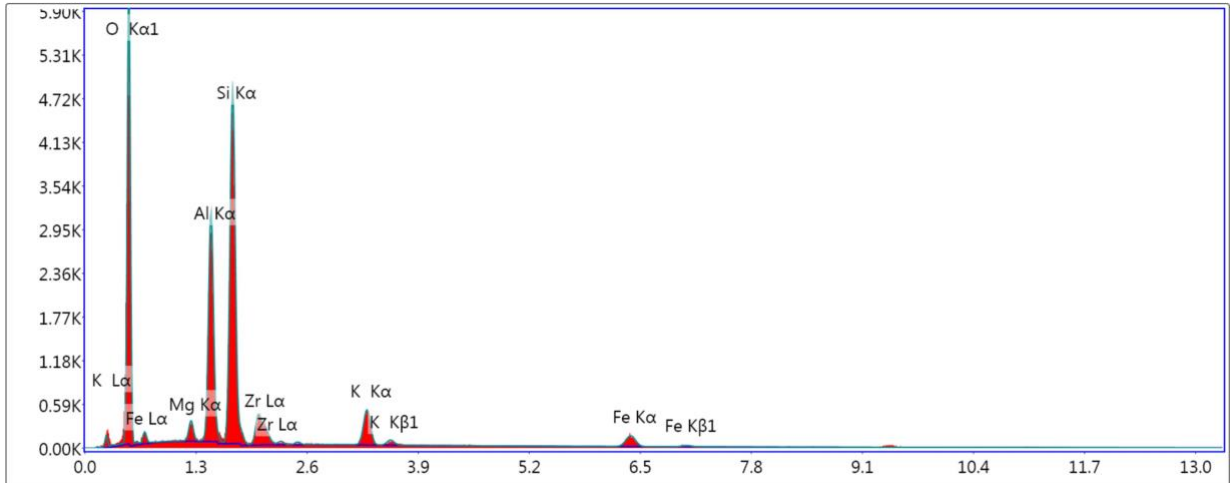
**eZAF Smart Quant Results**

Element	Weight %	Atomic %	Net Int.	Error %	Kratio	Z	R	A	F
C K	23.01	33.98	77.11	12.28	0.05	1.08	0.96	0.18	1
O K	41.29	45.78	411.08	9.55	0.10	1.03	0.98	0.23	1
MgK	0.83	0.60	33.12	11.62	0.00	0.95	1.01	0.54	1.01
AlK	10.40	6.83	510.73	5.08	0.07	0.92	1.02	0.69	1.01
SiK	15.42	9.74	762.42	4.69	0.10	0.94	1.03	0.7	1
ZrL	2.24	0.44	46.92	12.46	0.01	0.72	1.22	0.87	1.01
K K	3.36	1.52	126.69	4.65	0.03	0.87	1.05	0.93	1
FeK	3.46	1.10	54.03	7.95	0.03	0.79	1.08	1.01	1

EDS Spot 5

kV: 20      Mag: 5008      Takeoff: 6.2      Live Time(s): 30      Amp Time(μs): 3.84      Resolution:(eV)124

EDS Spot 5



Lsec: 30.0 0 Cnts 0.000 keV Det: Apollo X-SDD Det

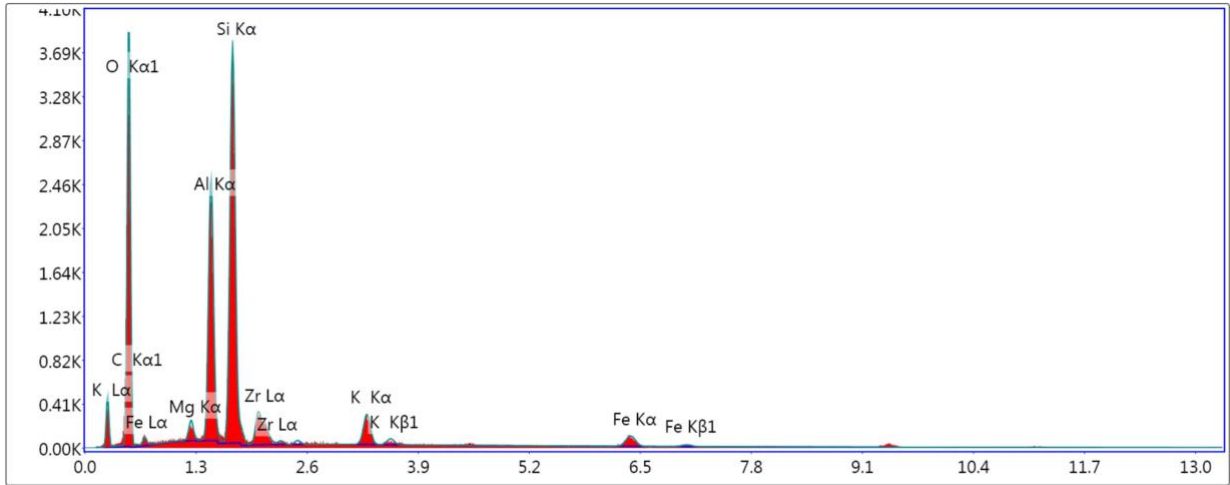
**eZAF Smart Quant Results**

Element	Weight %	Atomic %	Net Int.	Error %	Kratio	Z	R	A	F
O K	53.15	69.05	941.28	8.14	0.19	1.06	0.97	0.34	1
MgK	1.66	1.42	76.98	9.04	0.01	0.98	1	0.51	1.01
AlK	12.74	9.81	720.72	5.28	0.08	0.95	1.01	0.65	1.01
SiK	20.93	15.49	1,175.94	4.98	0.13	0.97	1.02	0.66	1
ZrL	4.36	0.99	100.58	7.97	0.03	0.75	1.21	0.79	1.01
K K	3.57	1.90	156.87	4.80	0.03	0.9	1.04	0.89	1
FeK	3.59	1.34	67.92	7.23	0.03	0.82	1.07	1	1

EDS Spot 6

kV: 20      Mag: 5008      Takeoff: 6.2      Live Time(s): 30      Amp Time(μs): 3.84      Resolution:(eV)124

EDS Spot 6



Lsec: 30.0 0 Cnts 0.000 keV Det: Apollo X-SDD Det

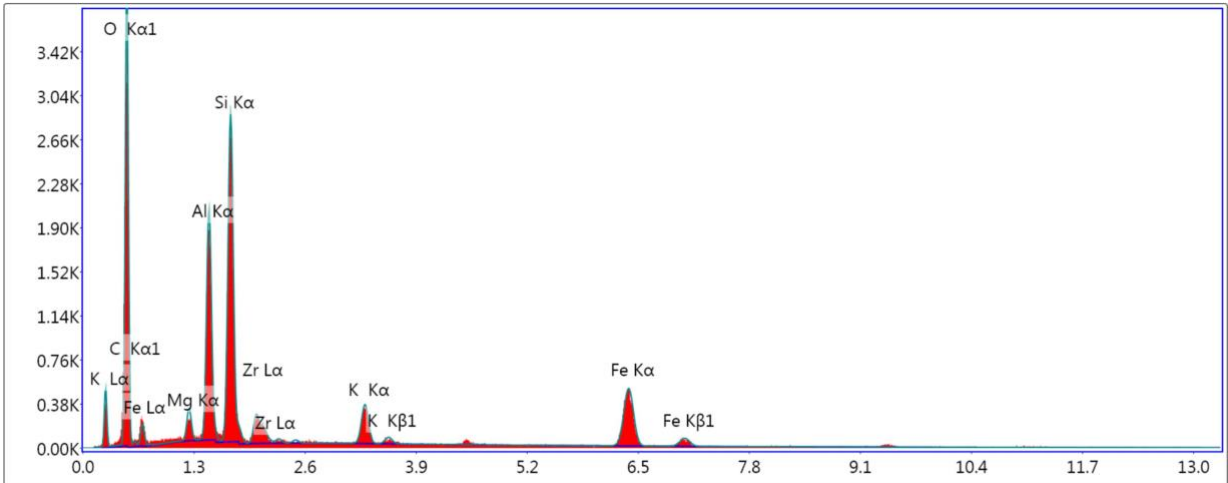
**eZAF Smart Quant Results**

Element	Weight %	Atomic %	Net Int.	Error %	Kratio	Z	R	A	F
C K	16.39	24.90	56.02	13.44	0.03	1.08	0.96	0.17	1
O K	47.06	53.65	592.97	9.02	0.13	1.04	0.98	0.27	1
MgK	1.08	0.81	46.99	11.08	0.01	0.96	1.01	0.54	1.01
AlK	10.62	7.18	565.16	5.07	0.07	0.92	1.02	0.68	1.01
SiK	16.86	10.95	903.54	4.67	0.11	0.94	1.02	0.69	1
ZrL	3.22	0.64	72.36	10.56	0.02	0.73	1.22	0.85	1
K K	2.21	1.03	90.43	6.11	0.02	0.88	1.05	0.92	1
FeK	2.56	0.84	43.91	9.21	0.02	0.79	1.08	1.01	1

EDS Spot 7

kV: 20      Mag: 5008      Takeoff: 6.2      Live Time(s): 29.9      Amp Time(μs): 3.84      Resolution:(eV)124

EDS Spot 7



Lsec: 29.9 0 Cnts 0.000 keV Det: Apollo X-SDD Det

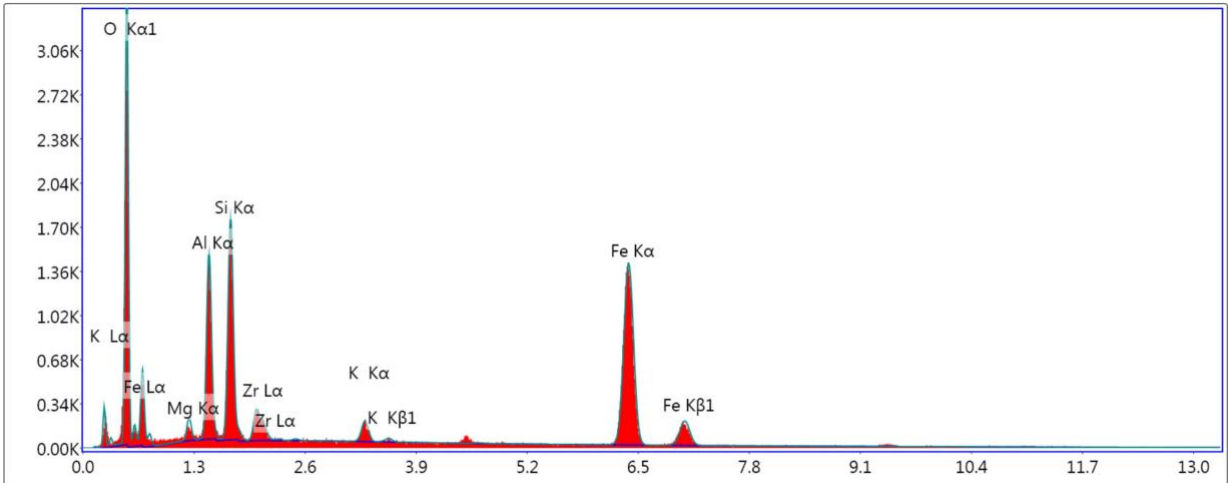
**eZAF Smart Quant Results**

Element	Weight %	Atomic %	Net Int.	Error %	Kratio	Z	R	A	F
C K	15.37	24.77	59.93	12.97	0.03	1.1	0.95	0.19	1
O K	43.19	52.26	606.61	8.87	0.13	1.05	0.97	0.28	1
MgK	1.55	1.23	61.86	9.78	0.01	0.97	1	0.47	1.01
AlK	9.21	6.61	461.20	5.96	0.05	0.94	1.01	0.61	1.01
SiK	13.03	8.98	694.77	5.22	0.08	0.96	1.02	0.65	1
ZrL	2.49	0.53	59.35	10.84	0.02	0.74	1.21	0.85	1.01
K K	2.53	1.25	110.52	5.51	0.02	0.89	1.05	0.92	1.01
FeK	12.64	4.38	229.14	3.31	0.10	0.81	1.07	1.01	1

EDS Spot 8

kV: 20      Mag: 5008      Takeoff: 6.2      Live Time(s): 30      Amp Time(μs): 3.84      Resolution:(eV)124

EDS Spot 8



Lsec: 30.0 0 Cnts 0.000 keV Det: Apollo X-SDD Det

**eZAF Smart Quant Results**

Element	Weight %	Atomic %	Net Int.	Error %	Kratio	Z	R	A	F
O K	32.17	55.39	539.10	7.85	0.14	1.13	0.93	0.39	1
MgK	1.52	1.72	38.87	13.38	0.01	1.05	0.96	0.35	1.01
AlK	9.78	9.99	331.97	7.45	0.05	1.01	0.97	0.47	1.01
SiK	10.96	10.75	422.85	6.59	0.06	1.04	0.98	0.54	1
ZrL	3.28	0.99	61.54	12.03	0.02	0.8	1.17	0.77	1.02
K K	1.43	1.01	53.16	9.52	0.01	0.97	1.01	0.88	1.03
FeK	40.87	20.16	643.03	2.26	0.36	0.88	1.05	1	1

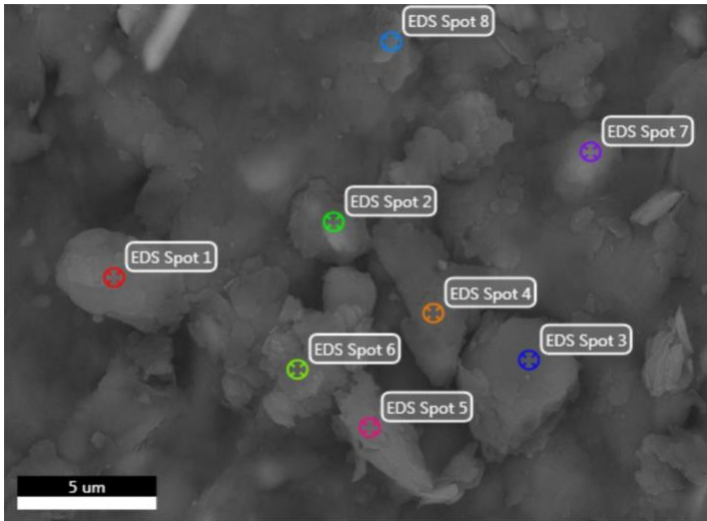
# B. EDX non-sintered Sample report

## EDAX TEAM

xiangxing

Author: edax  
Creation: 7/13/2018  
Sample Name: New Sample

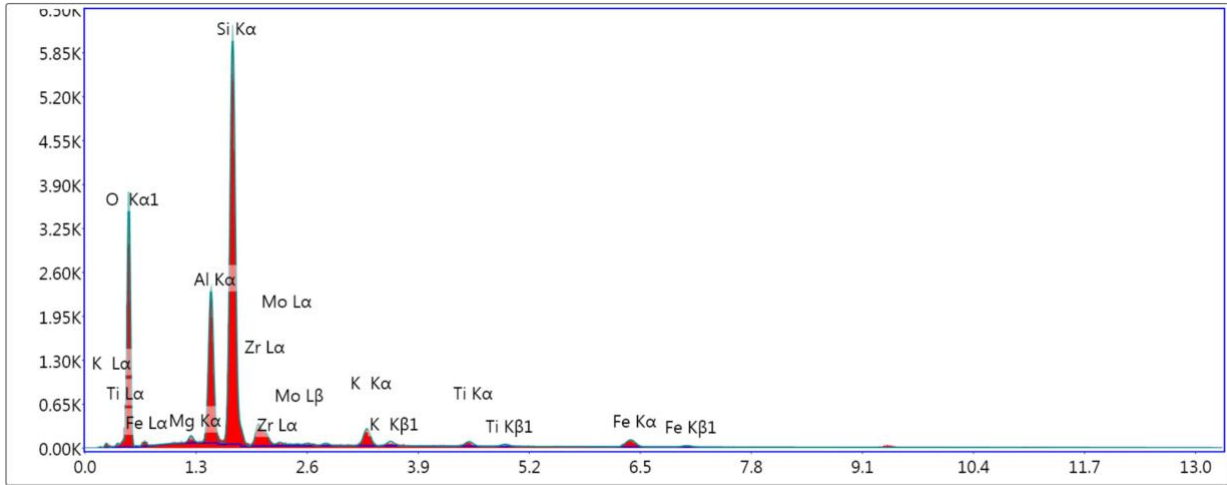
### Area 2



EDS Spot 1

kV: 20      Mag: 5008      Takeoff: 6.5      Live Time(s): 30      Amp Time(μs): 3.84      Resolution:(eV)124

EDS Spot 1



Lsec: 30.0 0 Cnts 0.000 keV Det: Apollo X-SDD Det

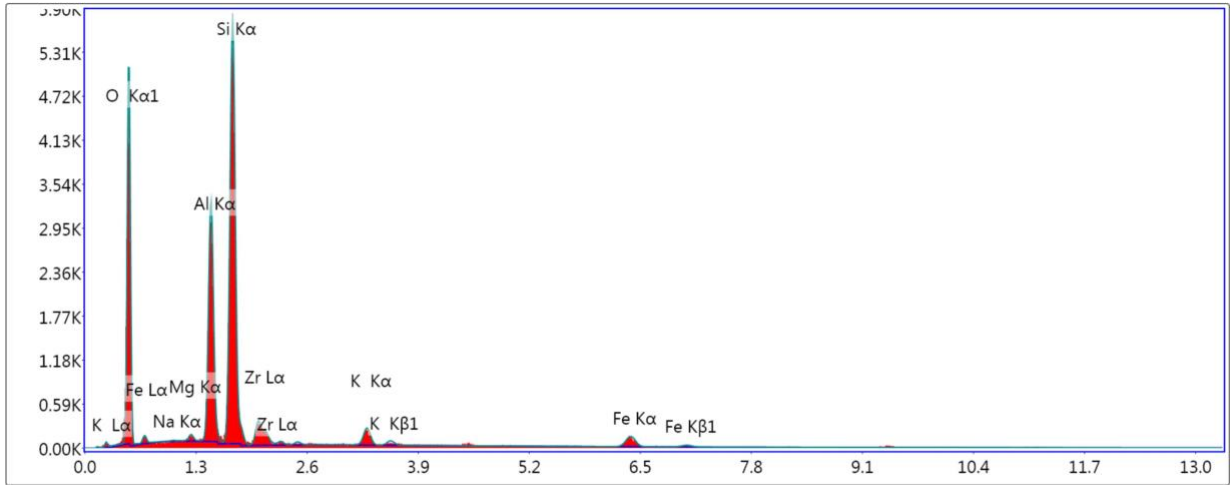
**eZAF Smart Quant Results**

Element	Weight %	Atomic %	Net Int.	Error %	Kratio	Z	R	A	F
O K	45.95	62.38	582.84	8.72	0.15	1.07	0.96	0.3	1
MgK	0.76	0.68	29.89	11.97	0.00	0.99	1	0.54	1.02
AlK	10.93	8.80	529.85	5.13	0.07	0.95	1	0.68	1.02
SiK	31.13	24.07	1,496.42	4.54	0.21	0.97	1.01	0.69	1
ZrL	4.37	1.04	76.54	9.30	0.02	0.75	1.2	0.74	1
MoL	0.49	0.11	9.08	36.23	0.00	0.75	1.21	0.8	1.01
K K	2.31	1.28	80.17	6.35	0.02	0.9	1.04	0.87	1
TiK	0.95	0.43	25.25	12.37	0.01	0.83	1.05	0.95	1.01
FeK	3.11	1.21	47.34	8.51	0.03	0.82	1.07	1	1

EDS Spot 2

kV: 20      Mag: 5008      Takeoff: 6.5      Live Time(s): 30      Amp Time(μs): 3.84      Resolution:(eV)124

EDS Spot 2



Lsec: 30.0 0 Cnts 0.000 keV Det: Apollo X-SDD Det

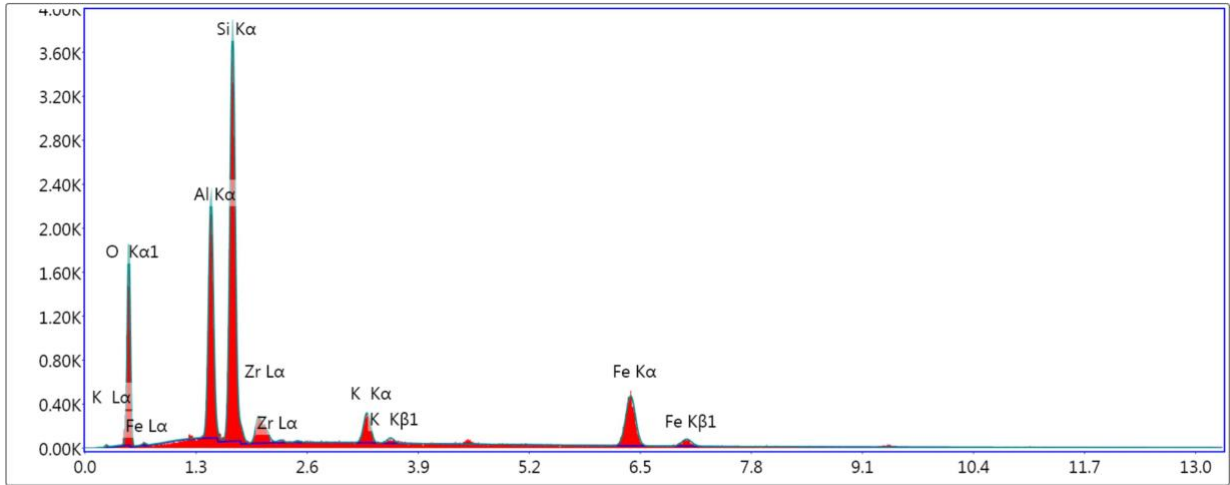
**eZAF Smart Quant Results**

Element	Weight %	Atomic %	Net Int.	Error %	Kratio	Z	R	A	F
O K	48.59	64.32	790.67	8.22	0.17	1.06	0.97	0.34	1
NaK	0.85	0.79	20.40	13.82	0.00	0.97	0.99	0.37	1.01
MgK	0.81	0.71	35.80	11.76	0.00	0.98	1	0.53	1.02
AlK	13.85	10.87	750.18	5.03	0.09	0.95	1.01	0.67	1.02
SiK	26.59	20.05	1,389.02	4.88	0.17	0.97	1.01	0.66	1
ZrL	3.81	0.88	77.01	9.76	0.02	0.75	1.2	0.75	1
K K	1.85	1.00	74.09	7.02	0.01	0.9	1.04	0.88	1
FeK	3.63	1.38	63.25	7.25	0.03	0.82	1.07	1	1

EDS Spot 3

kV: 20      Mag: 5008      Takeoff: 6.5      Live Time(s): 30      Amp Time(μs): 3.84      Resolution:(eV)124

EDS Spot 3



Lsec: 30.0 0 Cnts 0.000 keV Det: Apollo X-SDD Det

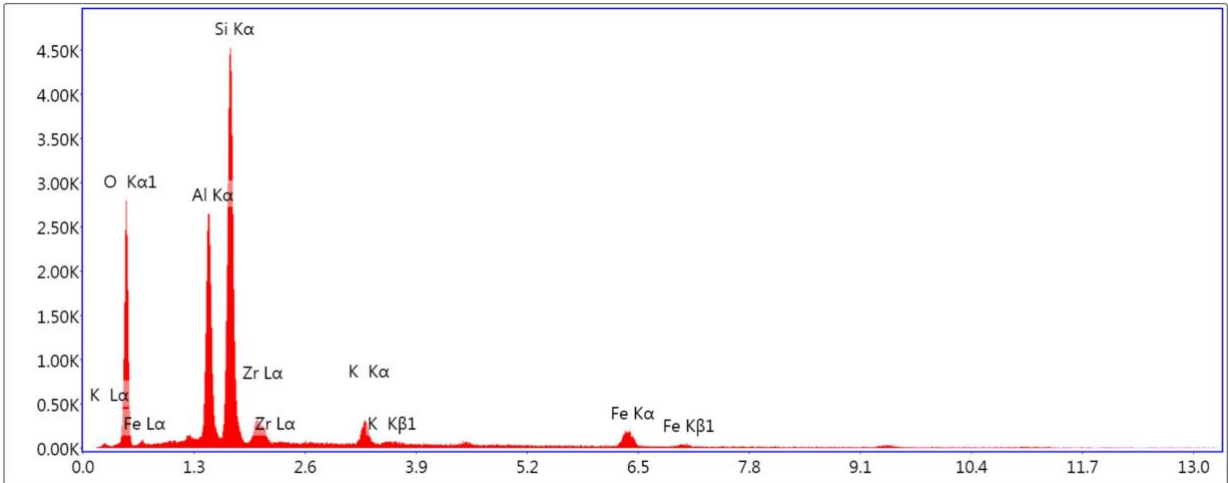
**eZAF Smart Quant Results**

Element	Weight %	Atomic %	Net Int.	Error %	Kratio	Z	R	A	F
O K	30.52	48.43	281.18	9.39	0.10	1.11	0.94	0.29	1
AlK	15.28	14.37	511.55	5.73	0.10	0.99	0.99	0.62	1.02
SiK	28.24	25.53	921.19	5.44	0.18	1.01	0.99	0.62	1
ZrL	4.54	1.26	58.27	13.48	0.03	0.78	1.18	0.71	1.01
K K	3.42	2.22	89.94	6.71	0.03	0.94	1.03	0.85	1.01
FeK	17.99	8.18	209.00	3.47	0.15	0.86	1.06	0.99	1

EDS Spot 4

kV: 20      Mag: 5008      Takeoff: 6.5      Live Time(s): 30      Amp Time(μs): 3.84      Resolution:(eV)124

EDS Spot 4



Lsec: 30.0 0 Cnts 0.000 keV Det: Apollo X-SDD Det

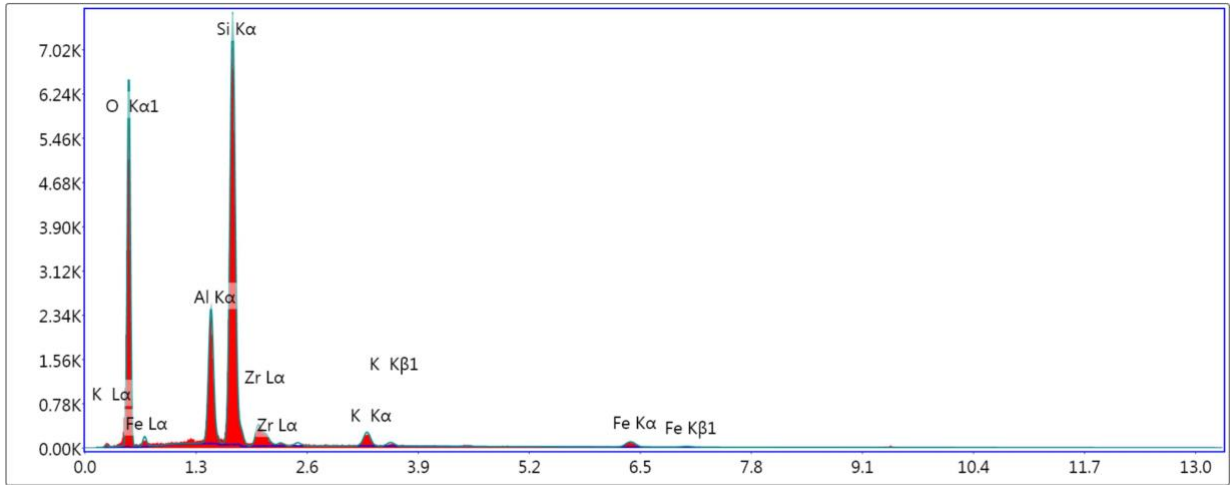
**eZAF Smart Quant Results**

Element	Weight %	Atomic %	Net Int.	Error %	Kratio	Z	R	A	F
O K	42.73	59.64	480.12	8.76	0.14	1.08	0.96	0.3	1
AlK	14.87	12.31	627.62	5.08	0.10	0.96	1	0.68	1.02
SiK	28.72	22.84	1,148.74	4.96	0.19	0.98	1.01	0.66	1
ZrL	4.79	1.17	72.81	11.04	0.03	0.76	1.2	0.74	1.01
K K	2.80	1.60	85.00	6.82	0.02	0.91	1.04	0.86	1
FeK	6.09	2.44	81.40	6.02	0.05	0.83	1.07	1	1

EDS Spot 5

kV: 20      Mag: 5008      Takeoff: 6.5      Live Time(s): 30      Amp Time(μs): 3.84      Resolution:(eV)124

EDS Spot 5



Lsec: 30.0 0 Cnts 0.000 keV Det: Apollo X-SDD Det

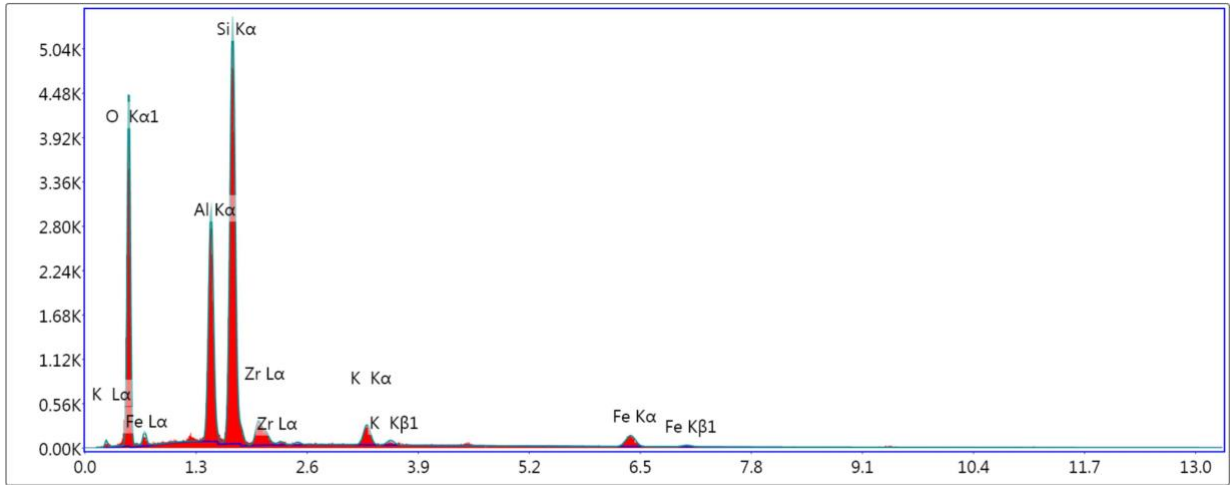
**eZAF Smart Quant Results**

Element	Weight %	Atomic %	Net Int.	Error %	Kratio	Z	R	A	F
O K	53.49	68.80	992.56	8.05	0.20	1.06	0.97	0.35	1
AlK	9.09	6.94	556.79	5.05	0.06	0.94	1.01	0.68	1.02
SiK	29.55	21.65	1,838.94	4.30	0.20	0.96	1.02	0.71	1
ZrL	3.91	0.88	89.24	7.58	0.02	0.74	1.21	0.77	1
K K	1.75	0.92	77.91	6.23	0.01	0.89	1.05	0.88	1
FeK	2.20	0.81	42.59	11.82	0.02	0.81	1.07	1	1

EDS Spot 6

kV: 20      Mag: 5008      Takeoff: 6.5      Live Time(s): 30      Amp Time(μs): 3.84      Resolution:(eV)124

EDS Spot 6



Lsec: 30.0 0 Cnts 0.000 keV Det: Apollo X-SDD Det

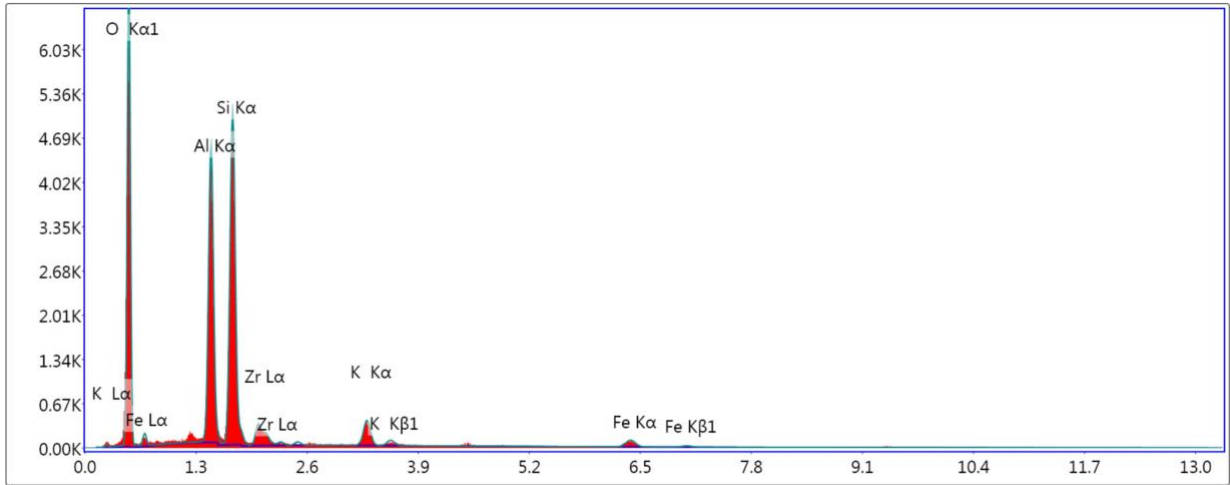
**eZAF Smart Quant Results**

Element	Weight %	Atomic %	Net Int.	Error %	Kratio	Z	R	A	F
O K	48.33	64.46	681.02	8.37	0.17	1.07	0.97	0.33	1
AlK	13.78	10.90	676.85	5.02	0.09	0.95	1.01	0.68	1.02
SiK	27.48	20.88	1,295.74	4.82	0.18	0.97	1.01	0.67	1
ZrL	4.02	0.94	72.37	10.67	0.02	0.75	1.2	0.75	1
K K	2.30	1.26	81.96	6.19	0.02	0.9	1.04	0.87	1
FeK	4.09	1.56	63.56	7.58	0.03	0.82	1.07	1	1

EDS Spot 7

kV: 20      Mag: 5008      Takeoff: 6.5      Live Time(s): 30      Amp Time(μs): 3.84      Resolution:(eV)124

EDS Spot 7



Lsec: 30.0 0 Cnts 0.000 keV Det: Apollo X-SDD Det

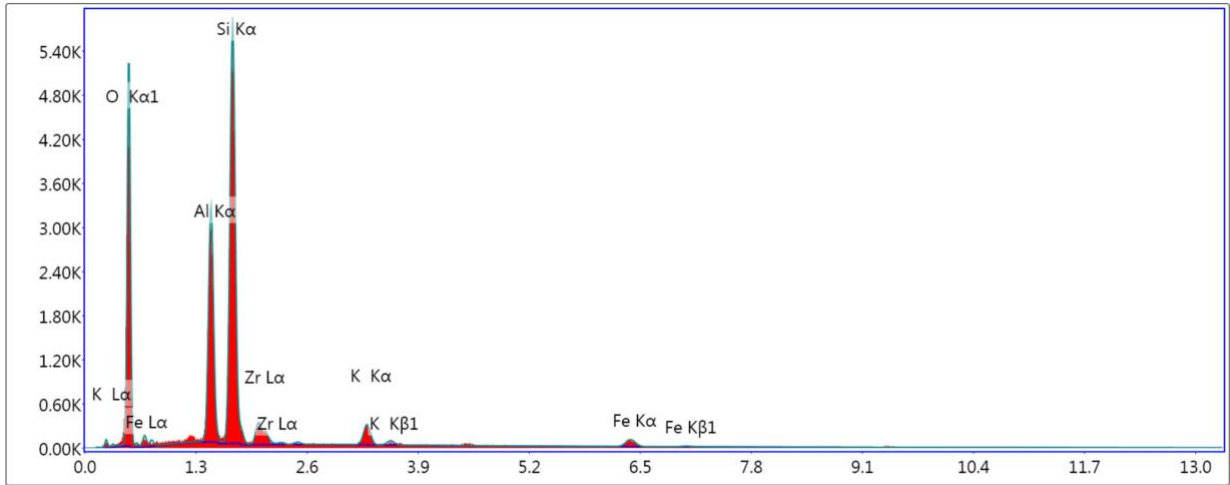
**eZAF Smart Quant Results**

Element	Weight %	Atomic %	Net Int.	Error %	Kratio	Z	R	A	F
O K	54.37	69.33	1,071.79	7.94	0.20	1.06	0.97	0.36	1
AlK	16.51	12.48	1,036.87	4.79	0.11	0.94	1.01	0.68	1.01
SiK	20.99	15.25	1,230.18	5.07	0.13	0.96	1.02	0.65	1
ZrL	3.18	0.71	76.72	8.49	0.02	0.74	1.21	0.78	1
K K	2.65	1.39	123.82	5.36	0.02	0.89	1.05	0.89	1
FeK	2.30	0.84	46.14	9.59	0.02	0.81	1.07	1	1

EDS Spot 8

kV: 20      Mag: 5008      Takeoff: 6.5      Live Time(s): 30      Amp Time(μs): 3.84      Resolution:(eV)124

EDS Spot 8



Lsec: 30.0 0 Cnts 0.000 keV Det: Apollo X-SDD Det

**eZAF Smart Quant Results**

Element	Weight %	Atomic %	Net Int.	Error %	Kratio	Z	R	A	F
O K	50.81	66.35	800.20	8.24	0.18	1.06	0.97	0.33	1
AlK	13.64	10.56	738.51	4.86	0.09	0.94	1.01	0.69	1.02
SiK	26.93	20.03	1,397.66	4.75	0.18	0.97	1.02	0.67	1
ZrL	3.73	0.85	74.19	10.00	0.02	0.74	1.21	0.76	1
K K	2.34	1.25	91.50	6.02	0.02	0.9	1.05	0.88	1
FeK	2.54	0.95	43.10	11.22	0.02	0.81	1.07	1	1

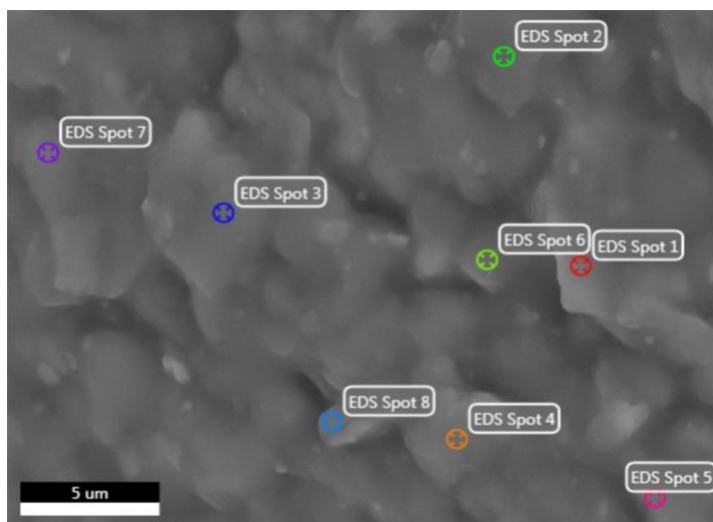
# C. EDX Sintered Sample report

## EDAX TEAM

xiangxing

Author: edax  
Creation: 7/13/2018  
Sample Name: New Sample

### Area 3

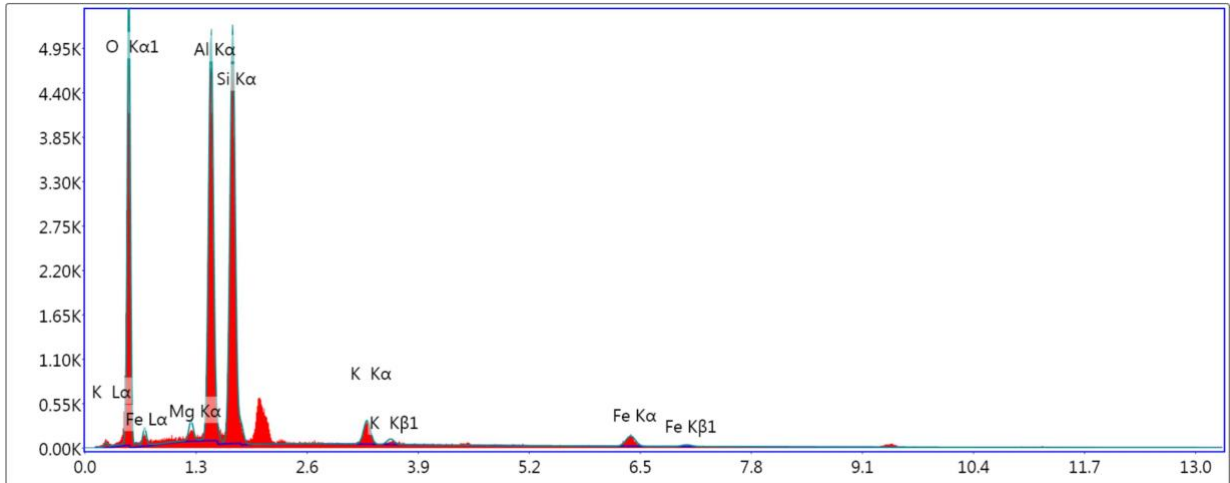


Notes:

EDS Spot 1

kV: 20      Mag: 5008      Takeoff: 6.9      Live Time(s): 30      Amp Time(μs): 3.84      Resolution:(eV)124

EDS Spot 1



Lsec: 30.0 0 Cnts 0.000 keV Det: Apollo X-SDD Det

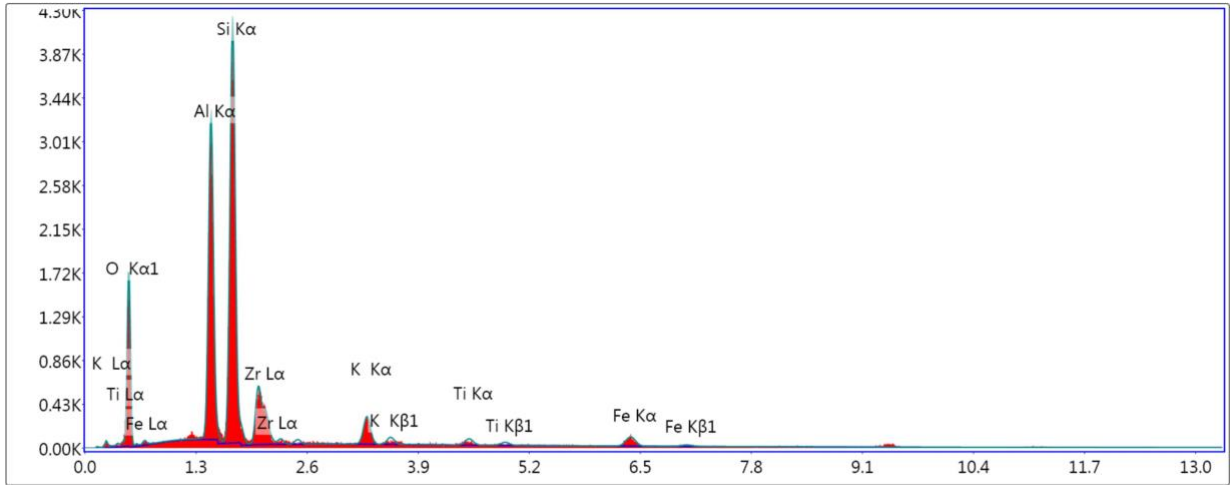
**eZAF Smart Quant Results**

Element	Weight %	Atomic %	Net Int.	Error %	Kratio	Z	R	A	F
O K	47.97	62.40	830.73	8.04	0.18	1.06	0.97	0.35	1
MgK	1.13	0.97	53.12	10.85	0.01	0.98	1.01	0.55	1.02
AlK	20.34	15.69	1,150.62	4.64	0.13	0.94	1.01	0.69	1.01
SiK	24.91	18.46	1,243.51	5.27	0.15	0.96	1.02	0.62	1
K K	2.37	1.26	97.51	5.90	0.02	0.89	1.05	0.89	1
FeK	3.27	1.22	57.95	7.96	0.03	0.81	1.07	1	1

EDS Spot 2

kV: 20      Mag: 5008      Takeoff: 6.9      Live Time(s): 30      Amp Time(μs): 3.84      Resolution:(eV)124

EDS Spot 2



Lsec: 30.0 0 Cnts 0.000 keV Det: Apollo X-SDD Det

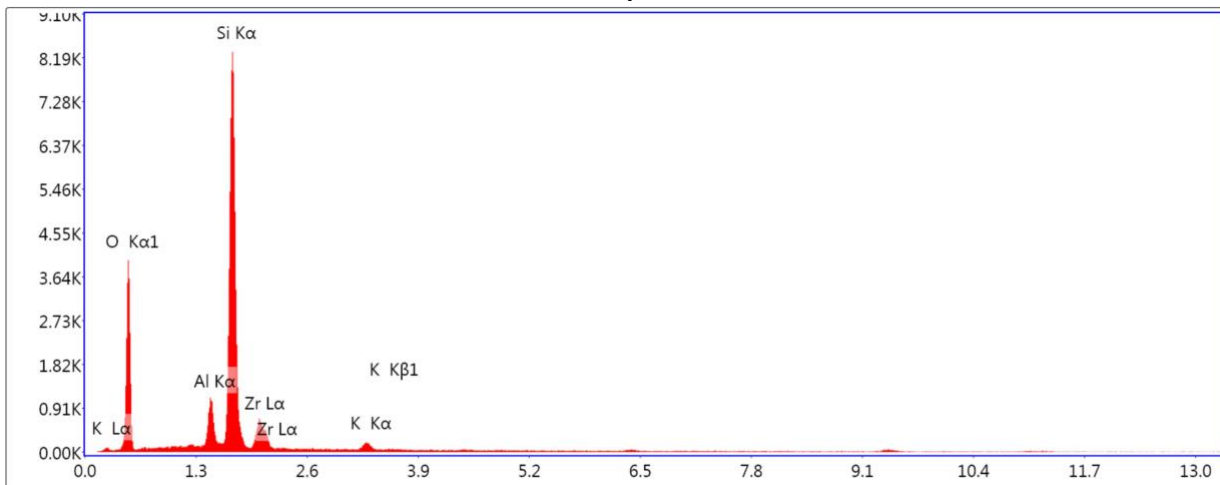
**eZAF Smart Quant Results**

Element	Weight %	Atomic %	Net Int.	Error %	Kratio	Z	R	A	F
O K	33.65	51.03	264.46	9.73	0.09	1.1	0.95	0.24	1
AlK	18.79	16.90	731.97	4.67	0.13	0.98	0.99	0.71	1.02
SiK	28.99	25.04	1,005.23	5.14	0.19	1	1	0.64	1
ZrL	10.47	2.78	138.43	6.88	0.06	0.77	1.19	0.72	1.01
K K	3.41	2.12	88.30	6.60	0.03	0.93	1.03	0.83	1
TiK	1.14	0.58	23.11	13.62	0.01	0.86	1.04	0.93	1.01
FeK	3.56	1.55	41.84	11.70	0.03	0.85	1.06	0.99	1

EDS Spot 3

kV: 20      Mag: 5008      Takeoff: 6.9      Live Time(s): 30      Amp Time(μs): 3.84      Resolution:(eV)124

EDS Spot 3



Lsec: 30.0 0 Cnts 0.000 keV Det: Apollo X-SDD Det

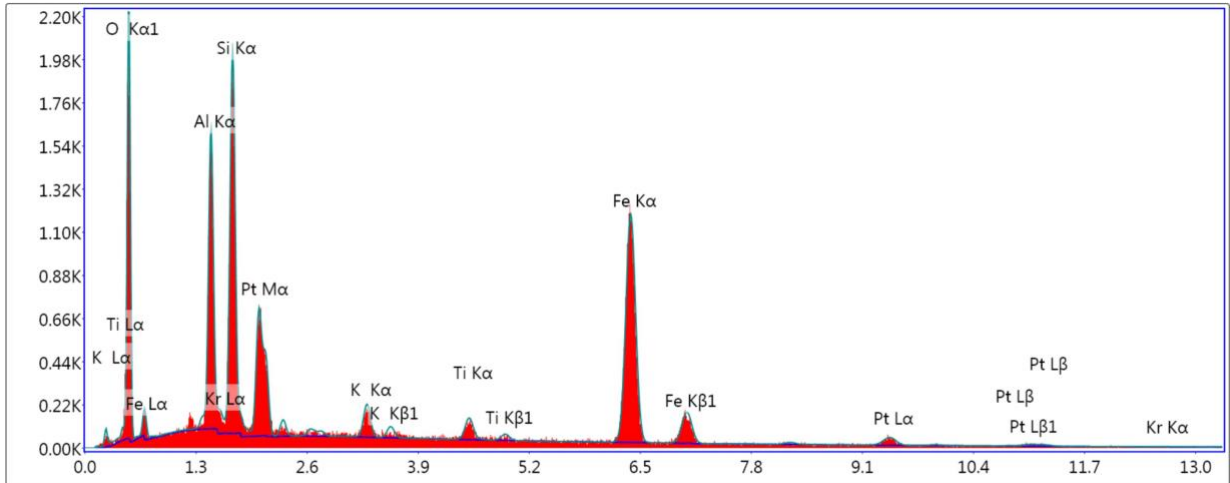
**eZAF Smart Quant Results**

Element	Weight %	Atomic %	Net Int.	Error %	Kratio	Z	R	A	F
O K	49.70	66.18	695.13	8.62	0.16	1.06	0.96	0.3	1
AlK	4.71	3.72	259.08	5.54	0.03	0.95	1.01	0.7	1.03
SiK	36.19	27.45	2,108.55	3.71	0.27	0.97	1.01	0.77	1
ZrL	7.92	1.85	153.97	6.45	0.04	0.75	1.2	0.75	1
K K	1.48	0.81	55.59	9.88	0.01	0.9	1.04	0.86	1

EDS Spot 4

kV: 20      Mag: 5008      Takeoff: 6.9      Live Time(s): 30      Amp Time(μs): 3.84      Resolution:(eV)124

EDS Spot 4



Lsec: 30.0 Cnts 0.000 keV Det: Apollo X-SDD Det

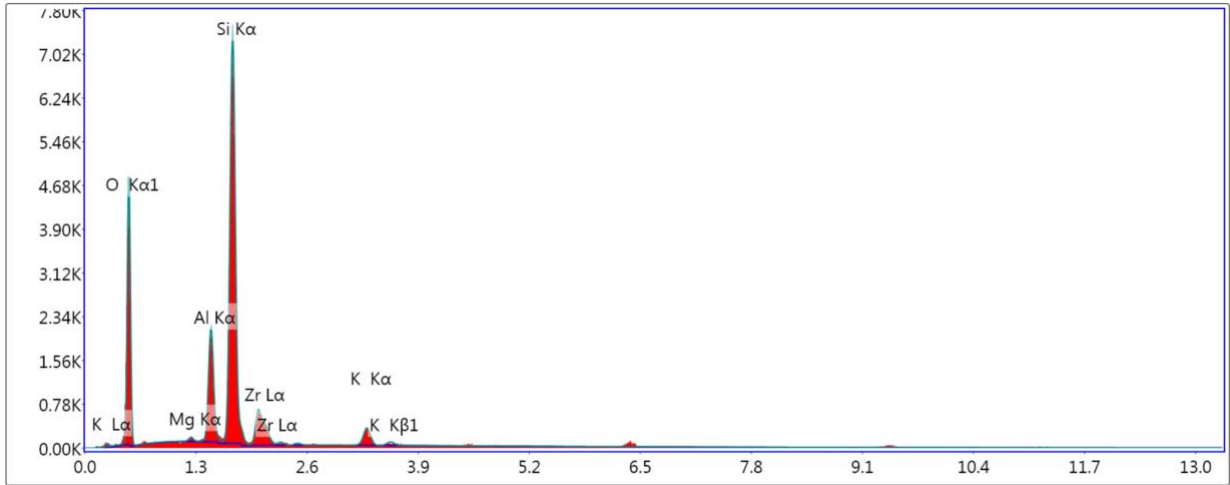
**eZAF Smart Quant Results**

Element	Weight %	Atomic %	Net Int.	Error %	Kratio	Z	R	A	F
O K	25.66	49.43	337.09	8.92	0.10	1.17	0.9	0.32	1
AlK	10.54	12.04	353.30	7.24	0.06	1.05	0.95	0.5	1.01
KrL	1.01	0.37	17.09	14.46	0.01	0.82	1.12	0.67	1.02
SiK	12.98	14.24	475.01	6.51	0.08	1.07	0.96	0.55	1
K K	1.58	1.24	51.88	8.89	0.01	1	1	0.83	1.02
TiK	1.51	0.97	40.79	11.81	0.01	0.93	1.01	0.93	1.07
FeK	36.35	20.06	535.25	2.55	0.33	0.92	1.03	0.99	1
PtL	10.37	1.64	23.82	31.59	0.07	0.63	1.13	1.02	0.99

EDS Spot 5

kV: 20      Mag: 5008      Takeoff: 6.9      Live Time(s): 30      Amp Time(μs): 3.84      Resolution:(eV)124

EDS Spot 5



Lsec: 30.0 0 Cnts 0.000 keV Det: Apollo X-SDD Det

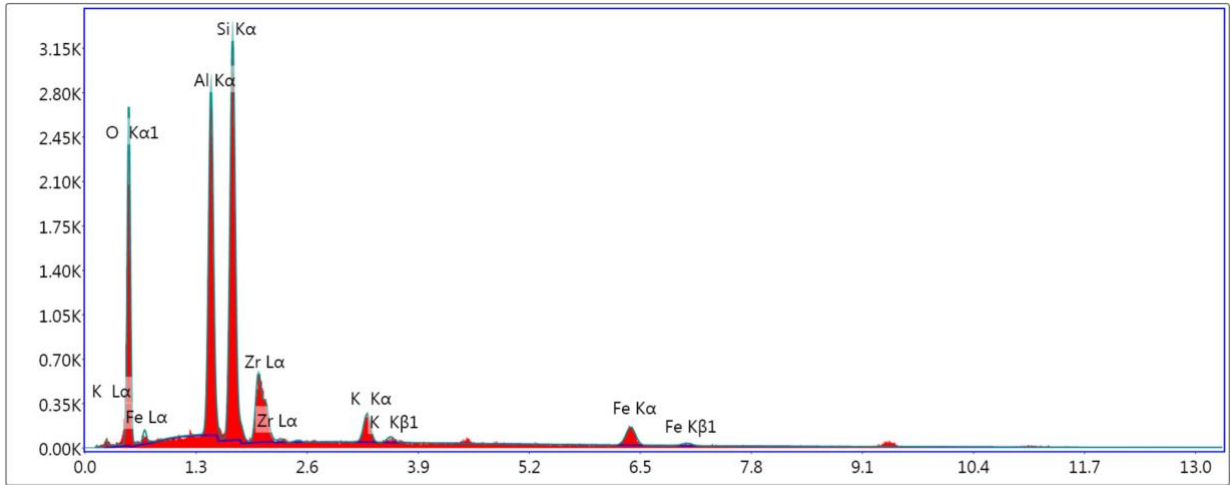
**eZAF Smart Quant Results**

Element	Weight %	Atomic %	Net Int.	Error %	Kratio	Z	R	A	F
O K	50.36	66.61	750.62	8.57	0.16	1.06	0.96	0.3	1
MgK	0.64	0.56	29.88	11.96	0.00	0.98	1	0.55	1.02
AlK	8.32	6.53	475.75	5.13	0.06	0.95	1.01	0.69	1.02
SiK	30.85	23.25	1,799.49	4.19	0.22	0.97	1.01	0.72	1
ZrL	7.33	1.70	153.35	7.29	0.04	0.75	1.2	0.77	1
K K	2.50	1.35	100.25	6.61	0.02	0.9	1.04	0.86	1

EDS Spot 6

kV: 20      Mag: 5008      Takeoff: 6.9      Live Time(s): 30      Amp Time(μs): 3.84      Resolution:(eV)124

EDS Spot 6



Lsec: 30.0 0 Cnts 0.000 keV Det: Apollo X-SDD Det

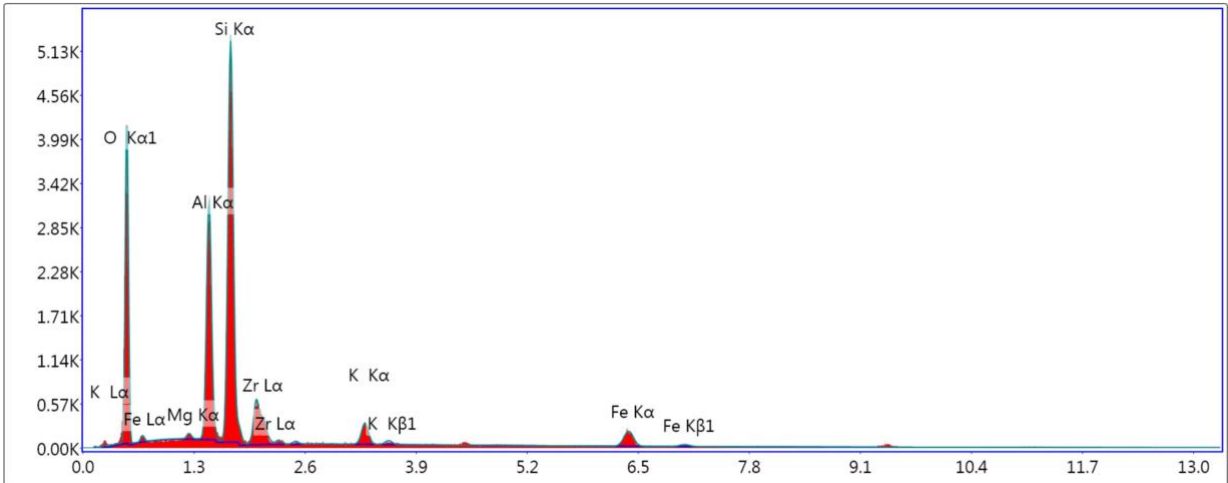
**eZAF Smart Quant Results**

Element	Weight %	Atomic %	Net Int.	Error %	Kratio	Z	R	A	F
O K	42.65	60.94	408.99	9.01	0.13	1.09	0.95	0.29	1
AlK	17.15	14.53	646.02	5.13	0.11	0.97	1	0.67	1.01
SiK	22.57	18.37	790.04	5.35	0.14	0.99	1	0.64	1
ZrL	9.54	2.39	136.01	7.61	0.06	0.76	1.19	0.76	1
K K	2.63	1.54	71.33	8.23	0.02	0.92	1.03	0.85	1
FeK	5.46	2.23	66.09	7.80	0.05	0.84	1.06	0.99	1

EDS Spot 7

kV: 20      Mag: 5008      Takeoff: 6.9      Live Time(s): 30      Amp Time(μs): 3.84      Resolution:(eV)124

EDS Spot 7



Lsec: 30.0 0 Cnts 0.000 keV Det: Apollo X-SDD Det

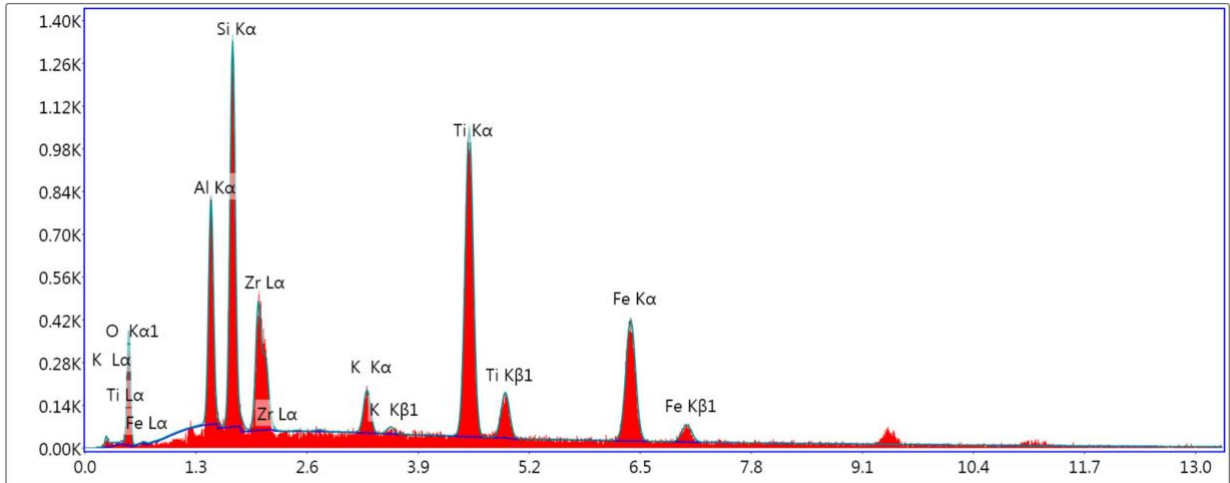
**eZAF Smart Quant Results**

Element	Weight %	Atomic %	Net Int.	Error %	Kratio	Z	R	A	F
O K	45.35	62.80	648.34	8.61	0.15	1.08	0.96	0.31	1
MgK	0.87	0.79	36.73	11.72	0.00	1	0.99	0.52	1.02
AlK	13.80	11.33	715.00	5.13	0.09	0.96	1	0.66	1.02
SiK	25.25	19.92	1,269.81	4.96	0.16	0.98	1.01	0.66	1
ZrL	7.11	1.73	140.58	7.16	0.04	0.76	1.2	0.76	1
K K	2.34	1.33	89.46	6.60	0.02	0.91	1.04	0.86	1
FeK	5.27	2.09	88.83	5.97	0.04	0.83	1.07	1	1

EDS Spot 8

kV: 20      Mag: 5008      Takeoff: 6.9      Live Time(s): 30      Amp Time(μs): 3.84      Resolution:(eV)124

EDS Spot 8



Lsec: 30.0 0 Cnts 0.000 keV Det: Apollo X-SDD Det

**eZAF Smart Quant Results**

Element	Weight %	Atomic %	Net Int.	Error %	Kratio	Z	R	A	F
O K	16.98	35.67	56.96	12.35	0.03	1.18	0.91	0.15	1
AlK	8.41	10.47	168.70	7.99	0.05	1.06	0.95	0.52	1.01
SiK	13.70	16.39	308.58	6.51	0.09	1.08	0.96	0.59	1.01
ZrL	10.21	3.76	106.64	6.78	0.07	0.84	1.15	0.79	1.03
K K	2.35	2.02	46.28	13.42	0.02	1.01	1	0.86	1.05
TiK	25.91	18.18	387.55	3.02	0.24	0.93	1.02	0.95	1.03
FeK	22.45	13.51	181.83	4.01	0.20	0.92	1.03	0.96	1